Functional characterization of the central auditory system using emission tomography



A thesis accepted for the degree of

Doctor of Natural Sciences (Dr. rer. nat.)

in the subject of Auditory Sciences

by

Martin Mamach, M.Sc. Physics

August 2018

Hannover Medical School

International PhD program "Auditory Sciences"

Hannover Biomedical Research School (HBRS)

Department of Nuclear Medicine

Acknowledged by the PhD committee and head of Hannover Medical School

President:	**Prof. Dr. Christopher Baum**
Supervisor:	**Prof. Dr. med. Georg Berding** Department for Nuclear Medicine Hannover Medical School
Cosupervisors:	**Prof. Dr. rer. nat. Peter Behrens** Institute of Inorganic Chemistry Leibniz University Hannover
	Prof. Dr. med. Karin Weißenborn Department of Neurology Hannover Medical School
External expert:	**Prof. Dr. Ronald Boellaard** Department of Nuclear Medicine and Molecular Imaging University of Groningen, Netherlands
Internal expert:	**Prof. Dr. med. Eckart Altenmüller** Institute of Music Physiology and Musicians' Medicine Hanover University of Music, Drama and Media

Day of final exam/public defense: November 5th 2018

‚Die Erschütterung der Luft wird erst Schall wo ein Ohr ist.‘

‚The vibration of the air first becomes a sound where there is an ear‘

Georg Christoph Lichtenberg
(1742–1799), German physicist

Summary

Hearing impairment is among the most common diseases affecting the life quality of more the 400 million people worldwide. It is of special interest in an aging society as it occurs naturally with advanced age. Beyond conventional amplifying hearing aids, the development of implantable hearing devices in the middle ear, the cochlea, the brainstem and the midbrain offers precise therapy for various causes of hearing loss. The ability to specify the source of the hearing impairment and predict the resulting hearing performance after corresponding therapy is highly demanded for optimized treatment. Functional and molecular imaging based on radiopharmaceuticals hold a high potential in this context as a translational tool useful from hearing research up to patient care. First, radiolabeled markers of cerebral perfusion have been used in hearing disorders about 3 decades ago in awake adult patients. Particularly in patients with auditory implants, they were applied in activation studies of the auditory system employing emission tomography with its limited spatial resolution at that time.

Against the background of earlier implantation nowadays – taking advantage of sensible phases for the development of hearing in the brain – we assessed in the first study reported here the usability of ^{15}O-water auditory activation PET studies in anesthetized children in comparison to awake adults. As all groups did not differ in their later speech performance, we hypothesized that similar activation patterns will to be measurable. Stimulations were applied in children either via cochlear implant or needle-electrode at the promontory, while adults were only stimulated by needle-electrode. We investigated different durations of scanning, kernels for smoothing of 3-dimensional data and cut-off levels of significance for statistical inference to reproduce similar results in all groups. No significant evidence could be found supporting to prefer either scan duration of 60 s or 90 s. Similar activation pattern in adults and children were achieved if a reduced statistical threshold of $p<0.01$ was used for anesthetized children compared to $p<0.001$ in awake adults. Stronger smoothing ([20-30mm]³) suppressed ‘artificial’ activations in extra-auditory areas. This study showed that PET can be successfully used in anesthetized children too.

In a second study, we tested the inverse translation of functional auditory PET imaging from humans into the rat animal model. The aim was to provide a diagnostic tool for hearing research. Multiple acoustic conditions were tested in a standardized sound shielded environment: (i) a stimulus called rippled noise designed to minimize adaption, (ii) a white noise stimulus and (iii) laboratory background noise. Additionally, animals were measured after bilateral cochlea ablation as a reference condition. Acoustic conditions were presented in awake animals during the uptake phase of ^{18}F-FDG. Imaging was performed during isoflurane anesthesia 1 h after intravenous tracer injection. Statistical analyses were performed area- and voxel-wise. Based on rippled noise, activation

in the inferior colliculus was so strong that it was even identifiable in individual animals. Significant activations with that stimulus were additionally found in statistical analyses for all major nuclei of the auditory pathway: the mediate geniculate body, the olivary complex, and the nucleus cochlearis – always comparing stimulus to laboratory background noise as a baseline in normal hearing rats. Furthermore, we could demonstrate stimulus based increased activity in the auditory cortex only if the cochlear ablated status was used as a reference, indicating the need for rigorous background suppression for baseline condition. Nevertheless, the functionality of the cortex was demonstrated by stimulus based deactivation by white noise compared to laboratory background noise. Finally, we observed after cochlea ablation an activation of the olfactory nucleus suggesting compensatory cross-modal activation.

Both studies underline the applicability of PET in auditory research as a tool providing objective measures. Different activation pattern in humans (cortical) and rats (subcortical) are most likely related to limitations in recovery from small structures of older PET systems and biological differences between species. Additionally, preliminary studies of the inhibitory GABAergic system using ^{18}F-Flumazenil PET in rats with profound hearing loss revealed decreased $GABA_A$-receptor binding in the auditory cortex together with a loss of activation. The finding points to a complementary value of functional and molecular imaging to improve understanding of the pathophysiology and treatment outcome in hearing loss.

Zusammenfassung

Hörbeeinträchtigungen gehörten zu den meistverbreiteten Erkrankungen, welche die Lebensqualität von mehr als 400 Millionen Menschen weltweit beeinflussen. Aufgrund ihres natürlichen Auftretens im gehobenen Alter sind sie dabei in einer alternden Gesellschaft von besonderem Interesse. Neben konventionellen verstärkenden Hörgeräten eröffnet die Entwicklung implantierbarer Hörhilfen, die vom Mittelohr über die Cochlea bis zum Hirnstamm und dem Mittelhirn eingesetzt werden können, präzise Therapiemöglichkeiten bei unterschiedlichen Ursachen des Hörverlustes. Die Fähigkeit ursächliche biologische Strukturen eines Hörverlustes zu identifizieren und den Erfolg von Hörhilfen vorherzusagen ist von Bedeutung für eine optimale Therapie. Die funktionale und molekulare Bildgebung besitzt mithilfe von Radiopharmaka ein hohes Potential in diesem Zusammenhang als translationale Methode, nutzbar von Hörforschung bis Patientenversorgung. Als erstes wurden radioaktive Marker der Hirndurchblutung bei Hörstörungen vor etwa 3 Jahrzehnten bei wachen, erwachsenen Patienten verwendet. Insbesondere bei Patienten mit auditorischen Implantaten wurden Aktivierungsstudien des auditorischen Systems unter Verwendung von Emissionstomographien mit ihrer zu der Zeit begrenzten räumlichen Auflösung durchgeführt.

Vor dem Hintergrund heutzutage frühzeitig durchgeführter Implantationen – die den Vorteil sensibler Phasen für die Entwicklung des Hörens im Gehirn nutzen – haben wir in der ersten Studie, über die hier berichtet wird, den Wert von auditorischen Aktivierungsstudien mit ^{15}O-Wasser PET bei Kindern unter Narkose im Vergleich zu wachen Erwachsenen untersucht. Wir erwarteten ähnlich messbare Aktivierungsmuster in allen Gruppen, da diese sich im späteren Sprachverständnis nicht unterschieden. Stimulationen erfolgen bei Kindern entweder über ein Cochlea-Implantat oder eine Nadelelektrode am Promontorium und bei Erwachsenen ausschließlich über eine Nadelelektrode. Es ergab sich kein signifikanter Hinweis, dass eine Scandauer von 60 s oder 90 s zu bevorzugen sei. Ähnliche Aktivierungsmuster bei Erwachsenen und Kindern wurden erreicht, wenn ein niedrigerer Grenzwert für statistisch signifikante Veränderungen von $p<0,01$ bei Kindern in Narkose im Vergleich zu $p<0,001$ bei wachen Erwachsenen verwendet wurde. Eine stärkere Glättung (20-30 mm^3) unterdrückte „artifizielle“ Aktivierungen in nicht-auditorischen Arealen. Eine Anwendung von PET bei narkotisierten Kindern ist somit sinnvoll möglich.

In einer zweiten Studie haben wir die inverse Translation der funktionalen PET-Bildgebung des auditorischen Systems vom Menschen zu Ratten als Tiermodel getestet. Das Ziel war es, eine diagnostische Methode für die Hörforschung zu entwickeln. Wir verwendeten dabei multiple akustische Konditionen in einer standardisierten schallabgeschirmten Umgebung: (i) einen “Rippled noise“ genannten Stimulus, der darauf ausgerichtet ist Adaptation zu minimieren, (ii) ein weißes Rauchen sowie (iii) Laborhinter-

grundsgeräusche. Zusätzlich wurden Tiere nach einer beidseitigen Cochlea-Ablation als Referenzkondition gemessen. Die akustischen Konditionen wurden wachen Tieren während der Aufnahmephase von ^{18}F-FDG präsentiert. PET Aufnahmen erfolgten dann in Isofluran-Narkose eine Stunde nach intravenöser Injektion des Radiotracers. Diese wurden statistisch areal- und voxelbezogen ausgewertet. Ausgehend vom „Rippled noise"-Stimulus war die Aktivierung im Inferior Colliculus so deutlich, dass sie bereits in einzelnen Tieren erkennbar war. Signifikante Aktivierungen mit diesem Stimulus waren in allen wesentlichen Nuklei der zentralen auditorischen Leitungsbahn zu beobachten: im auditorischen Thalamus, im olivären Komplex und im Nucleus Cochlearis – jeweils im Vergleich zu den Laborhintergrundsgeräuschen als Referenz bei normalhörenden Ratten. Darüber hinaus konnten wir eine Stimulus-basierte Aktivierung des auditorischen Kortex nachweisen, allerdings nur im Vergleich zum Status nach Cochlea-Ablation als Referenz. Dies weist hin auf die Notwendigkeit einer rigorosen Suppression der Hintergrundgeräusche für die Referenzkondition. Die Funktionsfähigkeit des Kortex konnte jedoch auch durch eine Aktivitätsreduktion beim Vergleich des weißen Rauschens gegenüber dem Laborhintergrund nachgewiesen werden. Zu guter Letzt beobachteten wir nach Cochlea-Ablation eine Aktivierung des olfaktorischen Nucleus, welche eine kompensatorisch cross-modale Aktivierung nahelegt.

Beide Studien belegen die Nützlichkeit von PET in der Hörforschung als eine Methode für objektive Messungen. Unterschiedliche Aktivierungsmuster zwischen Menschen (kortikal) und Ratten (sub-kortikal) sind höchstwahrscheinlich auf die Unterschätzung der Aktivität in kleineren Strukturen durch ältere PET Systeme und biologische Unterschiede zwischen den Spezies zurückzuführen. Zusätzlich zeigten Pilotversuche des inhibitorischen GABAergen Systems mit ^{18}F-Flumazenil in Ratten mit schwerwiegendem Hörverlust eine verminderte $GABA_A$-Rezeptorbindung im auditorischen Kortex, zusammen mit einem Abfall der neuronalen Aktivität. Die Ergebnisse weisen auf einen komplementären Wert von funktioneller und molekularer Bildgebung zur Verbesserung des Verständnisses der Pathophysiologie und der Therapieergebnisse beim Hörverlust hin.

Table of Contents

Summary ..... **III**

Zusammenfassung ..... **V**

Table of Contents ..... **VII**

1 Introduction **1**

1.1 The auditory system 2
1.1.1 The human auditory system 2
1.1.1.1 The ear 2
1.1.1.2 The central auditory pathway and auditory cortex 3
1.1.1.3 Physiological transmission of neuronal signals in the auditory pathway 5
1.1.1.4 Hearing impairment 6
1.1.1.5 Specific diagnostic tools for hearing loss 7
1.1.2 The auditory system in animals 7
1.1.2.1 Comparison of the auditory system between animals and humans 7
1.1.2.2 Animal models of hearing disorders 8
1.1.2.3 Special diagnostic tools 9
1.2 Imaging 9
1.2.1 Tracer and radiopharmaceuticals 10
1.2.2 Tomography 12
1.2.2.1 PET in patient diagnostics 13
1.2.2.2 PET in small animal imaging 14
1.2.3 Imaging properties 15
1.2.3.1 Spatial resolution 15
1.2.3.2 Sensitivity 16
1.2.3.3 Contrast 17
1.2.4 Data analysis 18
1.2.4.1 Spatial normalization 18
1.2.4.2 Volume- and voxel-wise analyses 19
1.3 Aims of studies 20

2 Study I – PET imaging of auditory system activation during general anesthesia 23

2.1 Abstract 24
2.2 Keywords 24
2.3 Background 25
2.4 Methods 27
2.4.1 Patients 27
2.4.2 Anesthesia 27
2.4.3 Auditory stimuli 28
2.4.4 Radiopharmaceutical 28

2.4.5 Data acquisition and reconstruction 28
2.4.6 Individual PET data analysis 29
2.4.7 Statistical analysis across subjects 29
2.5 Results 30
2.5.1 Impact of scan duration and anesthesia on peak-height in auditory cortex activations 30
2.5.2 Relative sizes of activations in AR and eAR with different parameters 30
2.5.3 Frequency of activations in AR and eAR depending on parameters and use of anesthesia 33
2.6 Discussion 33
2.7 Conclusion 39
2.8 Acknowledgements 39
2.9 References 39
3 Study II - Visualization of the auditory pathway in rats with ^{18}F-FDG PET 45
3.1 Abstract 46
3.2 Keywords 46
3.3 Introduction 47
3.4 Methods 48
3.4.1 Animals 48
3.4.2 Experimental procedure 48
3.4.3 Conditions 49
3.4.3.1 Stimulation environment 49
3.4.3.2 Training 50
3.4.3.3 Auditory Conditions 51
3.4.4 Cochlea ablation 51
3.4.5 PET/CT imaging 52
3.4.6 Data analysis 52
3.5 Results 53
3.5.1 Individual analysis 53
3.5.2 VOI analyses 53
3.5.3 SPM results 54
3.6 Discussion 59
3.6.1 Activation of the auditory system in normal hearing rats and differences to humans 59
3.6.2 Findings after cochlea ablation in rats 61
3.6.3 Limitations 62
3.7 Conclusions 62
3.8 Acknowledgment 63
3.9 References 63
4 General discussion 67
4.1 Summary 67
4.2 Translatability 68
4.2.1 Characterization of the auditory cortex 68

4.2.2 Studying sub-cortical activations 69
4.2.3 Selection of analysis parameter 70
4.3 Outlook and potentials 71
4.3.1 Radiopharmaceuticals for molecular imaging of the auditory system 71
4.3.2 Potentials in technological development 72
5 Conclusions 75
6 References 77
List of Figures XI
List of Tables XIII
List of Abbreviations XIV
Contribution XVIII
Declaration XXI
Acknowledgments XXIII
Curriculum Vitae XXV

1 Introduction

In a pure physical perspective, the perception of vibration or pressure changes of air or another medium is defined as hearing and is the basis for human communication. Expanding to the relevance of hearing for the individual, it is a fundamental key for communication and cognition as prerequisites for successful integration in the society. However, more than 16% of Germany's population are estimated to be affected by various degrees of hearing impairment [von Gablenz2017]. 1 in every 1000 children in Germany is born with hearing impairment. Furthermore, 50% of the population above the age of 65 have developed hearing impairment and this fraction will rise with the ongoing demographic transition. Worldwide, around 466 million people (6.1 % of the world's population) are affected of whom 34 million are children. The WHO estimates an increase up to 900 million people affected by 2050 [WHO2018]. The necessity of research on diagnostic and therapeutic procedures to tackle hearing loss is furthermore underlined in an aging society due to the discovered link between deafness and dementia [Lin2017].

In the last decades, the supply of hearing aids and the spectrum of devices have increased to incorporate even different types of hearing aids implanted into the brain [Lenarz2006]. This enables a larger range of affected people to regain this lost sense in limits. In this context, cochlear implantation for treatment of inner ear deafness with more than 500 000 clinical applications is already one of the most successful achievements in medical technology [Kral2010]. This is important in all ages as auditory deficiencies can affect a person's social life. The hearing is in children particularly import for the development of social skills [Mason2007]. Nevertheless, unexpectedly limited speech comprehension in about 30 % even of early implanted children without explanation in most cases prompts the necessity to further research [Akeroyd2008, Lazard2012]. This research includes the development of next generation, novel cochlear implants in a translational manner, including evaluation in animals [Le Prell2016]. Additionally, the central nervous system's auditory processing is a suspected reason for this large diversity of hearing performances after implantation [Wilson2008]. These factors imply a need for diagnostic methods applicable in translational neurological research – which is the case for emission tomography [Berding2017].

The present work contributes to this goal with two studies. One is elaborating auditory system activation studies using positron emission tomography (PET) with ^{15}O-water in deaf children during anesthesia. Such a procedure is needed for objective assessment of central auditory processing in this patient group which is not able to cooperate like adults. It is of special interest, as children preferentially receive auditory implants early in order to utilize sensitive periods of neuronal plasticity in the auditory system [Vincenti2014]. In the second study, activation studies of the auditory system using ^{18}F-

Fluorodeoxyglucose (FDG), which are established in humans, were re-translated into the rat animal model. Rat models for the evaluation of novel cochlear implants are feasible after the past development of surgical techniques and PET could serve as a tool to monitor the outcome *in vivo* [Lu2005].

Before the presentation of these two studies, the introduction gives a short background with respect to the components of the auditory system in humans, reasons of its functional impairment and differences between the auditory system in humans and rat (chapter 1.1). Subsequently, the general foundations of clinical and preclinical PET imaging and data analysis are described (chapter 1.2). After the complete presentation of both studies (chapter 2 and 3), their results are integrated into the bigger picture of the current state of the art of imaging equipment and radiopharmaceuticals to highlight the potential of further imaging studies in hearing research. Specifically improved scanner sensitivity and spatial resolution and the application of molecular markers of neurotransmission in the auditory system are to be considered in this context.

1.1 The auditory system

The process of hearing as in most senses in living organism is separated into an organ transforming the physical input e.g. pressure changes in the air into neuronal signals and further processing of the signals in the central nervous system. In the following section, a short overview of this process and its disturbances will be given.

1.1.1 The human auditory system

1.1.1.1 The ear

The external, middle and inner ear including the cochlea take on the task of transforming sound into a neuronal signal. The present work is focusing on further processing in the central nervous system and hence the signal forming organs are just described briefly. Detailed information can be found in textbooks such as [Møller2006, Pickles2013].

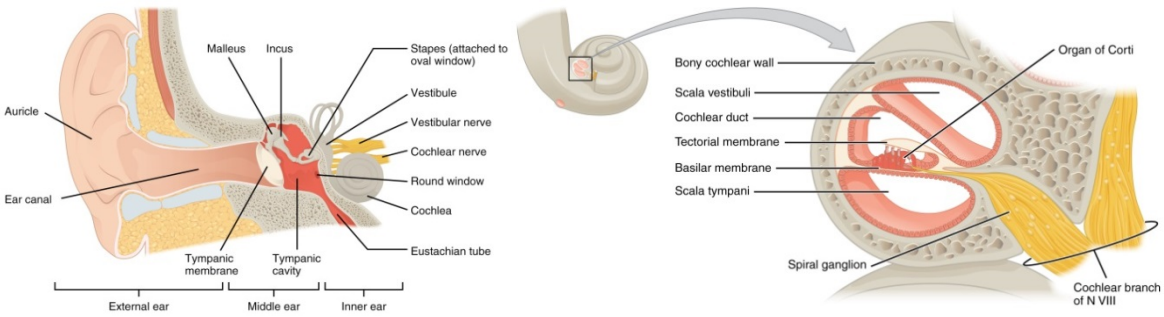


Figure 1 Anatomy of a) the human ear [OpenStax-College2016b] and the cochlea [OpenStax-College2016a]. Used on basis of Creative-Commons-License

The following description is based on Figure 1 taken from [OpenStax-College2016b, a]. Besides redirecting the sound to the tympanic membrane, the auricle and ear canal change properties of the signal due to their shapes contributing to directional hearing. Via the auditory ossicles malleus, incus, and stapes, the middle ear couples the tympanic membrane to the oval window of the cochlea and enables a transfer of energy from air to liquid with high efficiency due to the involved two smaller muscles. The involvement of these muscles might also provide additional functions such as sound attenuation as mentioned in [Pickles2013]. The snail-shaped cochlear contains three fluid filled compartments, especially the scala tympani and scala media, which are separated by the basilar membrane. The organ of Corti containing the sensory cells (hair cells) is located along this membrane. In the cochlea, the vibrations are transferred in a frequency-dependent manner from sensory cells to auditory nerve fibers. This is achieved mostly by different physical properties of the basilar membrane, which enable standing waves at frequency-depending locations with increasing distances to the oval window for lower frequencies.

1.1.1.2 The central auditory pathway and auditory cortex

Signal transmission from the cochlea to the auditory cortex (AC) involves particularly five main structures of the so-called central auditory pathway [Kretschmann1992]. They are in caudocranial order (Figure 2):

- Nucleus cochlearis (NC),
- Superior olivary complex (OC)
- Lateral lemniscus (LL)
- Inferior colliculus (IC)
- Medial geniculate body (MGB)

The NC consists of a ventral and a dorsal part. The arrangement of neurons and corresponding nerve fibers is related to the originating localization in the cochlea and represents a tonotopic map of frequency dependent neurons in both parts of the NC. The ventral and dorsal parts also differ in cytoarchitecture. The predominant cells in the dorsal part are fusiform cells while the ventral part mainly consists of stellated and bushy cells [Pickles2013].

The OC is dividable in three main nuclei with the lateral superior olive also organized in a tonotopic fashion. As the NC, the OC is located in the brainstem [Møller2006].

The LL is mostly a nerve fiber tract but also forms nuclei interrupting some neurons from the contralateral NC. It is about 25 mm long and connects to the auditory brainstem and midbrain regions [Kretschmann1992].

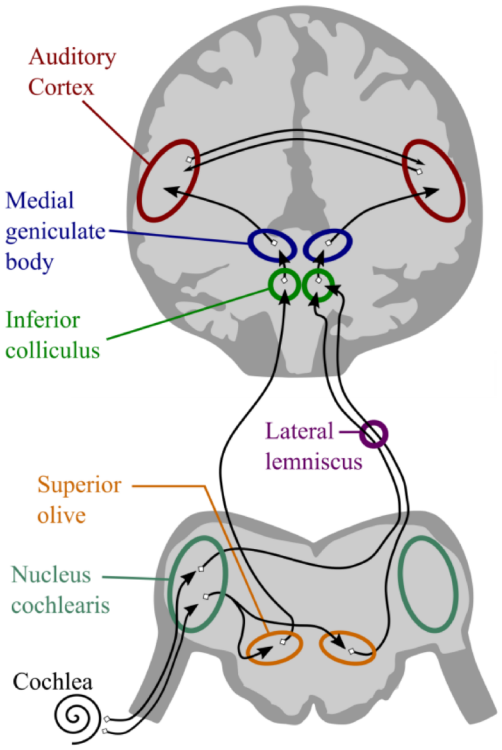


Figure 2 Schematic simplified view of the afferent auditory pathway

The main relay of the auditory pathway in the midbrain is the IC precisely located in the tectum. The IC consists of three divisions with different cytoarchitecture and correspondingly different functions. The central nucleus consists of mostly disc-shaped neurons, which arborize along planes creating laminations. This results in a tonotopic structure as well. Laminations are crossed over by stellated cells so that the isofrequency planes extend beyond laminations. Contra- and ipsilateral IC are connected to the thalamus on the respective side and by a commissure to each other. The IC projects to the thalamus among other paths via the brachium of the IC. In humans, the brachium is estimated to have 10-times the number of fibers compared to the auditory nerve, which by the way is seen as strong evidence for processing occurring before the auditory cortex [Møller2006].

As part of the thalamus, the MBG is integrated into the auditory pathway. The ventral nucleus of MGB has a laminar structure reflecting tonotopy. This tonotopy differs from that in the IC as layers cover larger frequency ranges [Cetas2001]. This results in jumps of frequency with best responses for multiple layers. Beside the auditory input, the MGB also received somatosensory and visual information. It has a strong reciprocal connection to the primary auditory cortex. Hence both areas are sometimes assumed to form one joint functional system and are studied together e.g. in [Lee2013].

The auditory cortex consists of distinct parts with respect to cyto- and receptor architecture, namely the primary auditory cortex and vicinal non-primary auditory areas [Clarke2012]. The primary auditory cortex is subdivided into Brodmann area 41 and 42,

shown in Figure 3 and receives mainly input from the MGB and responds primarily to acoustic stimuli [Clarke2012]. These areas project to associated non-primary auditory cortices. Non-primary auditory areas are involved in further processing such as sound localization and speech understanding. They are located in Brodmann areas 21 and 22. Multimodal integration of information takes place in these areas as they receive input from other afferent sensory pathways [Kretschmann1992]. Nevertheless, the knowledge of the exact anatomic classification of auditory cortices is still incomplete and varies between individuals [Møller2006]. Beyond these, temporal regions, e.g. regions in the inferior frontal cortex and the parietal cortex, are involved in brain networks of speech processing [Friederici2012].

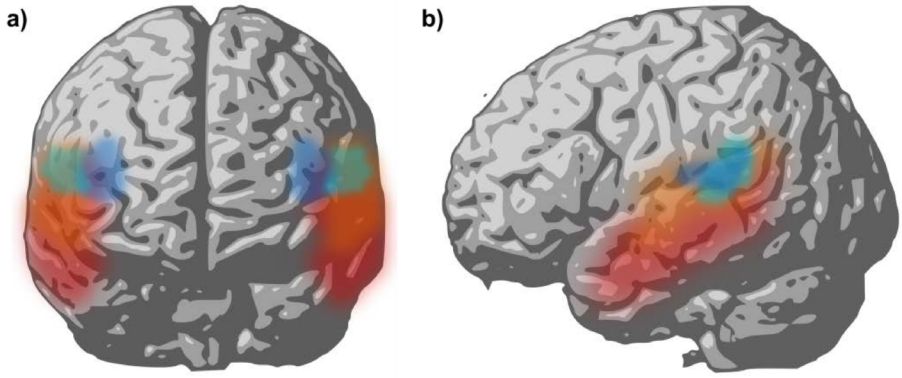


Figure 3 Schematic locations of auditory relevant Brodmann areas in humans. Primary auditory cortex (Brodmann area 41 in green and 42 in blue) and associated areas (Brodmann area 21 in red and 22 in orange) shown as projections on the a) front and b) side of a brain.

1.1.1.3 Physiological transmission of neuronal signals in the auditory pathway

In the cochlea, the first neurons of the auditory pathway are based in the spiral ganglions as seen in Figure 1b. They start the afferent auditory pathway as schematically depicted in Figure 2. The cochlear branch of the eighth cranial nerve projects to the dorsal and ventral part of the ipsilateral NC.

In the NC, the neuronal signals are analyzed and then further transmitted along three different pathways. One pathway originating in the dorsal NC changes sides and projects via the lateral lemniscus to the contralateral IC. The signals are then transmitted to the MGB and finally to AC. The second pathway projects from the ventral NC to the contralateral superior olivary nucleus. From there, signals are projected via the lateral lemniscus and continue similar to the first pathway. The third pathway projects from the ventral NC to the ipsilateral OC and continues ipsilateral via IC and MGB to the AC. The ipsilateral and contralateral sides of the AC are connected by nerve fibers through the corpus callosum [Kretschmann1992].

Several of the previously mentioned structures are not limited to relaying information from ear to cortex on the afferent pathway. They also project in reverse direction along efferent nerve fibers to generated reflexes, e.g. the middle ear muscle reflex originating in the brainstem [Pickles2013]. Most areas can be differentiated in substructures according to function and specific projection target.

1.1.1.4 Hearing impairment

A large variety of disorders can interfere with hearing. Nevertheless, in principle two types of hearing loss can be differentiated: First, conductive hearing loss affecting conduction of sounds to the sensory cells, e.g. by obstruction of the ear canal or disorders of the middle ear. Secondly, sensorineural hearing loss resulting from e.g. damage of the hair cells in the cochlea or degeneration of the auditory nerve [Møller2006]. Based on the anatomy and physiology, the hearing impairment can also be described by the place of origin. A frequent type of hearing impairment is associated with old age. Although the source or main reasons for this type of hearing impairment are not yet fully understood, it is probably due to a variety of 'naturally' occurring effects related to age.

Most types of hearing impairment are first realized by the patient and secondly confirmed by a measurable impairment of specific properties of hearing, for example, the hearing threshold. The identification of the underlying cause and corresponding location is especially important for the selection of treatment. Impairments originating ahead of the auditory pathway can be corrected or compensated in consideration of their severity e.g. by amplifying hearing devices as well as cochlear implants (CI) [Wilson2008]. CIs are placed in the scala tympani of the cochlea and stimulate the ending of the auditory nerve in the organ of Corti directly by electric pulses.

Hearing impairments originating further centrally in the auditory pathway pose a challenge in two ways – the diagnosis and the treatment. Most structures are difficult to access and cannot be tested exclusively. Nevertheless, with respect to treatment options advances in medical technology enable the electric stimulation at the two tonotopically structured sides, the IC in the midbrain (auditory midbrain implant – AMI) [Lenarz2006] and the NC in the brainstem (auditory brainstem implant - ABI) [Schwartz2008]. However, these types of auditory implants are normally not able to restore hearing to an extent similar to CIs and support lip reading and environmental awareness [Lenarz2002].

To achieve the best quality of hearing, it is of great importance to identify the source(s) of the hearing impairment in order to maximize the benefit by the choice of appropriate auditory implants. Especially in children, this is important as studies link better hearing performance with earlier time points of implantation in children at ages 1 to 2 years [Lee2001, Sharma2004, Vincenti2014].

1.1.1.5 Specific diagnostic tools for hearing loss

To determine the type of hearing impairment, specific diagnostic tools can be applied. For post-lingual hearing impairment e.g. due to age, most tests are designed to function in cooperation with the patient. They rely on active feedback or a lack thereof in order to identify deviations or quantify changes. For example, auditory parameters such as hearing threshold, loudness perception or sensitivity and frequency resolution can be quantified [Pickles2013].

Deafness, profound hearing loss or impairment due to disorders of the external and middle ear might lack feedback from the subject and hence require different procedures. While being more complex, such tests result in an objective classification independent of the subject's ability to cooperate. Some of these methods can measure responses to acoustic stimulation not consciously perceived by the subject, e.g. electrical signals measured from the cochlea as a result of an acoustic stimulation called cochlear microphonic. Other methods bypass possibly defect parts of the auditory systems by stimulating at alternative sites. One of such methods is the direct stimulation of the auditory nerve via electrical pulses applied via a needle electrode placed on the promontory. This method bypasses the cochlea. It is especially useful when predicting success rates for hearing performance after CI implantation by identification of post-cochlea causes of hearing impairment [Mortensen2005] and for studies in small children [Nikolopoulos1999]. However, up to now, the established objective diagnostic tools have limitations to identify precisely the level of disturbance for transmission along the auditory pathway.

1.1.2 The auditory system in animals

The establishment of objective diagnostic tools and novel therapeutic procedures applicable in humans require substantial investigation. Hence, the first steps of development usually incorporate *in vitro* studies and animal experiments [Le Prell2016]. A large part of our knowledge about the auditory pathway is based on preclinical studies. This suggests the usefulness of animal experiments for further development and refinement. Nevertheless, the comparability and translatability of knowledge between species must be taken into account.

1.1.2.1 Comparison of the auditory system between animals and humans

Animal and humans are most obviously different in absolute sizes of the involved structures from the external ear to the auditory pathway. Compared to rats and other animals, humans have longer nerve fibers inducing different limits on hearing e.g. with respect to the resolution of spatial accuracy. Other differences can be found in the anatomy such as of the cochlea [Nadol1988] which may result in different physiological responses.

The cortical areas are less structured in most laboratory animals in comparison to humans. Association of functional areas with clear lobes or gyri is limited and more geometrical references to stereotactic atlases and landmarks are consulted for identification. Differences can also be observed on the level of substructures and the expression of certain proteins [Baizer2018].

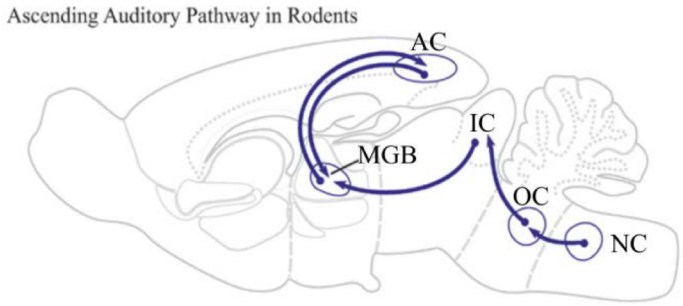


Figure 4 Schematic view of the structure of the auditory pathway in rats [Mueller2012], Use based on Creative-Commons-License

Nevertheless, animal models play a major role in hearing research which is reflected by a large number of publications i.e. more than 1000 annually publication related to animals and hearing are listed in PubMed [PubMed] since 2010. One reason is the general similarity of the translation of a mechanical to a nerval signal in the cochlea and the structure of the auditory pathway. Comparing the human afferent pathway in Figure 2 to the rat's afferent pathway in Figure 4, we see clear similarities. Other properties share similarities with humans as well e.g. the auditory evoked electric potentials from the nerve system. Among others, the absolute latency and the shape of the cortical evoked potential are similar in rats compared to humans [Shaw1988]. The same study showed analogous waveforms of auditory evoked potentials in the brainstem. Also in the MGB, single cell recordings exhibit similarities in humans and rats [Antunes2010]. Furthermore, functional brain imaging confirms a generally good translatability between rat and human [Jonckers2015]. A general comparability and translatability especially of rat models in hearing research can be endorsed.

1.1.2.2 Animal models of hearing disorders

The study of hearing impairment and corresponding treatment in animals is useful, as specific impairments can be studied in a controlled environment. This enables also to study the effects of specific auditory environments on the auditory system e.g. with respect to expression of inhibitory neurotransmission systems [Xu2010]. The development of specific auditory phenomena such as tinnitus can be compared between different causal (environmental) factors e.g. noise-induced tinnitus [Singer2013] compared to ototoxic-induced tinnitus [Selimoglu2007], which might contribute to improve understanding and treatment of that phenomenon.

Similar, specific changes along the auditory pathway can also be characterized in animal models with respect to hearing impairment. For example, in noise-induced hearing loss, as a common occurrence in humans, effects of long-term exposure might differ to that of short-term exposure. Rat models are used in the characterization of such noise-induced effects in the auditory system. Reduction of hair cells in the cochlear and inhibitory neurotransmission in the auditory cortex [Kang2013] as well as degenerative changes of the auditory nerve [Kujawa2009] have been demonstrated. Moreover, comparing profound hearing loss due to noise trauma with responses after an invasive cochlea ablation in Mongolian gerbils, as described in [Deutscher2006], revealed further insides in the cortical and subcortical processing of hearing.

Integrating models of treatment and models of hearing impairment will enable the study of prognostic factors. The cochlear implant is of particular interest in this context due to its widespread application in humans. Animals models for this procedure exist already in rats [Lu2005] and are applied in order to understand reversible and permanent effects e.g. of chemically induced hair cell loss, particularly with respect to inhibitory neurotransmission in the inferior colliculus [Argence2008].

1.1.2.3 Special diagnostic tools

An objective measure of the hearing capabilities of animals is necessary to validate and categorize the degree of hearing impairment in animal models. A method for this purpose, which is available in humans and animals, is the measurement of auditory brainstem responses (ABR). The applicability of this method is supported by the similarities of the brainstem auditory evoked potentials in rats and humans [Shaw1988]. ABR is a technique using multiple electrodes and a large number of repetitions to reduce other signals generated by the brain. It is widely used to confirm and categorize the implementation of models of hearing loss such as noise trauma [Kujawa2009, Kang2013]. As an objective measurement, it allows assessing the effects of factors not specifically related to the auditory system on that system. For example, ABR measurements have been used to quantify the impact of prenatal alcohol exposure on the development of the auditory system [Church2012].

Although the function of the auditory system and measurable shifts in hearing thresholds can be determined by ABR, the precise localization of the underlying alteration which causes the threshold shift cannot be unambiguously identified. Therefore, there is a need for other diagnostic tools – like imaging – to fill in this gap.

1.2 Imaging

Imaging gives us the opportunity to view different features of objects in multi-dimensional representations. The terminus itself can describe a large variety of *in vivo*,

ex vivo or *in vitro* methods of imaging superficial and complex structures. We applied imaging based on radioactive-labeled substances. Based on the ability of photons created by gamma or positron decay to cross tissue with limited interaction [Vogt2011], the source of this radiation within the body can be detected by measuring radiation emerging from the body. This allows to 'look' deeper into the brain and identify e.g. areas associated with the process of hearing and to assess their functionality and molecular characteristics.

1.2.1 Tracer and radiopharmaceuticals

To observe central neuronal processing, we employed radiopharmaceuticals as tracers. Tracers are defined as substances that do not influence the observed natural processes in a measurable way. Most tracer substances are not per se without influence. However, they are used in small concentrations and quantities in the order of pmol and ng, which results in negligible effects on the observed natural process and absence of side effects for the studied individual [Reivich1979]. These substances need to have easily identifiable characteristics e.g. fluorescence or emission of radiation which can be measured in such small amounts. The first scientific implementation of this principle in 1923 by Hevesy [Hevesy1923] used radionuclides and was awarded the Nobel Prize in chemistry in 1943. The measurement using radionuclides was later also employed to determine the flow of materials in living plants and other biological structures [Ljunggren1968, Orr1968]. The concept of linking stimulated brain activity with increased blood flow was proposed more than a century ago by [Roy1890] – using an apparatus with flexible membrane brought through a trepanation in the vertex directly to the brain surface of dogs. Combination of both principles (tracers and stimulated brain activity) is possible using radiolabeled tracers (radiopharmaceuticals) that have been developed to indicate the blood flow and correspondingly stimulated neural activity [Chu1980, Ell1987].

Radiopharmaceuticals are composed of two components. A pharmaceutical that fulfills the tracer's distinct biological properties such as the ability to bind to receptors or be metabolized by cells and a radionuclide enabling imaging which is bound to the pharmaceutical [Theobald2010]. Additionally, some radiopharmaceuticals contain components which do not interfere with the biological properties. Such components just act as bridges keeping biologically active substance and radionuclide together [Meyer2016]. In other radiopharmaceuticals, the imaging and functional component cannot be separated as the radionuclide can be part of the binding site or structure. This is the case in radiopharmaceuticals with small or short molecular structure.

A widely used radiopharmaceutical with such features is ^{15}O-water. It is given as a bolus intravenously, dilutes in the blood and diffuses freely from blood into cells. A measured increase in uptake of labeled water during stimulation against a resting condition

indicates a local increase in cerebral blood flow (CBF) which is associated with increased regional neuronal activity [Frackowiak1980]. This tracer can diffuse back to the blood space, which results in dynamic changes of tracer concentration. Thereby, ^{15}O-water is part of the group of tracers with dynamic or reversible uptake. Therefore, in theory, a comparison of activity in the blood and tissue is required for quantitative analyses of the CBF [Kanno1987]. Nevertheless, it has been shown, that integrative measurements, i.e. simply summing up the activity accumulated in a particular time span, yield results consistent with dynamic measurements for ^{15}O-water, at least with respect to the relative distribution of blood flow [Bol1990]. This tracer has been widely used in neuroscience in the nineties (before the advent of fMRI) [Kanno1987, Kanno1991, Volkow1991, Frackowiak1994] and is still used in auditory research, particularly related to auditory implants [Herzog1991, Naito1995, Okazawa1996, Jeffries2003, Schulz2005]. It is used based on the short physical half-life of ^{15}O with 122 s, which enables imaging of multiple conditions and repetitions of conditions in one imaging session. Due to the short physical half-life, tracer production using an on-site cyclotron and radiochemistry is mandatory [Mullani2008]. Furthermore, the optimal timing between auditory stimulation, tracer application, and PET measurement is crucial. These factors limit the availability and utilization of the method in auditory research and diagnosis.

A common radionuclide addressing the above-mentioned limitations is ^{18}F (fluoride). It has a half-life of 110 min and is thereby available from off-site sources with reasonable effort. ^{18}F labeled deoxyglucose, i.e. ^{18}F-2-fluoro-2-deoxy-D-glucose (^{18}F-FDG), is widely used [McIntosh1993, Krause2003, Ahn2004, Willis2008, Okuda2013] as tracers of energy metabolism. It is transported into cells more precisely brain astrocytes mostly via glucose transporters GLUT1 [Theobald2010] and is phosphorylated there to deoxyglucose-6-phosphate. This resulting substance cannot be further metabolized or transported [Alavi1986] due to the fluorine being in the C-2 position as shown in Figure 5a). Thereby this product of ^{18}F-FDG is irreversibly trapped in the cell with respect to the timeframe of measurement. As glucose consumption is an indicator of cell activity, increased uptake of ^{18}F-FDG identifies more active tissues and is commonly used in neuropsychiatric diseases [Elsinga2014] and oncology [Chu1980, Boellaard2015].

While most radiation escapes the body, a certain part interacts with tissue and can lead to harmful effect. This harmfulness, especially with respect to stochastically effects, is described by the effective dose [Vogt2011] given in the unit Sievert (Sv). It contains factors which take the radiation type, the energy, and the sensitivity of organs as well as the significance of corresponding damage into account. The International Commission on Radiological Protection (ICRP) states an additional cancer risk of 0.005 %/mSv for persons who are not professionally exposed to radiation [ICRP1991].

1.2.2 Tomography

For the measurement of radiation from radionuclides, a large variety of devices can be applied ranging from simple counter tubes measuring radiation with very limited spatial differentiation to standard scintillation based planar imaging of activity distributions and to dedicated semiconductor based tomography [Lange2002].

The general concept of tomography is independent of the detection modality. Tomography is a reconstruction of images or structures in a higher dimensional order using mathematical procedures based on images or projections in a low dimensional order [Carter1963]. In medical tomography 3- or 2-dimensional images are created by measurement and analyses of respective 2- or 1-dimensional images, possibly acquired sequentially over time.

The use of X-ray tomography is most widespread. It has the benefit of employing relatively low energy photons but requires an external source to generate the radiation. The application of tomographic imaging of radiopharmaceuticals enables *in vivo* measurements of radiation emitted from the subject and is therefore called emission tomography. It is used in particular to determine physiologic parameters related to energy-metabolism or blood flow as indicators of cerebral activity [Raichle1981, Lammertsma1983]. Two general systems are used in emission tomography [Lange2002]. They differ with respect to the types of the used emitted radiation.

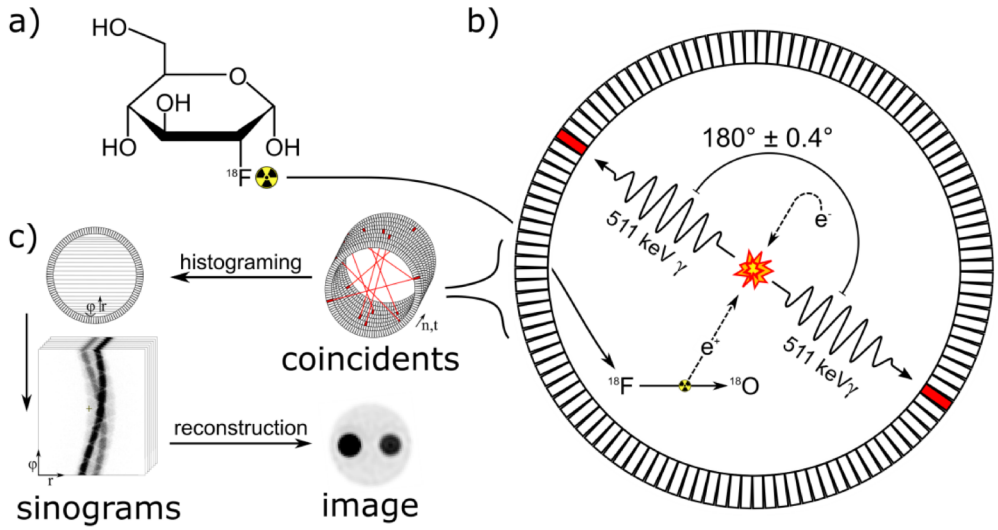


Figure 5 Structure of the radiopharmaceutical ^{18}F-FDG and imaging principle of PET. Of the a) chemical structure of ^{18}F-FDG, b) a positron (e^+) emitted by the decay of ^{18}F is detected by two coinciding photons with back-to-back geometry which result from the positron's annihilation with a surrounding electron. c) Multiple coincidences are histogrammed and reconstructed into the higher dimensional images.

Radioisotopes emitting single γ-radiation are measured in single-photon emission computed tomography (SPECT). This is done with the help of collimators which limit the detector element to be sensitive just in one specific spatial direction. SPECT needs a large number of detected photons to statistically reduce electrical and other noises. It has the benefit of enabling imaging of multiple tracers with radioisotopes emitting photons with distinguishable energies which improves accuracy in diagnostics e.g. in heart diseases [Caobelli2017].

The second method uses positron-emitting radionuclides. As shown in Figure 5b), not the primary emitted positrons are measured but two photons resulting from an annihilation of positrons with electrons in the vicinity [Lange2002]. Both photons are emitted with 180°±0.4° angular in a back-to-back geometry and with energies of each 511 keV. The specific properties are based on physical attributes of the elementary particles involved in the annihilation.

The photons can be measured in opposing detectors or a complete ring structure [Chu1980]. Due to the specificity in energy and spatial orientation, PET does not require collimators but uses coincidence of photon registration to reduce electrical and other noises. One disadvantage of PET is the physical limitation in the spatial resolution which will be further explained in sections 1.2.3.1. Nevertheless, in most studies, PET is appreciated as a superior diagnostic tool for neuropsychiatric disease compared to SPECT although evidence from comparative studies is limited [Davison2014].

1.2.2.1 PET in patient diagnostics

As the resolution of early PET scanners was limited, PET was first developed and tested with humans [Ter-Pogossian1992]. Due to this optimization with human subjects and patients, PET established itself as a valuable tool for various approaches in science and clinical medicine. It is applied in clinical routine for diagnostics [Elsinga2014, Schmuck2017] and furthermore widely used in neuroscience e.g. [Gunther1992, Logan1996, Schiffer2006, Qin2012]. Also in auditory sciences, PET has promising potential as an objective tool for diagnostics and research [Johnsrude2002]. It has been applied in several studies investigating the processing of auditory stimuli and speech, e.g. [Mazziotta1984, Nenov1991, Johnsrude2002, Willis2008] and demonstrated its unique feature in contrast to fMRI in enabling imaging of patients with auditory implants [Miyamoto2001, Berding2015]. As PET scanners are causing considerable less noise during operation, they also offer the possibility of a large variability in study designs. While advantageous, PET also causes some challenges. PET scans usually take more time than other imaging methods. As the movement of the subjects reduces the image quality, the necessity of anesthesia for patients not able to cooperate and its impact on the observed system needs to be addressed [Heinke2002, Absalom2014]. This and other factors must be considered in according study designs and for later implemen-

tation into clinical workflows [Fragoso Costa2016]. Such factors consist amongst others in the limited time resolutions of PET, which cannot compete with MRI, the radiation exposure for the patient, tracer compatibility with other pharmaceuticals et cetera. Nevertheless, the ability of imaging of neurotransmitter systems such as the inhibitory system utilizing gamma-aminobutyric acid (GABA) [Qin2012], is a further motivation for the inclusion of PET as a key feature for future studies particularly in auditory sciences according to [Johnsrude2002]. The large spectrum of available tracers [Fragoso Costa2016] and the potential for development of further specific targeted tracers are important factors in this regard.

1.2.2.2 PET in small animal imaging

While used first only with tracers which had been established in humans, small animal PET has advanced into a wide array of applications [Yao2012]. After its first use about 20 years ago, these dedicated systems have developed themselves into valuable tools for quantitative imaging in small animals [Constantinescu2009, Hsu2009].

The introduction of PET occurred reversed to the typical way for new methods because it has been first developed with humans and later been transferred into animals [Ter-Pogossian1992]. This resulted in the establishment of some models for PET in humans without a corresponding model in animals. While small animal PET can build on the experiences of human PET, it also faces some challenges. As animals are generally unable to cooperate by not moving especially for long scan durations (> 30min), scanning has to be performed in anesthesia, which in addition minimize stress and other long-time effects [Yao2012]. The impact of anesthesia on the interactions of tracer and target system has to be considered [Rajan2013]. Additionally, other options for imaging without the need for anesthesia have been studied [Vaska2004]. Other factors arise from the smaller bodies and different physiology of the animals. Smaller bodies mean that the volume in which the radiopharmaceutical is injected is limited too. To guarantee animal well-being, national and international recommendations are in effect. The compliance with them has to be reported according to codes of good practice [Kilkenny2010]. Physiological differences between different species including humans might result in variations in properties of the tracer such as stability [Mandema1991] and specific uptake [Froklage2012]. This can considerably influence the comparability between results in animals and humans. Hence, the properties of radiopharmaceutical and their applicability must be tested across species. Seeing that with animal size also the brain volume decreases [van Horik2011], there are further limits of the presentability of structures or substructures within a chosen animal based on the given spatial resolution of the PET system [Constantinescu2009].

1.2.3 Imaging properties

While PET systems got more and more distributed, significant technological advancements were achieved with multiple generations of scanners [Ter-Pogossian1992, Cherry2018]. As the development in technology progressed, different scan parameters were tested. This affected amongst others scan duration [Kanno1991, Volkow1991], waiting times for radioactive decay between scans [Chmielowska1998, Chmielowska1999], as well as study design and analysis procedures [Logan1996, Moreno-Cantu2000, Logan2001]. Nevertheless, the ability to compare results in science and the legal obligations to assure quality in medical diagnostics [DIN2016] require sets of parameters as an indicator for the status of the scanner.

A crucial issue for any imaging method is the image quality. As the visual determination of the quality of an image is to some extent subjective, mostly technical properties are used as basic indicators for image quality [Lange2002]. The most commonly used factors to characterize a PET scanner's performance are spatial resolution, sensitivity, contrast, homogeneity, linearity between measured and present activity and dead time, i.e. the time a detector cannot measure an event as it is still processing the readout of a previously measured event. Another factor that is not inherently controlled by the system is the scatter fraction – the fraction of photon 'pairs' that reaches the detectors within the coincidence time interval but just are random based on scattered photons and without according positron decay in the subject. Of all these factors, the spatial resolutions and sensitivity are primarily important and therefore explained a bit more in the following text [Constantinescu2009, Jakoby2011, Yao2012, Lee2014, Rausch2015].

1.2.3.1 Spatial resolution

Spatial resolution is one of the most commonly used criterions for scanner performance as it is determinative for the minimal extent of a structure necessary to detect the magnitude of radioactivity uptake correctly i.e. without loss. Studies showed a systematic underestimation of uptake depending on too small sizes of the measured structures. Consequently, limitations on detectability are given [Knoop2002]. Furthermore, the spatial resolution indicated the ability to distinguish two close structures as separate. Natural effects, which usually follow a Gaussian distribution, can be differentiated if they do not overlap too much. Interestingly, this is the case if they are further afar than their corresponding full widths at half maximum (FWHM) [NRC1989, Dávila2017]. Hence, the spatial resolution is often measured as FWHM of a point-source of radiation in a scanner [Constantinescu2009, Rausch2015].

For small animals [Constantinescu2009] and in children, this is of particular interest. Figure 6 compares an anatomical rat brain atlas to an image of a NEMA4U phantom taken with a µPET. By comparing the second smallest capillary of the phantom with

faintly higher uptake than the background to the sometimes even much smaller structures of the rat brain, it is evident that certain structures of the rat's brain cannot be qualitatively or even quantitatively measured.

Two sources need to be considered with respect to the spatial resolution of the PET method. The first is technical limitations for resolution by detector specifics such as size and shape as well as their spatial arrangement. The second source is a physical limitation of resolution based on the average traveling distance of an emitted positron and on the absence of collinear emission of photons [Yao2012]. With higher energy, the positrons travel on average farther from their point of origin, which would mean that even with idealized detectors and reconstruction, a point source would be visible as spherical volume. This is a theoretical resolution limit even though detector technology is improving with the implementation of time-of-flight and iterative reconstructions in consideration of point-spread functions [Jakoby2011, Rausch2015].

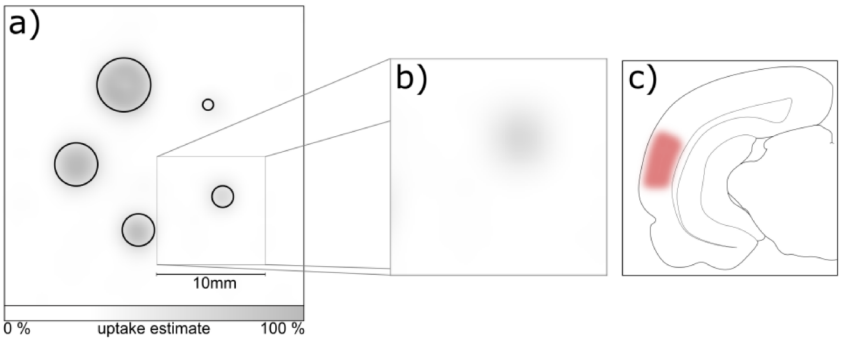


Figure 6 Comparison of spatial resolution of a dedicated small animal PET with an animal anatomical atlas. a) NEMA 4U image quality phantom superimposed with the sizes of the corresponding capillaries (linear increasing diameter 1-5 mm). The scale is the same for b) the 2x-magnified image section and c) the sketch of a rat's auditory cortex based on [Schwarz2006].

1.2.3.2 Sensitivity

A second important criterion is the sensitivity of the system. Similar to the resolution, it depends on detector properties and geometry of the device. Besides size and shape, the conversion efficiency of the detector is of interest [Yao2012]. It is a detector material depending property and describes the quota of photons converted into measurable electrons. This is depending on the scintillator, which converts the photons into electrons, and the photomultiplier, which multiplies the electrons into a measurable current. The modern generation of scanner uses mostly lutetium oxyorthosilicate (LSO) scintillators [Rausch2015, Schmidt2018] while devices of previous generations used e.g. scintillators made of bismuth germanate crystals (BGO) [Jin Su2004]. Considering the efficiency, the shape of the detector and the spatial alignment, the total rate of detectable photons can be estimated. This property is coupled to the resolution and generally given as

a factor converting the measured count rates of the PET device per given volume to an activity concentration [Lange2002].

As the quality in reconstructed imaged is directly linked to the number of events and the signal to noise ratio (S/N), this factor is of particular importance in technological development. Improvements of the sensitivity create multiple options for improvement of clinical methods. First, if the same amount of activity is used and patients are scanned shorter, the image quality would stay similar but more patients could be scanned and the burden of motionlessness would be reduced for each patient. Second, using similar activities and scan durations would lead to an increased number of events which enable reconstructions of images with enhanced quality which could improve diagnostic accuracy. Third, by applying less activity with similar scans durations, the quality of images would be similar to before, but each patient would get reduced doses of radiation. This would be particularly of interest for follow-up investigations after auditory implantation to assess neuronal plastic changes during rehabilitation.

1.2.3.3 Contrast

The contrast gives an estimate, which magnitude of effect is necessary in an image in order to be detectable. The contrast is defined by the S/N [Lange2002]. This ratio depends strongly on resolution and sensitivity. [Knoop2002] showed that effect magnitudes are not linearly recovered and correspondingly Figure 7 exemplifies the impact of resolution on the contrast. Higher resolution (diagrams further left) show better recovery of the signal against noise. Even though the background suppression is more advanced in PET than in SPECT [Fragoso Costa2016], it is non-negligible and can be caused by electronic noise, random coincidental measurements of natural occurring 511 keV photons or by measuring scattered photons. The contrast is sometimes specifically tested to quantify image quality [Rausch2015].

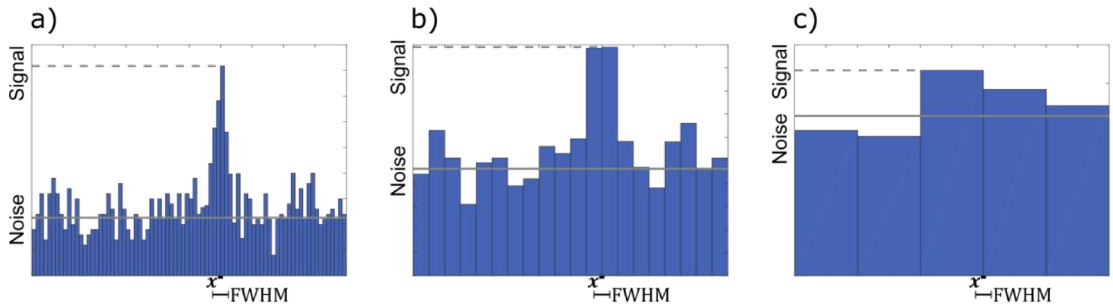


Figure 7 Impact of resolution on contrast. Noise and signal were generated by random linear distribution and respective Gaussian distribution with the same x, the same FWHM and the same noise for all distributions. The ratio FWHM to resolution is a) 4, b) 1 and c) 0.25. Accordingly, S/N decreases and effect localization is increasingly challenging.

1.2.4 Data analysis

All these different factors of imaging need to be taken into account when analyzing the data. Different software tools enabled us to optimize parameter selection for achieving the best possible image properties.

1.2.4.1 Spatial normalization

Every living being is unique. Nevertheless, different individuals share mutual features in brain images as shown exemplarily in Figure 8. When comparing the brain of humans and small animals, the structure of lobes and sulci is less distinct in animals particularly rats [Kretschmann1992, Paxinos1998]. However, due to similarities in brain structure within a species, specific atlases can be created using multiple individuals in order to give a spatial frame of reference in humans [Talairach1988, Lancaster2000] or animals [Paxinos1998, Schwarz2006]. Additionally, the use of different tracers with accordingly different pattern of uptake in the brain requires the generation of different atlases for best comparability [Vallez Garcia2015]. Two possible approaches can be applied to compare individual images with such anatomical standard spaces,.

First, the anatomical labeling of the atlas can be transferred into the individual space. Especially for clinical application with images from one subject this method is of interest. Second, the individual image can be transferred into the standard space. This is required if images of multiple subjects should be included. Automated algorithms can be applied to the image data to achieve reproducible results with consistent quality [Woods1998]. They employ minimization e.g. in gradients by scaling the dimensions of the image, rotate, or move it across three dimensions. This type of co-registering one image to another is called rigid matching.

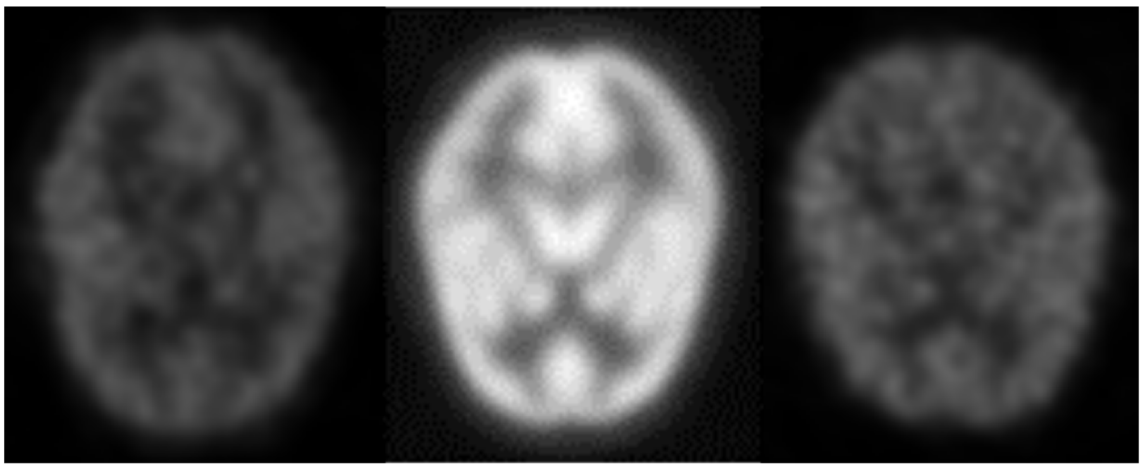


Figure 8 Exemplary interindividual differences shown on similar transaxial planes of patients (left, right) in comparison to a brain template (middle) and between each other.

As templates lose details in order to represent larger structures, the comparison of individualized images sometimes requires the masking of the details in individual images. This is achieved by applying a 3D-gaussian filter to every voxel of the image and is called smoothing [Woods1998]. However, this might result in an underestimation of the magnitude of biological effects as it creates an artificial resolution causing masking [Knoop2002]. This impacts effects in larger regions as well, as optimal representation is only achieved for effects in the size of the smoothing kernel [Blobel1998]. Advanced algorithms including warping allow evaluation of different regions with different parameters in order to achieve better correspondence through the use of non-linear matching. As these methods can change the morphology within the image, some information such as deficient blood flow can be underestimated. Therefore, most default registrations apply rigid matching, which is also used to test new algorithms [Vallez Garcia2015].

1.2.4.2 Volume- and voxel-wise analyses

After anatomical co-registration, the choice of observables has to be made. Depending on the tracer, various observables can be extracted like standardized uptake values (SUV) for example in ^{18}F-FDG studies [Mullani2008, Boellaard2015] or values describing perfusion such as K1 [Schmidt1991, Wu1995] based on bio-kinetic modeling of dynamically acquired ^{15}O-water studies [Kanno1987]. The observables of dynamically imaged tracers require advanced analyses methods and input functions such as blood-time-activity curves, which are not always feasible.

For most tracers, local uptake values are used. A common method of quantification is the use of SUV, which normalizes the specific uptake to injected dose and the subject's body weight. This assumes similar physiologic parameters for example metabolism of tracers and is not always applicable. Nevertheless, it enables comparison between subjects. As the values of single volume elements can vary, usually larger volumes of interest (VOIs) are formed. Such VOIs are typically predefined in atlases and group volumes of similar functions together [Tzourio-Mazoyer2002, Schwarz2006]. The corresponding volume-wise averaged values can be compared between subjects for the same regions to derive differences or enable the comparison of different paradigms such as listing to speech or multi-tones [Berding2015]. The strong points of these types of analyses are the quantification of effects. These types characterizing the volume-wise average uptakes will be further referred to as VOI-analyses. VOI-analyses require a definition of the areas before. They are thereby usually hypothesis-driven as only areas are compared in which significant changes are expected or regions are chosen to control the analyses for effects not intended i.e. systematic errors.

Another method – the statistical parametric mapping (SPM) – is based on analysis of each resolution element (2D - pixel, 3D - voxel). Co-registering all images into a spatial

standard space enables the statistic comparison of single voxels in multiple images. Depending on the study design, different parameters can be derived by applying statistical methods such as paired or grouped t-test on each voxel. The corresponding statistical parameters can then be displayed in 3D images representing the local effects. A very common observable is the integrated uptake compared to different paradigms [Berding2015]. Statistical tests reveal here relative activity of brain areas or inactivity according to the paradigm.

1.3 Aims of studies

Hearing impairment affects many people, but with advances in technology, a multitude of possible hearing aids or auditory implants offer restoration or partial relief. The outcome of different devices varies strongly and their optimization, as well as the implementation of new procedures, is still subject of hearing research. It requires objective diagnostic tools to understand the processes underlying normal hearing, the development of hearing loss, and the variability in the outcome of procedures for the restoration of hearing. Understanding these processes can be advanced using minimal invasive molecular imaging methods as shown e.g. in [Horga2014, Berding2015]. Especially PET has demonstrated its abilities in auditory research with awake human subjects. This tool has yet to be refined. Test have successfully been applied to older children [Fujiki2000] but not young children who require anesthesia for such diagnosis but are those who would benefit most from the assessment of prognosis. Effects of anesthesia on brain imaging are known [Heinke2002]. Moreover, the effects of anesthesia have been studied during cochlear implant surgery in children using electrophysiological methods [Jana2013].

Therefore, we studied for the first time the effects of anesthesia on imaging in a group of young children in conjunction with cochlear implantation. In a retrospective analysis of PET auditory activation studies on adults and anesthetized children, the transferability of the method was explored. As most analyses reported in the literature have been optimized and standardized with awake subjects, we additionally examined the need for adaption of analysis criteria. We addressed methodical parameters in order to derive the best representation of hearing ability. For this, individual analyses of activation studies in adults and children were compared for the same stimulus as well as differences in children with 2 different stimuli always considering 24 different analyses varying 3 different parameters of the same base data. Our aim was to find optimal parameters for analyses of awake subjects as a starting point to elaborate parameter for the best possible recovery of activations using data from anesthetized children.

In order to further establish PET as an objective diagnostic tool in hearing research, the methods, especially for children, can be further developed based on other models than

the human. Small animals, particularly rats, have been used to broaden the knowledge in hearing. A number of studies showed the applicability of PET in auditory research of rats, e.g. [Hsu2009, Jang2012], but with limited comparability to humans due to selected conditions and stimulation procedures.

Therefore, we conducted brain activations studies with ^{18}F-FDG employing multiple acoustic conditions in awake animals. Stimuli were selected to serve as reference or as stimuli promoting or avoiding habituation. Additionally, all conditions were compared to profound hearing loss as a baseline not influenced by any background noise. We aimed to assess the comparability between activation patterns in humans and rats. As human and rats have differences in size and physiology, we additionally aimed to elucidate the ability of PET to detect further structures along the auditory pathway previously not observed in humans or rats. In addition, an objective was the characterization of the profound hearing loss condition with respect to potential compensatory changes.

2 Study I – PET imaging of auditory system activation during general anesthesia

First published in 2018 in EJNMMI Res (European Journal of Nuclear Medicine and Molecular Imaging Research), Vol. 8(1), DOI: 10.1186/s13550-018-0362-z

Citations, tables, and figures are formatted and corresponding labels and legends edited to adhere to a coherent style of the dissertation with the permission of the publisher.

Feasibility of ^{15}O-water PET studies of auditory system activation during general anesthesia in children

Martin Mamach[1,2,3], Florian Wilke[3], Martin Durisin[4], Frank A. Beger[5], Mareike Finke[2,4], Andreas Büchner[2,4], Barbara Schultz[6], Arthur Schultz[6], Lilli Geworski[3], Frank M. Bengel[1], Thomas Lenarz[2,4], Anke Lesinski-Schiedat[4,*], Georg Berding[1,2,*]

[1] Department of Nuclear Medicine, Hannover Medical School, Germany

[2] Cluster of Excellence "Hearing4all", Hannover, Germany

[3] Department of Medical Physics and Radiation Protection, Hannover Medical School, Germany

[4] Department of Otolaryngology, Hannover Medical School, Germany

[5] Department of Anesthesiology and Intensive Care Medicine, Hospital Diakovere Annastift, Hannover, Germany

[6] Department of Anesthesiology and Intensive Care Medicine, Hannover Medical School, Germany

[*] Drs. Georg Berding and Anke Lesinski-Schiedat contributed equally to this study

2.1 Abstract

Background: ^{15}O-water positron emission tomography (PET) enables functional imaging of the auditory system during stimulation via a promontory electrode or cochlear implant, which is not possible using functional magnetic resonance imaging (fMRI). Although PET has been introduced in this context decades ago, its feasibility when performed during general anesthesia has not yet been explored. However, due to a shift to earlier (and bilateral) auditory implantation, the need to study children during general anesthesia appeared, since they are not able to cooperate during scanning. Therefore, we evaluated retrospectively results of individual SPM (statistical parametric mapping) analysis of ^{15}O-water PET in 17 children studied during general anesthesia and compared them to those in 9 adults studied while awake. Specifically the influence of scan duration, smoothing filter-kernel employed during preprocessing and cut-off value used for statistical inferences were evaluated. Frequencies, peak-heights and extents of activations in auditory and extra-auditory brain regions (AR and eAR) were registered.

Results: It was possible to demonstrate activations in auditory brain regions during general anesthesia, however, the frequency and markedness of positive findings was dependent on some of the above mentioned influence factors. Scan duration (60 vs. 90 seconds) had no significant influence on peak-height of auditory cortex activations. To achieve a similar frequency and extent of AR activations during general anesthesia compared to waking state a lower cut-off for statistical inferences ($p<0.05$ or $p<0.01$ vs. $p<0.001$) had to be applied. However, this lower cut-off was frequently associated with unexpected, "artificial" activations in eAR. These activations in eAR could be slightly reduced by the use of a stronger smoothing filter-kernel during preprocessing of the data (e.g. $[30\ mm]^3$).

Conclusions: Our data indicate that it is feasible to detect auditory cortex activations in ^{15}O-water PET during general anesthesia. Combined with the improved signal to noise ratios of modern PET scanners this suggests reasonable prospects for further evaluation of the method for clinical use in auditory implant users. Adapted parameters for data analysis seem to be helpful to improve the proportion of signals in AR versus eAR.

2.2 Keywords

^{15}O-water PET, scan duration, smoothing filter-kernel, cut-off for statistical inferences, cochlear implant, promontory needle electrode, auditory cortex activation, anesthesia, EEG monitoring

2.3 Background

Functional imaging of brain activation due to visual or auditory stimuli using radioactive biomarkers of blood flow or metabolism has been implemented for the first time in the 1980's [Celesia1982, Fox1984, Mazziotta1984, Petersen1988]. With the advent of fMRI in the 1990's most research in this context especially in healthy subjects shifted to this method avoiding radiation exposure [Johnsrude2002, Bandettini2012]. However, in adult patients with cochlear implants radioactive biomarkers still retained their role in research since fMRI is not possible for safety reasons [Herzog1991, Naito1995]. In the last 25 years the field of brain stimulation in general has witnessed an exponential growth in clinical applications – including diverse neurological, psychiatric, behavioral, and cognitive conditions – and research investigations [Hariz2013]. Functional imaging using PET provided substantial evidence with respect to the mechanisms of action in these therapies [Ballanger2009]. Regarding auditory implants especially two developments have occurred in parallel: (i) it has been recognized that implantation in children at an earlier age provides the best outcomes, since it takes advantage of sensitive periods of auditory development [Vincenti2014], (ii) new approaches with respect to targets more central in the auditory pathway (brainstem, midbrain) have been developed [Lenarz2006, Schwartz2008]. In consequence to the second development, functional imaging using PET and SPECT has been used as a monitoring tool helping to understand functional changes during auditory rehabilitation in adult users of novel types of implants [Miyamoto1999, Di Nardo2004, Coez2009, Berding2015]. However, small children with auditory implants have not yet been included in such studies due to their inability to cooperate in functional imaging while awake. This raises the question if those functional imaging studies are feasible during general anesthesia to circumvent this and how reliable such investigations would be.

Functional imaging studies during general anesthesia have been done in adult healthy subjects during auditory stimulation with words using fMRI [Kerssens2005, Plourde2006, Davis2007]. Specifically these studies revealed a reduced but maintained activation in auditory regions of the superior temporal cortex especially during light anesthesia while results were heterogeneous during deep anesthesia. Moreover, activations related to auditory stimuli in the auditory networks beyond the temporal cortex remained present at a light state of anesthesia [Kerssens2005]. Nevertheless, higher levels of auditory processing in the brain such as comprehension and memory were clearly impaired during anesthesia [Kerssens2005, Plourde2006, Davis2007]. With respect to the used anesthetic, there is evidence from patients undergoing cardiac surgery, that in opioid (fentanyl) based general anesthesia (combined with the benzodiazepine flunitrazepam) auditory evoked potentials are similar to the awake state, and implicit memories of auditory stimuli can be registered in a higher proportion as compared to other combinations of anesthetics [Schwender1994]. Correspondingly studies in non-human primate showed with electrophysiological methods using auditory stimuli during

opioid based anesthesia activations of primary auditory cortex and belt areas [Rajan2013]. In accordance with these findings opioid based anesthesia has been recommended for intraoperative monitoring of cochlear implant function [Jana2013].

In parallel to increasing challenges for functional imaging with PET in patients receiving electrical stimulation therapy to their brain, a substantial improvement in imaging technology occurred, with respect to sensitivity, spatial resolution and signal to noise ratio [Jakoby2011, Lee2014].

Against this background we systematically reanalyzed PET auditory activation studies of patients obtained in the context of patient care at Hannover Medical School. The studied patient population encompassed (awake) adult patients as well as a group of (anesthetized) children receiving functional ^{15}O-water PET with auditory stimulation during general anesthesia. Besides generating for the first time data on the feasibility of this approach (PET auditory activation studies during general anesthesia) we intended to optimize the procedure.

There are several issues with respect to PET acquisition and data analysis, in which different parameters have been suggested for activation studies with ^{15}O-water. These parameters are selected empirically without systematic reasoning and differ from one PET center to the other. One parameter is the acquisition duration. Early studies used relatively short durations of 40 s [Fox1984, Petersen1988]. In many studies up to now intermediate durations between 60 s and 90 s are employed [Morris1998, Chmielowska1999, Miyamoto1999, Nishimura2000, Fukuda2004, Demarquay2008, Klinge2008, Berding2015]. Working groups from Japan often use 120 s acquisition time [Naito1995, Okazawa1996, Fujiki2000, Hirano2000].

A further issue is smoothing of the 3-dimensional (3D) data set during preprocessing. Filter-kernels between 1 and 2 times of the spatial resolution (FWHM: full width at half maximum) of the used PET scanner (7-12 mm) tended to be more frequently employed [Morris1998, Miyamoto1999, Nishimura2000, Fukuda2004, Demarquay2008, Klinge2008, Coez2009] as compared to kernels between 2 and 3 fold the FWHM (15-20 mm) [Warburton1999, Schulz2005, Campbell2008, Berding2015].

Finally the cut-off used for statistical inferences from statistical parametric maps is variable. Although a p value less than 0.001 uncorrected for multiple comparisons is frequently employed [Giraud2001, Klinge2008, Coez2009, Berding2015] less rigid thresholds have been applied as well [Morris1998, Warburton1999, Nishimura2000, Fukuda2004].

Consequently the aims of the present study are: (i) explore the feasibility of functional imaging studies of the auditory system with PET in children during general anesthesia, (ii) assess the impact of the acquisition duration after ^{15}O-water application on the statistical outcome measures, (iii) elaborate adapted parameters for ^{15}O-water PET studies of auditory cortex activation with respect to pre-filtering and cut-off for statistical inferences – in particular for impaired activations during general anesthesia.

2.4 Methods

2.4.1 Patients

Altogether 26 patients with severe bilateral inner ear hearing loss were enrolled in this study. The entire group splits into one subgroup of children (10 male, 7 female) with a mean age of 6.3±4.7 years, and one subgroup of adults (4 male, 5 female) with a mean age of 45.0±26.1 years. In the children's subgroup, 13 received unilateral cochlear implantation 4.5±2.4 years before and four 0.5±0.4 years after ^{15}O-water PET. Twelve children received a second implant 0.6±0.4 years after the PET investigation. In the adult's subgroup, all received their first Implant after the PET study (0.4±0.2 years) and 3 received a second implant 2.4±1.0 years after the PET study. Cochlear Implants (CI) from different manufactures were implanted (Cochlear Nucleus®, Advanced Bionics Clarion™ and HiRes90K™, MED-EL Pulsar and Sonata). Final follow-up assessments of hearing capabilities were obtained in children 6.1±0.8 years and adults 5.6±2.3 years after the PET investigation. The speech intelligibility was scored between 0 and 100% for each of 4 tasks: (i) understanding of monosyllables at 65 dB, (ii) numbers at 65 dB, (iii) the Hochmair-Schulz-Moser (HSM) sentence test during silence and (iv) the HSM sentence test with 10 dB background noise [Hochmair-Desoyer1997]. The mean scores achieved in children and adults are given in Table 1. No significant differences were observed between the two subgroups.

Table 1 Comparison of speech intelligibility 6 years after PET, between patients studied with and without anesthesia

Age group	Anesthesia during PET	Percent understanding			
		of mono-syllables	of numbers	HSM sentence test in silence	HSM sentence test in 10 dB
Adults	No	54 ± 36	80 ± 33	70 ± 32	43 ± 38
Children	Yes	75 ± 11	98 ± 4	82 ± 20	37 ± 30

The speech intelligibility was determined using among others the HSM (Hochmair-Schulz-Moser) sentence test in silence or masked with a 10 dB (decibel) white noise. No significant differences were observed.

2.4.2 Anesthesia

Auditory stimulation and PET imaging was always performed during waking state in adults and flat electroencephalography (EEG) conducted general anesthesia in children. Anesthesia was induced with sevoflurane inhalation via mask. After establishing an intravenous access, endotracheal intubation was performed under additional analgesia with remifentanil (1 µg/kg/30s) and muscle paralysis with mivacurium. Sevoflurane was discontinued after intubation and ventilation was continued an air-oxygen mixture. During maintenance of anesthesia

remifentanil was given at a dose of 0.35 µg/kg/min and the sedative midazolam at a dose adjusted to achieve flat stages of anesthesia. The stage of anesthesia was assessed using the Narcotrend® monitor [Kreuer2003]. Base on a frontal EEG lead, this monitor allows to differentiate six stages from A = awake to F = very deep anesthesia. We targeted for stage B corresponding to an EEG pattern with dominating ß- and θ-waves in the present study.

2.4.3 Auditory stimuli

Stimulations of the auditory system were always applied unilaterally: via needle electrode placed at the promontory or CI. For promontory stimulation (always applied to not implanted ears) a dedicated device (Cochlear, Germany) was set to burst stimulation with a frequency of 100 Hz and current strength between 5 and 200 mA. In adults the current strength was adjusted according to the patient's comfortable hearing perception, in children (i.e. during general anesthesia) a standard value of 200 mA was used. For stimulations via cochlear implant (only done in children) music was directly fed from a compact disk (CD) player to the speech processor with loudness set to maximum. All stimuli were started 30 s before injection of the radiotracer. Each auditory condition was repeated 6 times with 10 min intervals between tracer injections to allow for decay of radioactivity. Consequently, full PET activation studies for both ears including scans during silence as a reference require 18 scans i.e. altogether more than 3 hours for the patient lying on the examination table. For the comfort of the patients studied while awake we divided acquisitions into two sessions of 9 scans with a pause of at least two hours in between. The conditions: (A) silence and stimulation via promontory needle electrode (PN) or CI on the left (B) or right side (C) were arranged as follows: in adult patients studied while awake: A-B-B-A-B-B-A-B-B, pause, A-C-C-A-C-C-A-C-C; and in children studied during anesthesia: A-B-C-A-B-C-A-B-C-A-B-C-A-B-C-A-B-C-A-B-C.

2.4.4 Radiopharmaceutical

^{15}O-water was produced employing a Scanditronix MC35 Cyclotron and administered using an advanced system as described previously [Matzke1993]. For each emission scan an age dependent activity amount of ^{15}O-water was administered always as a bolus within 7 seconds: up to the age of 5 years 185 MBq, up to 10 years 370 MBq, up to 15 years 555 MBq and in adults 740 MBq.

2.4.5 Data acquisition and reconstruction

For acquisition an ECAT EXACT 922/47 (Siemens, Erlangen, Germany) PET scanner with a spatial resolution of 7 mm (FWHM) was used. Before each session of 9 or 18 emission-scans a 10min transmission scan was acquired using ^{68}Ge rod sources. Emission scanning was always started 15 s after radiotracer injection to account for circulation time and allow the tracer to arrive in the brain. Two consecutive frames of 60 s and 30 s were acquired. The data

were reconstructed iteratively using an ordered subset expectation maximization (OSEM) algorithm with 6 iterations and 16 subsets. The dimensions of the reconstructed 3D data sets were 128/128/47 (x/y/z) with a voxel size of 1.87 mm / 1.87 mm / 3.38 mm. Data sets of ^{15}O-water uptake integrated for 60 s and 90 s were used in the further analyses.

2.4.6 Individual PET data analysis

Data were analyzed using the statistical parametric mapping (SPM) software (SPM8, Wellcome Trust Centre for Neuroimaging, London, UK). Data of each patient was analyzed individually (single-subject analysis). At first, all scans were realigned to one mean image, which had been obtained across all conditions, to correct for movement artifacts. Thereafter, all scans were spatially normalized using the parameters obtained with the mean image and the ^{15}O-water PET template provided in SPM8. Default settings of SPM8 software were applied. As a last step of preprocessing smoothing was applied to all scans using three different filter kernels: $[10\ mm]^3$, $[20\ mm]^3$ and $[30\ mm]^3$. Additionally unsmoothed data sets (filter kernel $[0\ mm]^3$) were considered in further analysis. A paired t-test was employed in all single subject analyses to compare stimulated and reference conditions. Pairs were always built: between scan during stimulation and the closest preceding scan during silence. Three levels of significance ($p<0.001$, $p<0.01$ and $p<0.05$) were applied with respect to statistical inferences. A volume of interest (VOI) template conforming the anatomical standard space and reflecting Brodmann areas (BA) was used to identify significant regional effects in primary and secondary auditory regions (AR): BA 41, BA 42, BA 22 and BA 21. The impact of data acquisition and reconstruction parameters on the demarcation of auditory activations was assessed using the following criteria: (i) the peak height (T_{max}-value) of activation in AR, (ii) the relative size of activations within AR and within extra-auditory regions (eAR) – both in relation to the total size of AR and (iii) the frequency of any activation in AR and eAR at all. For all assessments left and right sides of the cortex were always combined.

2.4.7 Statistical analysis across subjects

The impact of anesthesia and the above mentioned parameters selected for PET data acquisition and analysis on the demarcation of auditory activations has been evaluated based on 50 single-subject analyses (in 2 of 26 patients only unilateral auditory stimulation had been performed). Three groups were formed for further statistical comparisons: (i) n=17 studies of PN stimulation in adults during awake state, (ii) n=20 studies of PN stimulation in children during anesthesia (iii) n=13 studies of CI stimulation in children during anesthesia. Significances of differences in peak-heights, sizes or frequencies of activations between different groups or different parameters were assessed using JMP 10 software (SAS Institute Inc.) with a threshold of $p<0.05$.

2.5 Results

2.5.1 Impact of scan duration and anesthesia on peak-height in auditory cortex activations

In Table 2 mean T_{max} values obtained in SPM analyses based on different durations of the PET scan are compared for different conditions separately (i.e. studies with or without anesthesia and studies with auditory stimulation via PN or CI). No significant difference between the two scan durations was observed (Table 2). However, it could be observed, that studies without anesthesia (in adults) showed consistently higher T_{max}-values compared to those including anesthesia for all evaluated scan durations and smoothing kernels. P-values indicating the significance of the respective difference are given in Table 2. Moreover, we compared T_{max} values between sides contralateral vs. ipsilateral to the auditory stimulation. However, no significant side differences ($p>0.05$, paired t-test) were found for all groups listed in Table 2.

2.5.2 Relative sizes of activations in AR and eAR with different parameters

In Table 3 mean relative sizes of activations in AR and eAR are given for SPM analyses based on different smoothing filter-kernels applied in preprocessing and cut-off levels used for statistical inferences. Moreover, mean ratios of AR to eAR size are given. Mean sizes and ratios are listed separately for different conditions. In studies without anesthesia (in adults), stimulation via PN and employing a cut-off level of $p<0.001$ in the mean about 1% of the AR (i.e. of BAs 41, 42, 22 and 21) showed a supra-threshold activation. At the same time activations in eAR were considerably larger (4-8% in the mean). The highest ratio between AR and eAR of 0.16 was observed at that cut-off level and with a smoothing kernel of $[20\ mm]^3$.

For studies during anesthesia (in children) comparable mean sizes of activation in AR (around 1%) were observed with the less rigid cut-off level of $p<0.01$. At that cut-off level mean activations in eAR were considerably smaller during anesthesia (22-31%) compared to studies during waking state in adults (39-93%). This is illustrated in Figure 9a, showing results of one PET study during anesthesia (upper row) and one during waking state (lower row). A realistic size of auditory activation during anesthesia was only achieved with less rigid cut-off levels ($p<0.01$, $p<0.05$).

Table 2 Comparison of peak height (t_{max} values) of auditory activations obtained with different scan durations (60 vs. 90s) and depending on anesthesia (no vs. yes).

Age group	Condition		T_{max} values and significance p, of difference											
			S=[0mm]^3			S=[10mm]^3			S=[20mm]^3			S=[30mm]^3		
	Anesthesia	Stim.	60s.	90s	p	60s.	90s	p	60s.	90s	p	60s.	90s	p
Adults	No	PN	10.82±2.39	12.06±3.78	n.s.	11.68±3.25	10.98±5.24	n.s.	9.29±3.91	8.54±3.30	n.s.	7.14±3.74	7.31±6.57	n.s.
			n.s.	p=0.0313		p=0.0001	p=0.0071		p=0.0004	p=0.0194		p=0.0054	n.s.	
Children	Yes	PN	9.56±3.59	9.37±3.43	n.s.	6.27±2.52	6.86±2.49	n.s.	4.81±2.71	5.49±4.27	n.s.	3.90±2.54	4.09±2.95	n.s.
Children	Yes	CI	10.06±3.27	9.33±2.99	n.s.	6.80±2.10	8.07±3.04	n.s.	5.28±2.24	5.47±2.96	n.s.	3.38±1.16	4.40±1.97	n.s.

Mean values and standard deviations of t_{max} are given for different subgroups and smoothing kernels.
Stim. = Stimulation, PN = promontory needle electrode, CI = cochlear implant, S = smoothing kernel

Table 3 Mean relative sizes of activations in AR and eAR – both given as percent of the overall size of the auditory region.

				S = [0 mm]^3			S = [10 mm]^3			S = [20 mm]^3			S = [30 mm]^3		
Age group	p<	Anesthesia	Stimulation	AR	eAR	**AR/eAR**	AR	eAR	**AR/eAR**	AR	eAR	**AR/eAR**	AR	eAR	**AR/eAR**
	0.001	No	PN	0.3%	4.3%	**0.07**	0.7%	5.8%	**0.12**	*1.0%*	6.1%	**0.16**	0.8%	7.5%	**0.12**
Adults	0.01	No	PN	2.8%	39.4%	**0.07**	5.9%	62.5%	**0.09**	9.9%	83.6%	**0.12**	9.2%	92.8%	**0.10**
	0.05	No	PN	10.0%	163.0%	**0.06**	16.8%	242.1%	**0.07**	21.8%	324.6%	**0.07**	21.8%	358.7%	**0.06**
	0.001	Yes	PN	0.2%	2.4%	**0.05**	0.2%	2.5%	**0.02**	0.0%	4.3%	**0.03**	0.4%	5.0%	**0.02**
Children	0.01	Yes	PN	*1.1%*	22.0%	**0.04**	*1.2%*	23.0%	**0.03**	*1.3%*	25.4%	**0.02**	*1.6%*	31.00%	**0.05**
	0.05	Yes	PN	4.5%	108.6%	**0.04**	4.9%	112.0%	**0.04**	5.0%	114.1%	**0.03**	4.9%	120.2%	**0.03**
	0.001	Yes	CI	0.1%	2.9%	**0.04**	0.0%	2.2%	**0.03**	0.1%	1.6%	**0.22**	0.1%	0.3%	**0.15**
Children	0.01	Yes	CI	*1.0%*	19.9%	**0.05**	*1.1%*	20.9%	**0.07**	*0.8%*	19.9%	**0.07**	*0.7%*	16.4%	**0.05**
	0.05	Yes	CI	4.9%	101.2%	**0.05**	5.3%	103.2%	**0.06**	4.0%	103.4%	**0.06**	2.5%	100.5%	**0.05**

A ratio of auditory to extra-auditory activations (AR/eAR) is given (bold). The three parameters are listed for different smoothing filter-kernels (S) and thresholds for statistical inferences (p). About 1% activation in AR is reached with p<0.001 for studies without anesthesia and p<0.01 for those with (italic type). AR: Auditory regions, eAR: Extra-auditory regions, PN: Promontory needle electrode, CI: Cochlear implant, S: Smoothing filter-kernel

2.5.3 Frequency of activations in AR and eAR depending on parameters and use of anesthesia

In Table 4 mean frequencies of activations in AR and eAR are given for SPM analyses based on different smoothing filter-kernels applied during preprocessing and cut-off levels used for statistical inferences. Many times, for corresponding smoothing filter-kernels and cut-off levels the frequencies of activations in AR were significantly lower with anesthesia in children compared to without anesthesia in adults (e.g. with $[20\ mm]^3$ smoothing filter-kernel and cut-off level of $p<0.001$: 35% vs. 82%, $p<0.05$). A more comparable frequency of activations in AR for studies during anesthesia was observed with a less ridged cut-off level (e.g. for $[20\ mm]^3$ smoothing filter-kernel with a cut-off level of $p<0.01$ or $p<0.05$: 65% or 85%). For all conditions and at all cut-off levels the frequency of detected activations in AR increased with weaker smoothing. However, activations in eAR were detected for smoothing filter-kernels up to $[20\ mm]^3$ in 100% of the cases (for all conditions and cut-off levels). Only with the highest smoothing filter-kernel $[30\ mm]^3$ and a cut-off level of $p<0.001$ activations in eAR were seen in less than 100% (but not less than 75% of the cases). When looking at representative SPMs obtained in one patient based on different smoothing filter-kernels (always with cut-off level of $p<0.01$) as shown in Fig. 2, it is obvious that activation in eAR gets clearly reduced with higher smoothing filter-kernels. However, the size of activation in AR increases with stronger smoothing – which can also been extracted from Table 3. Nevertheless, the difference between the highest smoothing levels is small or even reversed as can be seen in the example case (Fig. 2).

2.6 Discussion

The functional performance after cochlear implantation can vary between simple sound detection and very good speech intelligibility [Coez2008]. The underlying mechanisms in the individual case often remain unclear. Furthermore, in the situation of unilateral implantation, the potential benefit of a second implant can be difficult to predict [Vincenti2014]. Therefore, objective functional measures reflecting individually either intactness of the central auditory pathway or correlates of central auditory processing are desirable. ^{15}O-water PET has been employed for that purpose using stimuli presented either via auditory implants or promontory needle electrodes [Mortensen2005, Coez2008]. The necessity of an objective measure is given all the more in patients not able to cooperate in testing procedures of auditory function like small children.

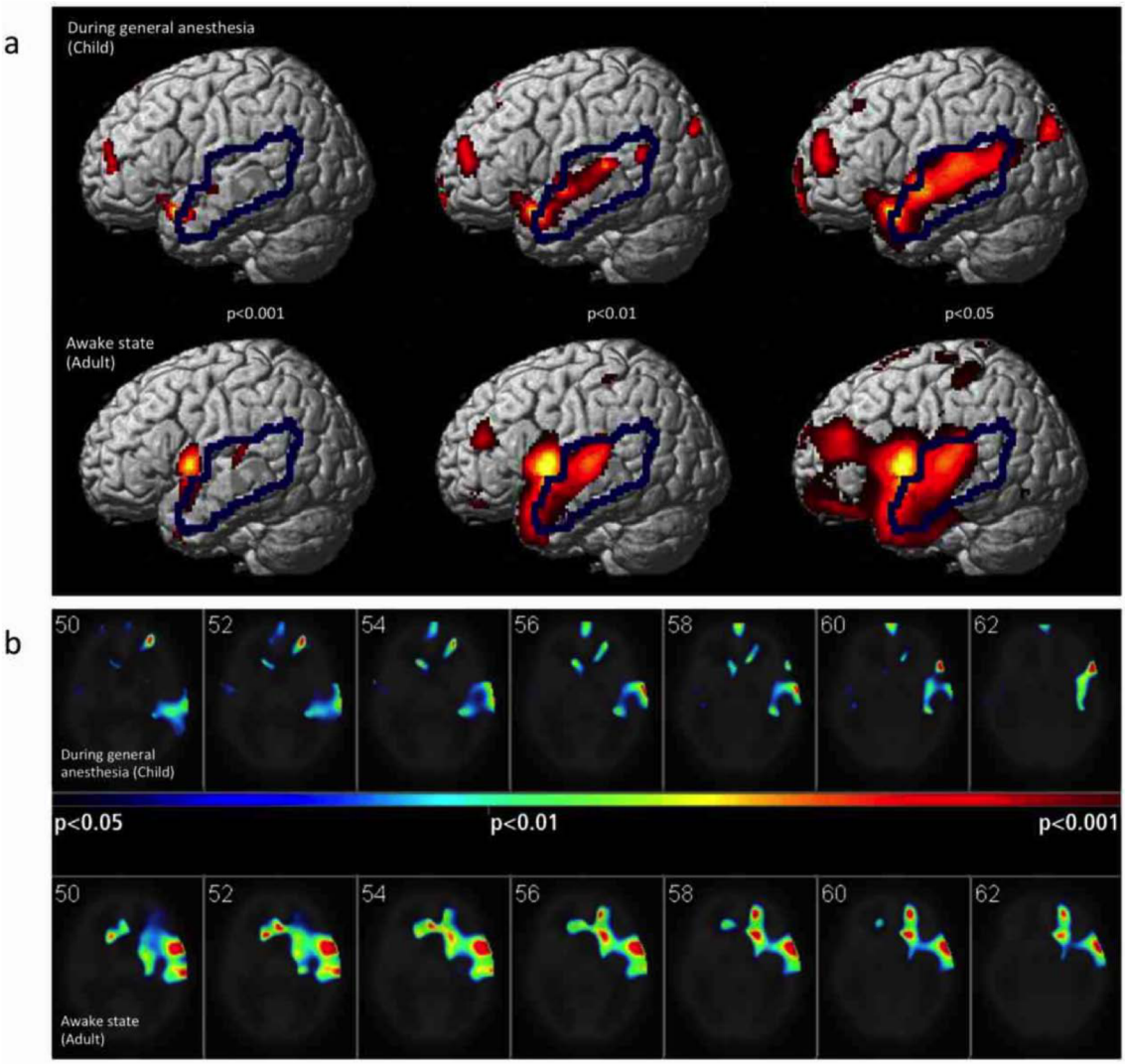


Figure 9 **a** Examples of activations in auditory and extra-auditory regions (AR and eAR separated by blue line), during general anesthesia in a child and awake state in an adult patient detected with different cut-off levels used for statistical inferences (all smoothed with a filter kernel of $[20mm]^3$). Stimulation was done via cochlear implant (upper row) and promontory needle electrode (lower row), respectively. Note: A realistic size of activations in AR during narcosis was only achieved using cut-off levels of $p<0.01$ or $p<0.05$. At the same time relatively less activation in eAR is seen during anesthesia compared to waking state with these cut-off levels. **b** Corresponding t-maps to the examples displayed in **a**. The t-map from the study acquired during general anesthesia in a child nicely depicts the activated auditory cortices with $p<0.01$ (color scale green/blue), while the t-map reflecting the waking state study in an adult patient did the same with $p<0.001$ (color scale dark red/brown). Using $p<0.01$ for the latter would result into pseudo-activation up to ventral frontal.

Table 4 Frequency of activations in AR and eAR – dependency on selected threshold for statistical inferences and applied smoothing filter-kernel.

Age group	p<	Anesthesia	Stimulation	Frequency of activation in AR in [%] S = [0 mm]^3	S = [10 mm]^3	S = [20 mm]^3	S = [30 mm]^3	Frequency of activation in eAR in [%] S = [0 mm]^3	S = [10 mm]^3	S = [20 mm]^3	S = [30 mm]^3
	0.001	No	PN	100	100[a,b]	**82**[a,b]	65[a,b]	100	100	100	94
Adults	0.01	No	PN	100	100	88	77[c]	100	100	100	100
	0.05	No	PN	100	100	100[c]	100	100	100	100	100
	0.001	Yes	PN	95	50[a]	35[a]	10[a]	100[1]	100[2]	100[3]	75[1,2,3]
Children	0.01	Yes	PN	100	85	**65**	45	100	100	100	100
	0.05	Yes	PN	100	100	85[c]	70[d]	100	100	100	100
	0.001	Yes	CI	92	54[b]	31[b]	8[b]	100[1]	100[2]	100[3]	85[1,2,3]
Children	0.01	Yes	CI	100	100	**77**	38[c]	100	100	100	100
	0.05	Yes	CI	100	100	100	100[d]	100	100	100	100

Frequency of activation in AR around 65-82% were reached with p<0.001 for studies without anesthesia and p<0.01 for those with anesthesia (bold, S = [20 mm]³). Grey background indicates which values have been compared with respect to significance of difference (explicitly assigned by superscripts).

AR: auditory regions, eAR: extra-auditory regions, PN: promontory needle electrode, CI: cochlear implant, S: smoothing filter-kernel,

[a, b, c, d] significant differences within columns (t-test: p<0.05), [1, 2, 3] significant differences within rows (t-test: p<0.05)

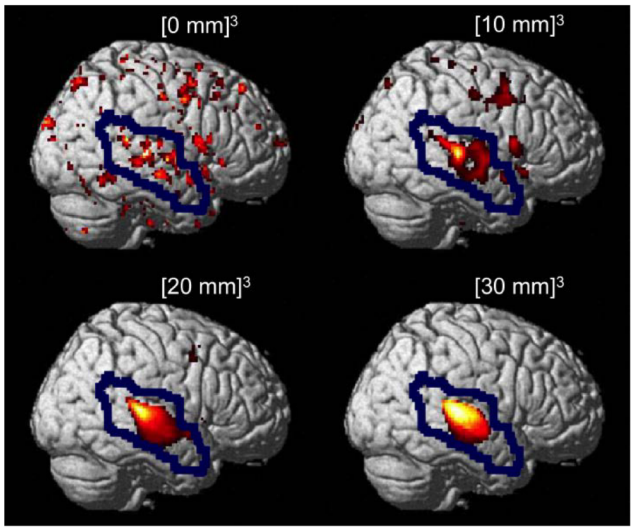


Figure 10 Examples of activations in auditory and extra-auditory regions (AR and eAR separated by blue line) detected with different smoothing filter kernels (always using a cut-off for statistical inferences of p < 0.01). Stimulation was done in an adult patient via promontory needle electrode during awake state. Note: The highest proportion of activation in the auditory cortex was detected with the second highest degree of smoothing (filter kernel of approximately three times of the full width at half maximum, [20 mm]^3). Higher degrees of smoothing result in the detection of less extra-auditory activation

Therefore, we investigated the feasibility of ^{15}O-water PET activation studies of the auditory system during general anesthesia. During a flat opioid-based EEG conducted general anesthesia we could demonstrate in children activations of the auditory cortex during stimulation via a promontory needle electrode or a cochlear implant. However, when applying the same parameters for PET data analysis as in awake adults, activations during anesthesia were less frequent and significant (with respect to peak-height and extent). This observation corresponds to findings in healthy subjects using fMRI [Kerssens2005, Plourde2006, Davis2007]. Nevertheless, it would be desirable that diagnostic accuracy of auditory activation studies during anesthesia at least partially approaches that of studies in waking state.

The present data indicate that specifically adapted parameters for PET images are helpful in this regard. Particularly similar sensitivity can only be obtained if the cut-off for statistical inferences is lowered for studies during anesthesia. Typically for single-subject analyses of PET studies in awake patients an uncorrected p-value less than 0.001 is used for cut-off [Signorini1999, Berding2015]. Other investigators have suggested less rigid cut off values of $p<0.05$ or $p<0.01$ particularly for studies of the auditory system [Warburton1999, Giraud2001]. One argument in favor of this is, that the open hypothesis with respect to the location of detected activations typically associated with a level of $p<0.001$ is not fitting to the situation of an auditory activation study with a high likelihood of an activation predominantly in the auditory system. We observed a similar sensitivity in the detection of auditory cortex activation during anesthesia compared to waking state using a cut-off level of $p<0.05$ or $p<0.01$ instead of $p<0.001$.

Furthermore, the present study indicates, that in activation studies during anesthesia a relatively high degree of smoothing (e.g. filter kernel equivalent to 2-3 fold the FWHM) results into considerably less frequent "activations" in extra-auditory regions (Table 4, Figure 10). These extra-auditory "activations" during anesthesia and stimulation via promontory needle electrode or CI (music) are unexpected and likely to be primarily artificial [Kerssens2005, Davis2007, Angulo-Perkins2014]. On the other side adequate filtering to detect the expected signal in the auditory cortex (despite narcosis) might be achieved by setting it according to the matched filter theorem. This theorem suggests that the optimal smoothing filter-kernel should match the spatial size of the signal to be detected [Reimold2006, Lange2015]. In auditory activation studies, the main structure in which a signal should be detected is obviously the primary auditory cortex and it should be possible to separate it from the secondary and association areas. The extent of the primary auditory cortex (Heschl's gyrus, Brodmann area 41) might be assumed to be about 20 to 30 mm – despite a considerable inter-individual variation [Talairach1988, Morosan2001]. Thus, matching the filter kernel to the extent of the primary auditory cortex according to the filter theorem results again into a relatively high degree of smoothing (equivalent to 2-3 fold the FWHM of the scanner used in our study). Employing this in the present study produced similar frequencies of auditory cortex activations with and without anesthesia (with the respective cut-offs). Higher frequencies of auditory cortex activations during anesthesia achieved with less smoothing filter kernels are likely to reflect in part false positive findings. This is further illustrated in Figure 10 $[0\ mm]^3$ displaying activations in auditory and non-auditory regions appearing as comparable "noise" consisting of small accidentally "significant" clusters. Further evidence, that the detection of a diagnostically relevant signal (in that case of reduction), is not hampered by stronger filtering comes for studies in neurodegenerative diseases. In these, it has been demonstrated for a large range of filter kernels (between 8 mm and 18 mm), that a higher degree smoothing had only a very small impact on the detection of the relevant signal, i.e. diagnosis [Lange2015]. Nevertheless, it has to be kept in mind, that with very large filter kernels (e.g. $[30\ mm^3]$, also evaluated in the present study) signals might be compromised. This is illustrated by consistently lower mean t_{max} values observed with $[30\ mm^3]$ compared to $[20\ mm^3]$ for both acquisition durations in all subgroups (see Table 2). Moreover, too large filter kernels might be detrimental with modern generations of PET scanners – providing in particular at least twice as much spatial resolution compared to the PET scanner used in the present study. These modern scanners enable sufficient recovery of signal for substructures of the auditory system of half of the size compared to the scanner used in the present study, which could be lost by excessive smoothing.

As mentioned above, another issue potentially influencing the accuracy of ^{15}O-water PET activation studies of the auditory system is scanning duration. Shorter as well as

longer acquisition durations have been proposed. Kanno et al. [Kanno1991] demonstrated an increase of signal to noise (S/N) ratio with acquisition time. In the mean they found S/N ratio to be about 1/3 higher at 120 s compared to 40 s scan time. On the other hand Volkow et al. [Volkow1991] showed the largest activations in occipital cortex due to light stimulation based on acquisitions during "uptake phase" (the initial 30-35 s). Moreover, they demonstrated that activations depend on the duration of stimulation. Continued stimulation after the peak of uptake phase for further 40 s during the "washout phase" resulted into lower uptake compared to stimulation restricted to the uptake phase. The authors explained this observation and also lower activation with longer acquisitions by increased clearance of radioactivity from areas of high blood flow. In our study we did not observe a significant difference in activation height (T_{max}) dependent on the acquisition duration (60 s vs. 90 s). This is particularly in contrast to a study by Sibersweig et al. [Silbersweig1993] reporting improved significance (greater signal to noise ratio and higher Z-score) of results obtained with 90 s compared to 60 s. One reason for these conflicting results might be differences in the injection procedure – particularly with respect to the duration of the bolus injection. Silbersweig et al. [Silbersweig1993] described a slow bolus injection (over 20 s), which is considerably slower compared to Volkow's and our study (3 s and 7 s, respectively). A slower injection might promote improved results with longer acquisition durations. Thus, a final conclusion with respect to the most favorable scan duration is not yet possible based on the presently available data. Nevertheless, future studies employing modern PET equipment with the capability of list mode acquisition enabling flexible retrospective definition of reconstructed time frames would allow to address this issue more precisely. Furthermore, due to achievements in PET technique like time of flight measurements an enhanced signal to noise ratio for a given acquisition duration can be expected [Jakoby2011]. Finally this will help to adapt the acquisition duration rather on biological / physiological grounds than on technical limitations of the scanner for improved results of PET activation studies.

Some limitations of our study have to be considered. First that it is a retrospective study. A prospective study would have offered the possibility e.g. to select age matched patients studied with and without anesthesia. Moreover, auditory stimulations were performed routinely on the left side first (without randomization) – therefore an order effect cannot be excluded. A further limitation is caused by the use of the standard SPM template for adults for spatial normalization in children. Muzig et al. [Muzik2000] explored this issue. They found acceptable errors in children down to 6 years. In younger children mean deviations of the brain contour around 2-3 mm have to be expected. However, this might be more relevant in the localization of epileptogenic foci (as in Muzig's [Muzik2000] patient population) as compared to more extended auditory cortices. Furthermore, some beneficial effect might be expected due to higher degrees of

smoothing as applied in the present study. And finally, at least visual inspection of the normalization result in all cases of the present study did not reveal any artifacts. Furthermore, with respect to the impact of the acquisition duration it would have been desirable to compare more than two time periods. However, this was unfortunately not possible retrospectively since our scanner did not allow performing list mode acquisitions and therefore we hat to stick with the originally used frame sequence. At last an impact of the use of CI's from different vendors could not be completely excluded. However, due to the facts that music was used as a robust stimulus not that dependent on the speech processor and most of the implants reflected the technique available during a relatively short period between 2001 and 2007 a major impact is not expected. Despite the abovementioned limitations, we considered it as an added benefit to obtain insights regarding the feasibility of auditory activation studies with ^{15}O-water PET during anesthesia based on available data obtained on clinical grounds.

2.7 Conclusion

The present data indicate that auditory activation studies with ^{15}O-water PET in children during general anesthesia are feasible. They can approach results of studies obtained during waking state in adults if an adapted less rigid cut-off for statistical inferences ($p_{\text{uncorrected}}<0.01$ or $p<0.05$) is employed and strong smoothing during preprocessing (filter-kernel $\geq$ [20 mm]^3) – like in studies without anesthesia. Nevertheless, further research is needed to ascertain whether activation studies with ^{15}O-water PET in children during general anesthesia are a valuable diagnostic tool before and after auditory implantation in clinical routine situations. The issue of optimal scan duration is still not clarified on the basis of the presently available data. However, modern PET scanners providing fundamentally higher signal to noise ratios – in comparison to the generation of PET scanners employed to elaborated procedures for auditory activation studies with PET decades ago –will open novel possibilities to explore the circuitry of the auditory system in implant users.

2.8 Acknowledgements

The authors would like to thank the technical staff at the PET center and Radiochemistry of the Department of Nuclear Medicine of Hannover Medical School for providing ^{15}O-water and excellent technical assistance.

2.9 References

Angulo-Perkins, A., Concha, L. (2014). "Music perception: information flow within the human auditory cortices." Adv Exp Med Biol 829: 293-303.

Ballanger, B., Jahanshahi, M., Broussolle, E., Thobois, S. (2009). "PET functional imaging of deep brain stimulation in movement disorders and psychiatry." J Cereb Blood Flow Metab 29(11): 1743-1754.

Bandettini, P. A. (2012). "Twenty years of functional MRI: the science and the stories." Neuroimage 62(2): 575-588.

Berding, G., Wilke, F., Rode, T., Haense, C., Joseph, G., Meyer, G. J., et al. (2015). "Positron Emission Tomography Imaging Reveals Auditory and Frontal Cortical Regions Involved with Speech Perception and Loudness Adaptation." PLoS ONE 10(6): e0128743.

Campbell, M. C., Karimi, M., Weaver, P. M., Wu, J., Perantie, D. C., Golchin, N. A., et al. (2008). "Neural correlates of STN DBS-induced cognitive variability in Parkinson disease." Neuropsychologia 46(13): 3162-3169.

Celesia, G. G., Polcyn, R. D., Holden, J. E., Nickles, R. J., Gatley, J. S., Koeppe, R. A. (1982). "Visual evoked potentials and positron emission tomographic mapping of regional cerebral blood flow and cerebral metabolism: can the neuronal potential generators be visualized?" Electroencephalogr Clin Neurophysiol 54(3): 243-256.

Chmielowska, J., Coghill, R. C., Carson, R. E., Ishii, K., Chen, R., Hallett, M., et al. (1999). "Comparison of PET [15O]water studies with 6-minute and 10-minute interscan intervals: single-subject and group analyses." J Cereb Blood Flow Metab 19: 570-582.

Coez, A., Zilbovicius, M., Ferrary, E., Bouccara, D., Mosnier, I., Ambert-Dahan, E., et al. (2008). "Cochlear implant benefits in deafness rehabilitation: PET study of temporal voice activations." J Nucl Med 49(1): 60-67.

Coez, A., Zilbovicius, M., Ferrary, E., Bouccara, D., Mosnier, I., Ambert-Dahan, E., et al. (2009). "Processing of voices in deafness rehabilitation by auditory brainstem implant." Neuroimage 47(4): 1792-1796.

Davis, M. H., Coleman, M. R., Absalom, A. R., Rodd, J. M., Johnsrude, I. S., Matta, B. F., et al. (2007). "Dissociating speech perception and comprehension at reduced levels of awareness." Proc Natl Acad Sci U S A 104(41): 16032-16037.

Demarquay, G., Royet, J. P., Mick, G., Ryvlin, P. (2008). "Olfactory hypersensitivity in migraineurs: a H215O-PET study." Cephalalgia 28(10): 1069-1080.

Di Nardo, W., Picciotti, P., Di Giuda, S., De Rossi, G., Paludetti, G. (2004). "SPET assessment of auditory cortex stimulation and tonotopic spatial distribution in auditory brainstem implant." Acta Otorhinolaryngol Ital 24: 321-325.

Fox, P. T., Raichle, M. E. (1984). "Stimulus rate dependence of regional cerebral blood flow in human striate cortex, demonstrated by positron emission tomography." J Neurophysiol 51(5): 1109-1120.

Fujiki, N., Naito, Y., Hirano, S., Kojima, H., Shiomi, Y., Nishizawa, S., et al. (2000). "Brain activities of prelingually and postlingually deafened children using cochlear implants." Ann Otol Rhinol Laryngol Suppl 185: 12-14.

Fukuda, M., Barnes, A., Simon, E. S., Holmes, A., Dhawan, V., Giladi, N., et al. (2004). "Thalamic stimulation for parkinsonian tremor: correlation between regional cerebral blood flow and physiological tremor characteristics." Neuroimage 21(2): 608-615.

Giraud, A. L., Truy, E., Frackowiak, R. (2001). "Imaging plasticity in cochlear implant patients." Audiol Neurootol 6: 381-393.

Hariz, M., Blomstedt, P., Zrinzo, L. (2013). "Future of brain stimulation: new targets, new indications, new technology." Mov Disord 28(13): 1784-1792.

Herzog, H., Lamprecht, A., Kuhn, A., Roden, W., Vosteen, K. H., Feinendegen, L. E. (1991). "Cortical activation in profoundly deaf patients during cochlear implant stimulation demonstrated by H215O PET." J Comput Assist Tomogr 15(3): 369-375.

Hirano, S., Naito, Y., Kojima, H., Honjo, I., Inoue, M., Shoji, K., et al. (2000). "Functional differentiation of the auditory association area in prelingually deaf subjects." Auris Nasus Larynx 27: 303-310.

Hochmair-Desoyer, I., Schulz, E., Moser, L., Schmidt, M. (1997). "The HSM sentence test as a tool for evaluating the speech understanding in noise of cochlear implant users." The American journal of otology 18: S83.

Jakoby, B. W., Bercier, Y., Conti, M., Casey, M. E., Bendriem, B., Townsend, D. W. (2011). "Physical and clinical performance of the mCT time-of-flight PET/CT scanner." Phys Med Biol 56(8): 2375-2389.

Jana, J. J., Vaid, N., Shanbhag, J. (2013). "Effect of total intravenous anaesthesia on intraoperative monitoring of cochlear implant function in paediatric patients." Cochlear Implants Int 14(3): 169-173.

Johnsrude, I. S., Giraud, A. L., Frackowiak, R. S. (2002). "Functional imaging of the auditory system: the use of positron emission tomography." Audiol Neurootol 7: 251-276.

Kanno, I., Iida, H., Miura, S., Murakami, M. (1991). "Optimal scan time of oxygen-15-labeled water injection method for measurement of cerebral blood flow." J Nucl Med 32: 1931-1934.

Kerssens, C., Hamann, S., Peltier, S., Hu, X. P., Byas-Smith, M. G., Sebel, P. S. (2005). "Attenuated brain response to auditory word stimulation with sevoflurane: a functional magnetic resonance imaging study in humans." Anesthesiology 103(1): 11-19.

Klinge, P. A., Brooks, D. J., Samii, A., Weckesser, E., van den Hoff, J., Fricke, H., et al. (2008). "Correlates of local cerebral blood flow (CBF) in normal pressure hydrocephalus patients before and after shunting - A retrospective analysis of O-15 H2O PET-CBF studies in 65 patients." Clinical Neurology and Neurosurgery 110(4): 369-375.

Kreuer, S., Biedler, A., Larsen, R., Altmann, S., Wilhelm, W. (2003). "Narcotrend monitoring allows faster emergence and a reduction of drug consumption in propofol-remifentanil anesthesia." Anesthesiology 99(1): 34-41.

Lange, C., Suppa, P., Frings, L., Brenner, W., Spies, L., Buchert, R. (2015). "Optimization of Statistical Single Subject Analysis of Brain FDG PET for the Prognosis of Mild Cognitive Impairment-to-Alzheimer's Disease Conversion." J Alzheimers Dis 49(4): 945-959.

Lee, Y. S., Kim, J. S., Kim, K. M., Kang, J. H., Lim, S. M., Kim, H. J. (2014). "Performance measurement of PSF modeling reconstruction (True X) on Siemens Biograph TruePoint TrueV PET/CT." Ann Nucl Med 28(4): 340-348.

Lenarz, T., Lim, H. H., Reuter, G., Patrick, J. F., Lenarz, M. (2006). "The auditory midbrain implant: a new auditory prosthesis for neural deafness-concept and device description." Otol Neurotol 27: 838-843.

Matzke, K. H., Meyer, G. J., Hundeshagen, H. (1993). "An advanced system for the administration of 15O-water." J Labelled Comp Radiopharm 32: 459-460.

Mazziotta, J. C., Phelps, M. E. (1984). "Human sensory stimulation and deprivation: positron emission tomographic results and strategies." Ann Neurol 15 Suppl: S50-60.

Miyamoto, R. T., Wong, D., Pisoni, D. B., Hutchins, G., Sehgal, M., Fain, R. (1999). "Positron emission tomography in cochlear implant and auditory brain stem implant recipients." The American journal of otology 20: 596-601.

Morosan, P., Rademacher, J., Schleicher, A., Amunts, K., Schormann, T., Zilles, K. (2001). "Human primary auditory cortex: cytoarchitectonic subdivisions and mapping into a spatial reference system." Neuroimage 13(4): 684-701.

Morris, J. S., Friston, K. J., Dolan, R. J. (1998). "Experience-dependent modulation of tonotopic neural responses in human auditory cortex." Proc Biol Sci 265: 649-657.

Mortensen, M. V., Madsen, S., Gjedde, A. (2005). "Cortical responses to promontorial stimulation in postlingual deafness." Hear Res 209(1-2): 32-41.

Muzik, O., Chugani, D. C., Juhasz, C., Shen, C., Chugani, H. T. (2000). "Statistical parametric mapping: assessment of application in children." Neuroimage 12(5): 538-549.

Naito, Y., Okazawa, H., Honjo, I., Hirano, S., Takahashi, H., Shiomi, Y., et al. (1995). "Cortical activation with sound stimulation in cochlear implant users demonstrated by positron emission tomography." Brain Res Cogn Brain Res 2: 207-214.

Nishimura, H., Doi, K., Iwaki, T., Hashikawa, K., Oku, N., Teratani, T., et al. (2000). "Neural plasticity detected in short- and long-term cochlear implant users using PET." Neuroreport 11: 811-815.

Okazawa, H., Naito, Y., Yonekura, Y., Sadato, N., Hirano, S., Nishizawa, S., et al. (1996). "Cochlear implant efficiency in pre- and postlingually deaf subjects. A study with H215O and PET." Brain 119 (Pt 4: 1297-1306.

Petersen, S. E., Fox, P. T., Posner, M. I., Mintun, M., Raichle, M. E. (1988). "Positron emission tomographic studies of the cortical anatomy of single-word processing." Nature 331(6157): 585-589.

Plourde, G., Belin, P., Chartrand, D., Fiset, P., Backman, S. B., Xie, G., et al. (2006). "Cortical processing of complex auditory stimuli during alterations of consciousness with the general anesthetic propofol." Anesthesiology 104(3): 448-457.

Rajan, R., Dubaj, V., Reser, D. H., Rosa, M. G. (2013). "Auditory cortex of the marmoset monkey - complex responses to tones and vocalizations under opiate anaesthesia in core and belt areas." Eur J Neurosci 37(6): 924-941.

Reimold, M., Slifstein, M., Heinz, A., Mueller-Schauenburg, W., Bares, R. (2006). "Effect of spatial smoothing on t-maps: arguments for going back from t-maps to masked contrast images." J Cereb Blood Flow Metab 26(6): 751-759.

Schulz, G. M., Varga, M., Jeffires, K., Ludlow, C. L., Braun, A. R. (2005). "Functional neuroanatomy of human vocalization: an H215O PET study." Cereb Cortex 15(12): 1835-1847.

Schwartz, M. S., Otto, S. R., Shannon, R. V., Hitselberger, W. E., Brackmann, D. E. (2008). "Auditory brainstem implants." Neurotherapeutics 5(1): 128-136.

Schwender, D., Kaiser, A., Klasing, S., Peter, K., Poppel, E. (1994). "Midlatency auditory evoked potentials and explicit and implicit memory in patients undergoing cardiac surgery." Anesthesiology 80(3): 493-501.

Signorini, M., Paulesu, E., Friston, K., Perani, D., Colleluori, a., Lucignani, G., et al. (1999). "Rapid assessment of regional cerebral metabolic abnormalities in single subjects with quantitative and nonquantitative [18F]FDG PET: A clinical validation of statistical parametric mapping." Neuroimage 9: 63-80.

Silbersweig, D. A., Stern, E., Frith, C. D., Cahill, C., Schnorr, L., Grootoonk, S., et al. (1993). "Detection of thirty-second cognitive activations in single subjects with positron emission tomography: a new low-dose H215O regional cerebral blood flow three-dimensional imaging technique." J Cereb Blood Flow Metab 13(4): 617-629.

Talairach, J., Tournoux, P. "Co-Planar Stereotaxic Atlas of the Human Brain. Stuttgart: Thieme; 1988.

Vincenti, V., Bacciu, A., Guida, M., Marra, F., Bertoldi, B., Bacciu, S., et al. (2014). "Pediatric cochlear implantation: an update." Ital J Pediatr 40: 72.

Volkow, N. D., Mullani, N., Gould, L. K., Adler, S. S., Gatley, S. J. (1991). "Sensitivity of Measurements of Regional Brain Activation with Oxygen-15-Water and PET to Time of Stimulation and Period of Image Reconstruction." J Nucl Med 32(1): 58-61.

Warburton, E., Price, C. J., Swinburn, K., Wise, R. J. (1999). "Mechanisms of recovery from aphasia: evidence from positron emission tomography studies." J Neurol Neurosurg Psychiatry 66: 155-161.

3 Study II - Visualization of the auditory pathway in rats with ^{18}F-FDG PET

First published in 2018 in PLOS ONE, Vol. 13(10):e0205044, DOI: 10.1371/journal.pone.0205044

Citations, tables, figures, label and legends are formatted to adhere to a coherent style of the dissertation.

Visualization of the auditory pathway in rats with ^{18}F-FDG PET activation studies based on different auditory stimuli and reference conditions including cochlea ablation

Martin Mamach[1,2], Mariella Kessler[2,3], Jens P. Bankstahl[3], Florian Wilke[1], Lilli Geworski[1], Frank M. Bengel[3], Simone Kurt[2,4,5&], Georg Berding[2,3&]

[1] Department of Medical Physics and Radiation Protection, Hannover Medical School, Hannover, Germany

[2] Cluster of Excellence Hearing4all, Hannover Medical School, Hannover, Germany

[3] Department of Nuclear Medicine, Hannover Medical School, Hannover, Germany

[4] Department of Otolaryngology, Hannover Medical School, Hannover, Germany

[5] Department of Biophysics, Center for Integrative Physiology and Molecular Medicine CIPMM, Saarland University, Homburg, Germany

[&] Equal contribution

3.1 Abstract

Activation studies with positron emission tomography (PET) in auditory implant users explained some of the mechanisms underlying the variability of achieved speech comprehension. Since future developments of auditory implants will include studies in rodents, we aimed to inversely translate functional PET imaging to rats. In normal hearing rats, activity in auditory and non-auditory regions was studied using ^{18}F-fluorodeoxyglucose (^{18}F-FDG) PET with 3 different acoustic conditions: sound attenuated laboratory background, continuous white noise and rippled noise. Additionally, bilateral cochlea ablated animals were scanned. 3D image data were transferred into a stereotaxic standard space and evaluated using volume of interest (VOI) analyses and statistical parametric mapping (SPM). In normal hearing rats alongside the auditory pathway consistent activations of the nucleus cochlearis (NC), olivary complex (OC) and inferior colliculus (IC) were seen comparing stimuli with background. In this respect, no increased activation could be detected in the auditory cortex (AC), which even showed deactivation with white noise stimulation. Nevertheless, higher activity in the AC in normal hearing rats was observed for all 3 auditory conditions against the cochlea ablated status. Vice versa, in ablated status activity in the olfactory nucleus (ON) was higher compared to all auditory conditions in normal hearing rats. Our results indicate that activations can be demonstrated in normal hearing animals based on ^{18}F-FDG PET in nuclei along the central auditory pathway with different types of noise stimuli. However, in the AC missing activation with respect to the background advises the need for more rigorous background noise attenuation for non-invasive reference conditions. Finally, our data suggests cross-modal activation of the olfactory system following cochlea ablation – underlining, that ^{18}F-FDG PET appears to be well suited to study plasticity in rat models for cochlear implantation.

3.2 Keywords

PET, FDG, activation study, animals, rats, auditory, normal hearing, cochlea ablation

3.3 Introduction

Since their first clinical application in the early 1960s cochlear implants (CI) enabled a remarkable success story in the treatment of inner ear deafness [Wilson2008]. Nevertheless, the variability of individual performance in speech comprehension after CI implantation is not fully understood. In 30% of the cases, despite early implantation in childhood, the expected hearing performance is not achieved – without explanation in 78% of these [Niparko2010, Lazard2012, Blamey2015]. In this context, functional neuroimaging after implantation using positron emission tomography (PET) improved already the pathophysiologic understanding of underlying plasticity in specialized auditory regions as well as at the level of neuronal circuits required for a successful outcome [Giraud2001, Ruytjens2006, Berding2015]. Nevertheless, since it is complicated to address some of the basic factors related to the success of cochlear implantation in patients, like it is done e.g. in molecular biological / proteomics research, animal models and related diagnostic approaches are required. Specifically, cochlear implantation has been implemented in rats – chosen due to their low mortality rate following surgical intervention and the extensive auditory research already performed in this species [Lu2005, Hsu2009]. With respect to diagnostic approaches for rat brain imaging, PET achieved sufficient spatial resolution with the development of dedicated small animal scanners about 15 years ago [Constantinescu2009]. Subsequently, specific tools e.g. stereotaxic VOI atlases for spatial assignment of specific effects have been developed [Schiffer2006, Schwarz2006]. For auditory research, this technique has mostly been used employing ^{18}F-2-fluoro-2-deoxy-D-glucose (^{18}F-FDG) as a marker of neuronal activity. Auditory and visual stimuli as well as cochlea ablation and tinnitus condition have been investigated [Hsu2009, Paul2009, Soto-Montenegro2009, Jang2012]. However, these were pioneering studies, demonstrating the general potential of the methodology, but including shortcomings with respect to the development of ^{18}F-FDG PET as a standardized quantitative diagnostic method to serve in the further development of treatment options for hearing loss in particular via rat models of cochlear implantation. Shortcomings include for example: (i) no consideration of adaptation to stimulation paradigms, (ii) lack of standardization of environment with background or reference conditions, (iii) lack of comparison to bilateral complete hearing loss as absolute reference in order to estimate observed effects sizes and (iv) no exclusion / proof of effects due to auditory stimulation in non-auditory regions (including potential cross-modal activations).

To address these questions, we (i) used refined stimuli designed to avoid adaptation which were previously employed in electrophysiology [Laudanski2012], (ii) utilized a sound attenuating box as environmental standardization and tested with 2 possible auditory baseline conditions, (iii) added longitudinal tests after bilateral cochlea ablation as physiological baseline for a subset of animals and (iv) implemented a volume of interest

(VOI) template for automated spatial assignment and relative quantification of effects in 5 essential brain structures of the auditory system and additionally 3 reference brain regions.

3.4 Methods

This study was approved by the Lower Saxony State Office for Consumer Protection and Food Safety (LAVES, ID: 33.14-42502-04-14/1625) in accordance with German and European regulations for animal experiments. Part of this approval was validation by an ethics committee of the LAVES. This study was designed and is reported in accordance with the ARRIVE guidelines [Kilkenny2010].

3.4.1 Animals

In this study 12 healthy, normal hearing, young adult, female Sprague-Dawley rats (Charles River, Sulzfeld, Germany) in 2 groups of 6 animals were included. The animals were 16 weeks old when bought and were habituated to the laboratory environment for 1 week and trained for 3 additional weeks for habituation to the acoustic stimulation setup. All animals were housed in pairs in individually ventilated cages with (50±5) % humidity at (22±1) °C with 14-10 hours day-night cycle. They had ad libitum access to autoclaved tap water and a standard laboratory diet (1324 TPF, Altromin, Lage, Germany). The rats (weight 289 g ± 19 g) were scanned at ages 20-39 weeks.

3.4.2 Experimental procedure

Figure 11a) illustrates the general experimental setup in a timeline.

Figure 11b) shows the timing of the applied acoustic conditions, tracer injection and subsequent ^{18}F-FDG PET imaging. The animals were shortly anesthetized with an isoflurane (FORENE, AbbVie, Wiesbaden, Germany) in humidified oxygen for placement of an intravenous (i.v.) catheter into a tail vein and afterwards placed into the restriction tube into the sound attenuation box. The anesthesia was initialized with 3 % isoflurane concentration and a flow of 3 l/min. After a wake-up period of 10 min, the box (Figure 12) was fully closed and the sound level reduced to unavoidable background noises for 14 min. Subsequently, an auditory condition was started lasting for 41 min. 60 sec after the start, ^{18}F-FDG was applied as bolus injection with a closed box into the tail vein via a catheter. After the condition ended, the animals were anesthetized again with isoflurane and scanned 1 h post injection. In continuous anesthesia, the concentration of isoflurane was reduced to 1-2 % and the flow to 0.8 – 1.0 l/min according to a target respiratory rate of 30 - 40 rpm. The animals were warmed during anesthesia.

All animals were placed into their home cages when fully awake. Between imaging sessions, a resting period of at least 2 days was kept for each individual animal.

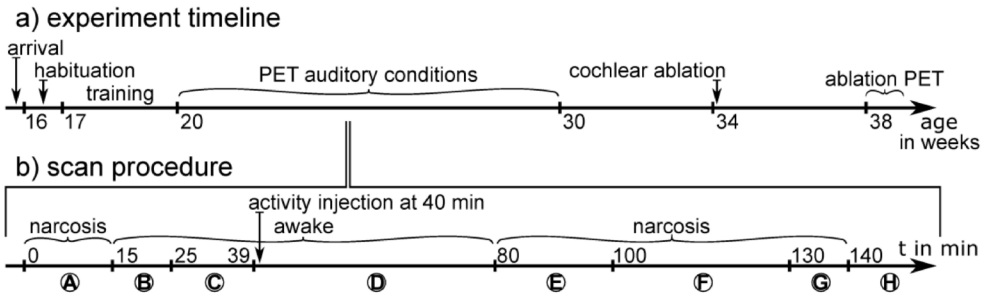


Figure 11 Timelines for a) general experimental setup and b) a single scan procedure. The scan procedure includes (A) placement of the tail vein catheter and insertion of the rat in the restriction tube into the box, (B) wake-up period, (C) adaption period to sound deprivation, (D) acoustic conditions, (E) preparation for scan, (F) PET scan, (G) CT scan and (H) the return to the home cage.

All 12 animals were exposed to all auditory conditions. Since we could scan on average 3 animals per day, 4 subgroups were built for pseudo-randomization of the order of animals (A, B and C) and stimulation conditions (1, 2 and 3) on three scan days. On these days the order of animals and conditions complied with the following rules: (1) each animal was scanned at first, second and third position on different scanning days, (2) at each scanning day all stimulation conditions were presented at a different position. A typical sequence of animals and conditions would be: Scanning day 1: A1 B2 C3; day 2: C2 A3 B1 and day 3: B3 C1 A2. After completion of the entire study we confirmed in a statistical analysis (ANOVA) the independence of the PET uptake values from the order of stimulus presentation ($p > F: 0.5670$) and order of animals ($p > F: 0.5716$). With respect to the status of cochlear ablation – since auditory stimulation conditions are only possible before ablation, this status had always to be performed last. After the completion of all experiments, animals were sacrificed by cervical dislocation in isoflurane anesthesia.

3.4.3 Conditions

3.4.3.1 Stimulation environment

All auditory conditions were applied in a standardized acoustic environment consisting of a transparent motion restriction tube placed in an unlit custom made sound-attenuating box as shown in Figure 12. Opening on the top and the front of the restriction tube enable acoustic stimulation and a notch in the hatch enables access to the tail for i.v. administration. The length and diameter of the tube were designed to ensure maximal comfort for the animals after habituation training, but to avoid turning around or considerable backward of forward movement. The box reduced default laboratory

background noises by 10 dB to 55 dB SPL (decibel sound pressure level) as measured with Brüel & Kjær 2636 amplifier (Brüel & Kjær, Bremen, Germany) and condenser microphone 4135 (Brüel & Kjær, Bremen, Germany) on a representative position in the restriction tube. This ensured similar acoustic conditions across all conditions via a closable opening directly above the tube indicated in Figure 12. In the lid a Wavemaster Mobi 2 speaker (Wavemaster, Bremen, Germany) was placed. The animals were observed in the closed box via an infrared camera (Syngonix 43176Y, Nürnberg, Germany) to ensure their well-being and complication-free application. The box was always placed in the same room with controlled climatic environment. All procedures were done by the same staff creating per se constant acoustic, climatic and olfactory conditions.

3.4.3.2 Training

As stress would affect the performance of the animals during awake acoustic stimulation, all animals were trained to this environment over 3 weeks. To familiarize the rat with the setup, they were placed in the motion restriction tube and box three times awake on subsequent day. Further habituation to waking up in the setup was performed twice under initial isoflurane anesthesia. In each training session, the animals were in the box in the tube for a 10 min wake-up period and 20 min of training conditions were applied. No catheters were applied or sham injections performed during training sessions as this was seen as unnecessary burden. Additionally, both way open tubes made of the same material with similar diameters and lengths were placed into the home cages for enrichment and habituation.

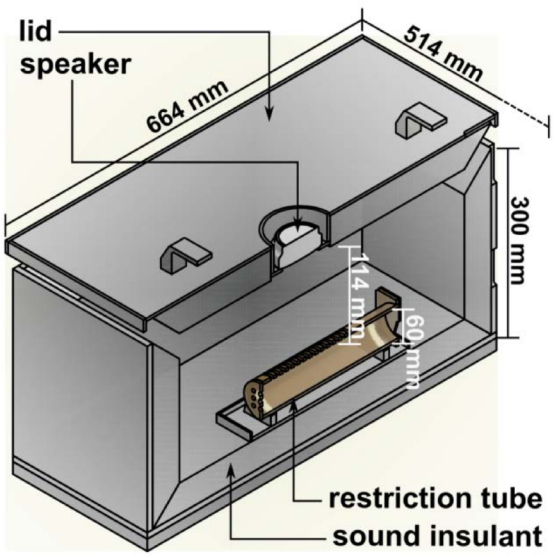


Figure 12 Schematic view of the custom-made sound-attenuating box. The speaker is placed in the cover lid. Holes in the front, top and end of the animal restriction tube allowed respectively for sufficient ventilation, sound permeability and access to the tail of the animals.

3.4.3.3 Auditory Conditions

Three auditory conditions were selected in this study to provide different effects with respect to (i) adaptation to the stimulus and (ii) degree of activation achieved in auditory brain regions. Conditions are identified by the type of noise (two letters) and the sound pressure level in brackets.

Condition 1: Background noise - *BG(55dB)*

Condition 2: Continuous white noise - *WN(65dB)*

Condition 3: Pulsed rippled noise - *RN(95dB),* consisting of broadband randomized frequency depending phase and amplitude modulations for 500 ms followed by 200 ms silence [Laudanski2012]

Proceeding from these conditions, an additional condition was constructed with slight modifications for training purposes in order to avoid adaptation effects to the auditory conditions. In order to avoid habituation to specific frequency pattern or loudness, a white noise stimulus with intermediate loudness was used in the training sessions. The purpose was to train the animals to a noisy environment without adapting to the specific stimulus. The laboratory background was used in order to train a stimulus-free environment. We alternately exposed the animals during the training to the respective conditions for a very limited duration (5 min) in comparison to the much longer exposure during FDG uptake phase for prevention of adaptation to the stimuli.

Training condition: 4 min *BG(55dB)* + 5 min *WN(75dB)* + 5 min *BG(55dB)* + 5 min *WN(75dB)* + 1 min *BG(55dB)*

All auditory stimuli were prepared using the open-source-software Audacity 2.0.5. The sound levels in dB SPL were measured using Brüel & Kjær 2636 amplifier (Brüel & Kjær, Bremen, Germany) and a condenser microphone 4135 (Brüel & Kjær, Bremen, Germany) placed within the restriction tube at an ear-representative location.

3.4.4 Cochlea ablation

Bilateral cochlea ablations (*ABL*) were included as a reference of complete deprivation of the auditory system and therefore better assessment of differences in normal hearing animals due to different auditory conditions. The cochlea ablations were performed on 6 animals after their completion PET scans of the auditory conditions as described in Deutscher et al.[Deutscher2006]. 1 animal died after surgery resulting in 5 animals for which pairwise analysis was possible. Under anesthesia using a mix of 80 mg/kg keta-

mine (Ketamin, WDT, Garbsen, Germany) and 5 mg/kg xylazine (Sedaxylan, WDT, Garbsen, Germany) the skin was opened over the bulla tympanica and muscles were moved to reveal the bulla. Via a small drill, the bulla was opened and the organ of Corti destroyed with a sterile needle. An antibacterial salve (Tyrosur, Engelhard Arzneimittel, Niederdorfelden, Germany) was inserted into the bulla to avoid infections. The bulla opening was closed by applying composite glue (Tetric EvoFlow, Ivoclar Vivadent AG, Schaan, Liechtenstein), suture material (Ethicon, Johnson & Johnsen Medical GmbH, Norderstedt, Germany) and Histoacryl (B.Braun, Melsungen, Germany). To provide analgesic care, metamizole (Novaminsulfon 500mg Lichtenstein, Zentiva, Prague, Czechia) was added to the drinking water 2 days preoperative for max. 2 weeks and given subcutaneously after the operation (200 mg/kg metamizole). PET imaging was performed 3-4 weeks after ablation.

3.4.5 PET/CT imaging

All rats were imaged using a hybrid Inveon PET/CT system (Siemens AG, Berlin, Germany). A dose of 18.2±0.7 MBq of the radiotracer ^{18}F-FDG was injected i.v. via the lateral tail vein catheter. A 30 min PET list mode scan was started 1 h post injection and reconstructed using an OSEM3D follow by FastMAP iterative reconstruction algorithm. After two OSEM3D iterations, FastMAP generated an image of 128x128x159 voxels with a voxel size of 0.776 mm x 0.776 mm x 0.796 mm using 18 iterations and 16 subsets. A ^{57}Co-transmission based attenuation correction was applied during reconstruction. PET acquisitions were followed by CT imaging using a tube voltage of 80 kV, a current of 500 µA and 120 ms exposure time of the head acquired in continuous rotation (full rotation with 180 projections) and reconstructed as filtered back projection using a Feldkamp algorithm and Shepp-Logan filter with 0.5 cutoff. The resulting CTs had a size of 512x512x512 voxels with a resolution of $[0.096\ mm]^3$ and were used to validate coregistration.

3.4.6 Data analysis

For a regional statistical analysis on group level, brain regions were extracted using a VOI atlas for rats [Schwarz2006] adapted to a rat ^{18}F-FDG image template [Schiffer2006] via corresponding MR images. Additional VOIs were drawn according to the Paxinos and Watson rat brain atlas [Paxinos1998]. The images were processed using PMOD3.6 software (PMOD Technologies, Zurich, Switzerland). Individual images were manually pre-aligned and followed by rigid-matching to the FDG. These spatially normalized images were then cropped to include the brain within a matrix of 93x93x120 voxels with a voxel size of $[0.2\ mm]^3$ as given by the template. In line with clinical methods, the image values were normalized to the observed average whole brain activity for further analysis.

We evaluated the activities in VOIs of the nucleus cochlearis (NC), the olivary complex (OC), the inferior colliculus (IC), the medial geniculate body (MGB) and the auditory cortex (AC) as auditory target regions. The somatosensory cortex (SC), cerebellum (CB) and olfactory nucleus (ON) were used as non-auditory control regions. All VOIs were analyzed in individually paired t-tests of two respective auditory conditions for all animals. All positions of coronal slides are given with reference to the ^{18}F-FDG templates bregma coordinates [Schiffer2006]. Additionally, statistical parametric maps (SPM) including significantly activated or deactivated voxels at a threshold of $p<0.001$ without correction for multiple comparisons were generated based on normalized images by comparing conditions using pairwise t-testing in SPM8.0 (Wellcome Department of Cognitive Neurology, London, UK). These analyses were chosen as in preliminary analysis with $p<0.05$ and FEW corrections no supra-threshold voxels were found in the target region of the auditory cortex. A minimum fraction of activated voxels of 1 % of the VOI was selected as extent threshold to account for random effects. The actual percentage of activated voxels in a VOI was called coverage, and listed for each comparison of conditions alongside with the T_{max}-values and the ratio of T_{max} to T-value at $p<0.001$ for assessment of extent and peak height of differences between different auditory conditions.

3.5 Results

The used stimuli and applied reference condition determined which sub-regions of the auditory system revealed activation respectively. For individually analyzed animals activations were only observable in up to two regions, while group analyses revealed activations in up to 4 of 5 evaluated auditory regions.

3.5.1 Individual analysis

In individual images, higher normalized ^{18}F-FDG uptake could be visually assessed for RN(95dB) stimulation in IC and AC, while no distinct difference to other conditions was detected in MGB, NC or OC. In individual difference images of RN(95dB) and BG(55dB) which had the largest sound level difference in normal hearing animals in our experiment, visual activation evidences were limited to the IC (images not shown). Therefore group analyses were required. Figure 13 shows corresponding average images based on all individual images for each auditory condition.

3.5.2 VOI analyses

In Table 5, mean percent differences in normalized uptake between stimulated and reference conditions are given for auditory and non-auditory VOIs. Significant differences indicated with grey background in Table 5.

Using BG(55dB) as a reference, stimulation with either RN(95dB) or WN(65dB) resulted into significant activation in IC, OC and NC. The highest activation by (15.6±3.6) % occurred in the IC. No increase in activation could be seen with the BG(55dB) referencein the AC. Instead, stimulation by WN(65dB) induced a low but significant deactivation compared to BG(55dB) (-2.8±1.6) %, which formally introduced an increased activation, if RN(95dB) is compared to WN(65dB). Moreover, MGB activation was only induced by RN(95dB) but not with WN(65dB) stimulation. In normal hearing animals (i.e. without cochlea ablation) neither activation nor deactivation could be observed in non-auditory regions (SC, CB ON).

Employing ABL as reference condition, significant activations were observed with all other conditions (RN(95dB), WN(65dB) and BG(55dB)) in IC, OC and AC. Activations were considerably higher for all three regions – e.g. (35.0±3.8) % in the mean with RN(95dB) in IC – in comparison to those obtained with BG(55dB) as reference (15.6±3.6) %. Moreover, no activation was seen consistently in MGB – and in NC activation was only observed with RN(95dB). With respect to non-auditory regions, activity in ON was significantly higher in ABL condition compared to all acoustic conditions in healthy rats (> 20 % in the mean, see Table 5 – negative algebraic sign there, for the comparison RN(95dB) - ABL indicate higher values for ABL condition). For all other non-auditory regions no activation or deactivation was found.

3.5.3 SPM results

Corresponding to the comparisons carried out at a VOI level, pairwise voxel-based analyses were performed using SPM8.0. The results are given in Table 6 and Figure 14. They resemble by and large those obtained in VOI analyses. Maximum T-values are shown in Table 6. For improved comparability of activation strength between condition-comparisons and between anatomical regions, Table 6 contains additionally a T_{max}-fraction with respect to the corresponding T-threshold for $p<0.001$ and the percentage of voxels significantly activated in the respective VOI (i.e. the coverage).

With BG(55dB) as a reference, SPM revealed in healthy animals like VOI analyses for RN or WN as stimulation condition significant activations in IC, OC and NC. Up to 89 % of the IC-VOI were covered with T_{max} being 2.66 times of the $T_{p=0.001}$ threshold. The nearly total coverage/activation of the IC due to RN(95dB) stimulation vs. BG(55dB) is illustrated in Figure 14 by representative slices of the SPM overlaid to CT and VOI outlines (1st column, 1st and 2nd row). Moreover, as in VOI analyses, SPM showed a deactivation of the AC under WN(65dB) stimulation compared to BG(55dB) (coverage 3%) and MGB activation induced by RN(95dB) but not with WN(65dB) stimulation.

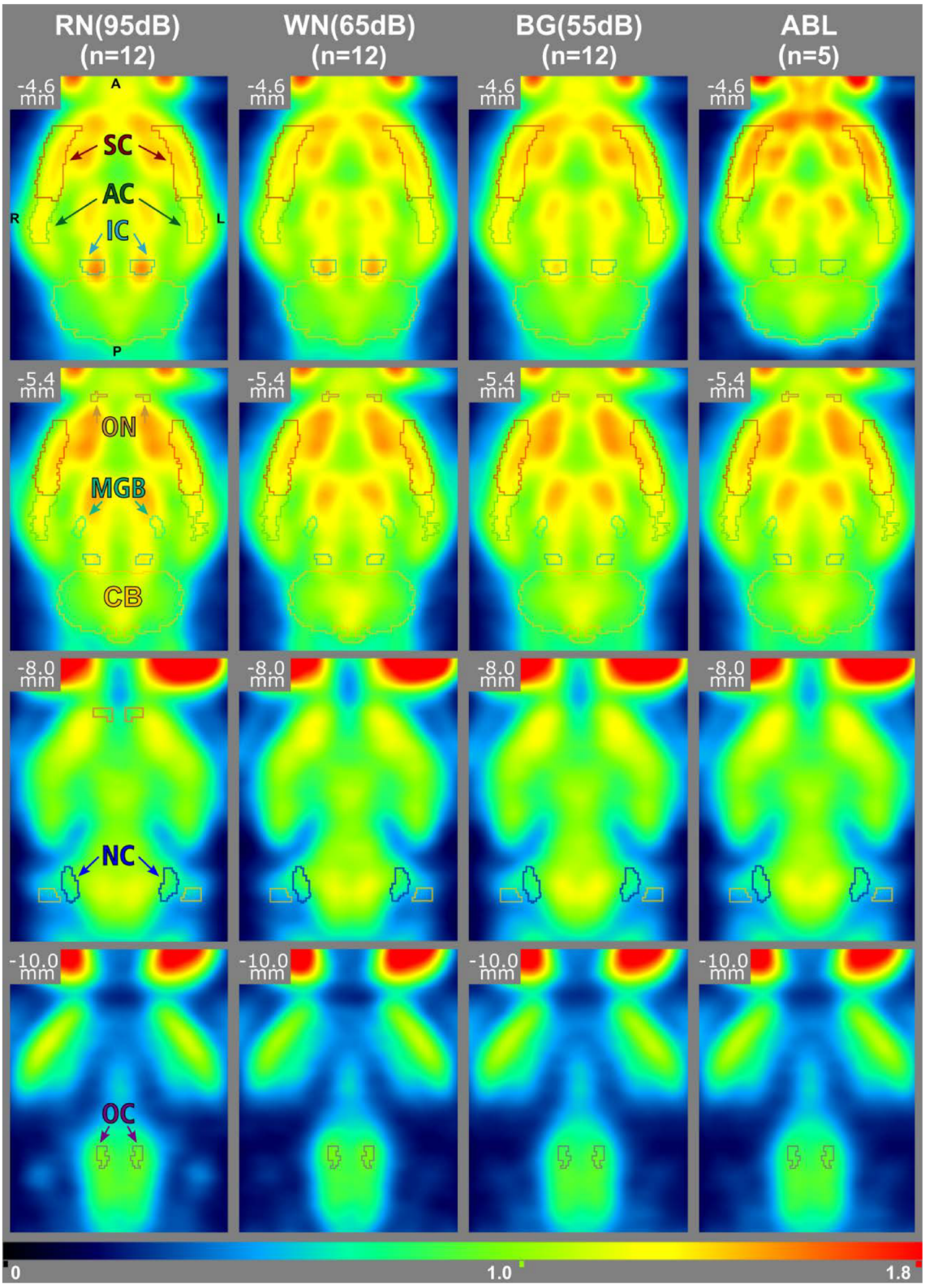


Figure 13 Mean normalized images for all conditions and in different coronal levels. Different activation can be visually assessed in different regions (AC – auditory cortex, IC – inferior colliculus, MGB – mediate geniculate body, OC – olivary cortex, NC – nucleus cochlearis, SC – somatosensory cortex, CB – cerebellum, ON – olfactory nucleus). The activation of the IC shown in the first two rows is strongest for the rippled noise stimulus RN(95dB) and visible with white noise WN(65dB). It is reduced to the brain mean with laboratory background BG(55dB) and below mean after ablation ABL.

Table 5 Mean and standard deviation (SD) of pairwise differences of average normalized VOI values shown for all comparisons of conditions.

	RN – BG (n=12)		RN – WN (n=12)		WN – BG (n=12)		RN – ABL (n=5)		WN – ABL (n=5)		BG – ABL (n=5)	
	Mean SD	p-Value	Mean SD	p-Value	Mean SD	p-Value	Mean SD	p-Value	Mean SD	p-Value	Mean SD	p-Value
AC	(0.0±2.4) %	0.9943	(2.8±3.1) %	0.0101	(-2.8±1.6) %	0.0001	(10.0±3.1) %	0.0018	(6.5±2.4) %	0.0036	(10.0±2.1) %	0.0004
IC	(15.6±3.6) %	0.0001	(3.1±7.4) %	0.1817	(12.5±6.4) %	0.0001	(35.0±3.8) %	0.0001	(27.5±5.7) %	0.0004	(18.4±4.3) %	0.0007
MGB	(6.1±3.4) %	0.0001	(5.6±3.5) %	0.0002	(0.6±2.6) %	0.4591	(8.0±7.1) %	0.0649	(2.6±6.9) %	0.4524	(1.8±6.4) %	0.5614
OC	(6.3±9.7) %	0.0445	(-0.5±6.3) %	0.7829	(6.9±9.0) %	0.0223	(20.3±9.1) %	0.0075	(17.8±9.2) %	0.0125	(8.2±6.5) %	0.0485
NC	(6.6±4.6) %	0.0004	(2.0±3.5) %	0.0761	(4.6±5.1) %	0.0091	(14.5±8.2) %	0.0168	(11.0±9.5) %	0.0600	(6.1±7.8) %	0.1572
SC	(-1.5±3.2) %	0.1278	(-1.2±3.8) %	0.2934	(-0.3±2.0) %	0.5881	(-3.1±3.4) %	0.1115	(-3.1±3.7) %	0.1684	(-2.0±2.6) %	0.1369
CB	(0.6±3.9) %	0.6053	(-0.8±4.1) %	0.5220	(1.4±2.9) %	0.1208	(1.3±3.1) %	0.4157	(1.5±2.3) %	0.2158	(-0.3±3.2) %	0.8448
ON	(0.6±6.3) %	0.7598	(1.4±5.5) %	0.3835	(-0.9±2.7) %	0.2958	(-23.4±6.7) %	0.0014	(-21.9±8.0) %	0.0037	(-20.5±7.9) %	0.0044

The corresponding p-values are shown and significances of $p<0.05$ are highlighted by grey shading. In normal hearing animals (RN – rippled noise, WN – white noise, BG - laboratory background), different auditory structures (AC – auditory cortex, IC – inferior colliculus, MGB – mediate geniculate body, OC – olivary cortex, NC – nucleus cochlearis) are significantly activated for different comparisons. In non-auditory regions (regions (SC – somatosensory cortex, CB – cerebellum, ON – olfactory nucleus), significant deactivation shown by the negative values are only detected comparing to ablation (ABL).

Table 6 T-values and coverage of VOIs for each condition comparison with SPM

	RN – BG (n=12)			RN - WN (n=12)			WN - BG (n=12)			RN - ABL (n=5)			WN - ABL (n=5)			BG - ABL (n=5)		
	$T_{\max}$	$\frac{T_{\max}}{T_{p=0.001}}$	Cov.	$T_{\max}$	$\frac{T_{\max}}{T_{p=0.001}}$	Cov.	$T_{\max}$	$\frac{T_{\max}}{T_{p=0.001}}$	Cov.	$T_{\max}$	$\frac{T_{\max}}{T_{p=0.001}}$	Cov.	$T_{\max}$	$\frac{T_{\max}}{T_{p=0.001}}$	Cov.	$T_{\max}$	$\frac{T_{\max}}{T_{p=0.001}}$	Cov.
AC			<1%			<1%	-5.47	-1.36	3%	17.06	2.38	6%	12.09	1.69	3%	14.73	2.05	7%
IC	10.70	2.66	89%	5.43	1.35	5%	8.23	2.04	55%	33.70	4.70	67%	22.99	3.20	32%	14.39	2.01	15%
MGB	5.49	1.36	16%	5.83	1.45	14%			<1%			<1%			<1%			<1%
OC	4.77	1.19	5%			<1%	5.43	1.35	15%	13.24	1.85	12%	8.32	1.16	3%			<1%
NC	5.71	1.42	5%			<1%	5.53	1.37	2%			<1%			<1%			<1%
SC			<1%			<1%			<1%			<1%	-12.85	-1.79	1%			<1%
CB			<1%			<1%			<1%			<1%			<1%			<1%
ON			<1%			<1%			<1%	-19.58	-2.73	39%	-14.30	-1.99	26%	-13.38	-1.86	20%

(Cov.) shows the coverage of the corresponding VOIs with significant activated voxel according to SPM for all auditory regions (AC – auditory cortex, IC – inferior colliculus, MGB – mediate geniculate body, OC – olivary cortex, NC – nucleus cochlearis) and control regions (SC – somatosensory cortex, CB – cerebellum, ON – olfactory nucleus). Negative T-values indicate higher activity in the second condition (RN – rippled noise, WN – white noise, BG - laboratory background, ABL – cochlea ablation). An activation threshold of 1% of the corresponding VOI was assumed to account for random activations.

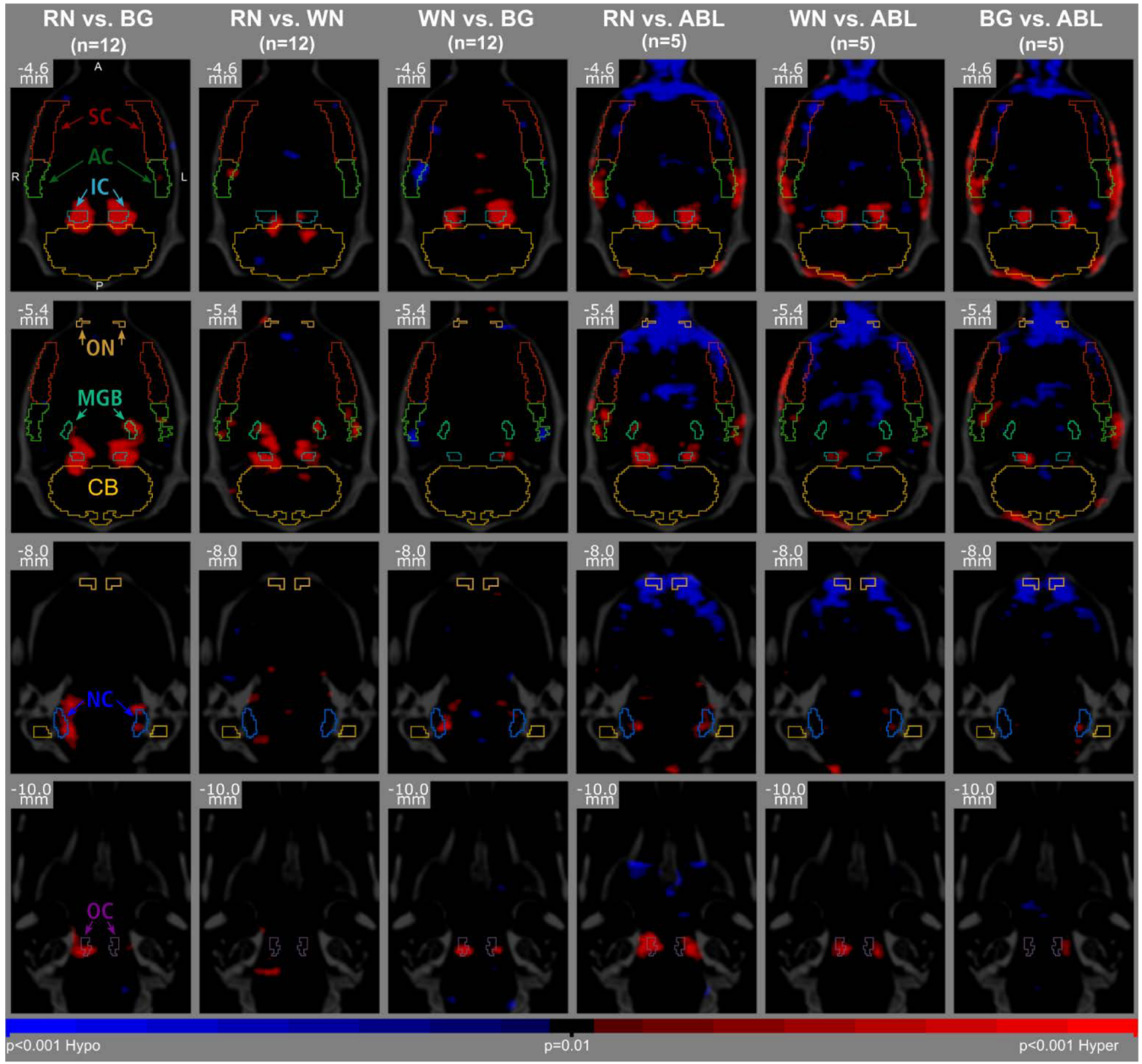


Figure 14 Results of voxel-wise pairwise comparison in SPM. The first 3 columns show all comparison of auditory conditions in normal hearing animals (RN – rippled noise, WN – white noise, BG - laboratory background) and the last 3 columns show all comparisons with respect to cochlea ablation (ABL). Red shows significantly increased ^{18}F-FDG uptake of the first condition versus the second, while blue shows respectively decreased uptake comparing first to second condition in the corresponding regions (AC – auditory cortex, IC – inferior colliculus, MGB – mediate geniculate body, OC – olivary cortex, NC – nucleus cochlearis, SC – somatosensory cortex, CB – cerebellum, ON – olfactory nucleus).

Bilateral deactivation in the AC (due to WN(65dB) stimulus against BG(55dB)) can also be spotted in Figure 14 (3rd column, 2nd row). Furthermore in line with VOI analyses, neither activation nor deactivation could be in SPM analyses for non-auditory regions (SC, CB and ON) of normal hearing animals.

Employing ABL as reference condition in SPM analyses nearly identically to VOI analyses significant activations could be observed with all other conditions (RN(95dB), WN(65dB) and BG(55dB)) in IC, OC and AC. The only exception was a lack of activation in OC due to BG(55) condition. This can also be extracted from Figure 14, showing activations with all conditions (RN(95dB), WN(65dB) and BG(55dB)) in IC and AC (column 4-6, row 1-2), and in OC only with RN(95dB) and WN(65dB) but not with BG(55dB) according to the VOI atlas (column 4-6, row 4). Significant activations in the above three regions were at a considerably higher level (according to T_{max}-fractions) with ABL compared to BG(55dB) reference – e.g. for the IC and RN(95dB) stimulation 4.70 vs. 2.66.

Moreover, SPM analyses with ABL reference did not reveal any activation in MGB or NC. With respect to non-auditory regions - again in line with VOI analyses - SPM detected significantly higher activity in ON in ABL condition compared to all acoustic conditions in healthy rats (T_{max}-fractions -1.86 to -2.73). SPMs displayed in Figure 14 show, that these "activations" due to ABL condition (recognizable in blue as "deactivations" during stimulation) considerably exceed the ON into the frontal cortex (column 4-6, rows 1-3).

3.6 Discussion

3.6.1 Activation of the auditory system in normal hearing rats and differences to humans

Using ^{18}F-FDG PET, we were able to show activations in several anatomical structures along the central auditory pathway of normal hearing rats. Likewise Jang et al. [Jang2012] employed ^{18}F-FDG PET to study stimulus-related changes of activity in the same regions of the central auditory pathway as we did. However in their study white noise stimuli at different sound pressure levels between 40 dB (for reference) and 100 dB (strongest stimulus) were applied. This type of stimulus is different compared to the pulsed rippled noise used as strongest stimulus in our study. We chose a lesser sound pressure level (95 dB) as prolonged 100 dB stimulation can induce noise trauma in rats [Abbott1999, Rao2000] and shows negative effects even with short exposure [Clark1991, Kujawa2009]. Nevertheless, considering results obtained with the strongest stimuli, both studies demonstrate significant activations in the NC, the OC and the IC –

reaching up to 15 % in the mean. Moreover, we detected a significant increase in MGB, which was reported only not-significant by Jang et al. [Jang2012].

Different results with strongest stimuli were observed for AC with no change in our study (±0 %) and a significant decrease of more than -5 % in the mean in Jang's study [Jang2012]. Nonetheless, we observed a less pronounced but significant reduction of activity in the AC (-3 %) with the less strong 65dB white noise stimulus similar to Jang's observation at 80dB [Jang2012]. These findings of reduced activity in the AC due to white noise stimulation might be explained by adaptation to this uniform stimulus presented in both studies for 30 min [Wehr2005]. The lesser reduction with our lower stimulus intensity fits the intensity related reduction observed by Jang et al. [Jang2012]. The lack of reduced activity in AC due to stimulation with the more complex pulsed rippled noise used by us is most likely due to the nature of this stimulus. It is characterized by temporal and spectral modulations varying randomly through time (representative for a multi-component signal) in a way that matches aspects of animal vocalization. Therefore adaptation effects are to be expected in a lesser amount [Laudanski2012]. Besides that, the observation of activations in subcortical structures (NC, OC, IC) in contrast to AC (made in our and Jang's study) despite using white noise stimuli might be explained by the fact that synaptic depression by habituation mostly occurs in cortical areas [Zucker2002].

On the other side, the lack of AC activation in rats might in addition have species-specific reasons. In humans, activation of the AC due to different and not specifically adaptation-avoiding stimuli presented during ^{18}F-FDG uptake phase has been demonstrated [Pietrini2000, Parellada2008, Chonde2013]. Furthermore one might speculate that limitations in demonstrating AC activation in rats (and subcortical structures in humans) can be related to the respective sizes of these structures in relation to the spatial resolution of the respective PET equipment. The diameter of AC in humans (≈ 50 mm) equals approximately 7-times the spatial resolution (FWHM ≈ 7 mm) while in rats (AC ≈ 3.2 mm) it is only 2-times (FWHM ≈ 1.5 mm) [Lancaster2000, Schwarz2006, Constantinescu2009, Mamach2018]. Therefore, the expected loss of signal from AC due to partial volume effects is much higher in rats compared to humans [Knoop2002]. Vice versa, the diameter of subcortical structures like the MGB in rats (≈ 1.5 mm) equals approximately at least the spatial resolution, while in humans (≈ 4.5 mm) it corresponds to only 0.6-times the resolution [Lancaster2000, Schwarz2006, Constantinescu2009, Mamach2018]. Consequently, the expected loss of signal from MGB and/or other subcortical structures due to partial volume effects in humans exceeds that in rats[Knoop2002]. In fact, the recovery of signal from activation of subcortical auditory structures in humans seems to be so low that it has only rarely been reported by now [Giraud2001], which is the strength of using animal models. Nevertheless, it should in general be possible to detect activation in subcortical structures in hu-

mans much better using the most recent PET technology with a spatial resolution approaching the diameter of these structures [Rausch2015].

3.6.2 Findings after cochlea ablation in rats

Effects of cochlea ablation on activity in the central auditory pathway and cortex have been previously studied using ^{14}C-2-Deoxyglucose (2-DG) ex-vivo autoradiography [Ahn2004] and ^{18}F-FDG PET [Hsu2009]. Ahn et al. [Ahn2004] performed bilateral cochlea ablation in rats and injected 2-DG under ambient noise. They observed a significant reduction of 2-DG uptake (compared to normal rats) in AC at 2 and 8 weeks post-ablation and IC at 2 and 4 weeks post-ablation – more pronounced in the latter region – and no significant change at 1 and 28 weeks post-ablation. Furthermore, in the MGB significant reduction was only found 2 weeks post-operatively. Our finding of significantly lower ^{18}F-FDG uptake in AC and IC together with no significant change in MGB four weeks after ablation compared to measurements during background noise condition preoperatively correspond to the changes observed in these regions by Ahn et al. [Ahn2004]. In our study uptake reductions were most pronounced in the IC as well. In addition, we could demonstrate reduced activity in the OC after cochlea ablation. Hsu et al. [Hsu2009] compared after unilateral cochlea ablation ipsilateral and contralateral activity in AC and IC – during ambient noise condition and stimulation 50-60 dB SPL above the ambient noise (i.e. with 115 dB). Ratios expressing activity during ambient noise on the side mainly associated with the preserved cochlea against activity on the side mainly associated with the ablated cochlea equaled 1.24±0.08 for the IC and 1.18±0.07 for the AC. Acoustic stimulation increase activity in the IC to 1.36±0.14 but not in the AC. These results are basically well in line with our present results. Likewise, we observed (compared to cochlea ablated status) higher activity due to ambient noise (BG(55dB)) preoperatively in the IC as compared to the AC (18±4 % vs. 10±2 %) and an increase due to auditory stimulation (RN(95dB)) for the IC (35±4 %) but not for the AC (10±3 %). SC and CB as reference regions showed (as expected) no significant change due to auditory stimulation and after cochlea ablation. On the contrary, an increase in activity of more than 20 % after ablation in comparison to each of the three auditory conditions preoperatively was seen in the ON. Such extra-auditory effects were not described in the studies of Ahn et al. [Ahn2004] and Hsu et al. [Hsu2009]. It is known particularly for the visual and auditory system that deprivation of sensory input to one sense can lead to cross-modal neuronal plastic changes with enhanced activity in cortex region primarily belonging to the other sense [Arno2001, Merabet2010]. With respect to the olfactory system, a regulatory impact of the auditory system via a noradrenergic cortical modulation on the olfactory system has been demonstrated in a learning paradigm [Smith2009]. Furthermore, based on behavior tasks and local field potential recordings, Zhou et al. [Zhou2017] showed that cross-modal enhancement of olfac-

tory perception was present 7 days after visual deprivation. We observed this analogously in our study while testing in a dark environment. A corresponding effect of higher olfactory activity about 22 % after cochlea ablation was found.

3.6.3 Limitations

As ^{18}F-FDG PET is performed as an integrative measure over 30min, detection probability of cortical activation of small regions, such as single cells, or with low frequency of activation is only limited. Visualization of information transmission by sparse coding as discussed for the AC [Willmore2009] might not be possible with ^{18}F-FDG-PET.

Furthermore, use of standard VOI atlases in analyses might result in misalignment and low coverage due to the variability among animals even of the same breed. For small regions, this could cause loss of detected activations which are identifiable in SPM by visual assessment. In our study, the SPM results displayed in Figure 14 (column 6, row 4) shows an activation which could be located in the OC. Nevertheless, we limited our analyses to the standard VOI atlas in order to be comparable to established methods in humans.

We decided to selected hypothesis-driven representative control regions – ON and CB as non-cortical control and SC as cortical control – instead of data-driven VOI regions. .

Even though constant acoustic, climatic and olfactory conditions have been maintained, a small possibility remains that changes in the olfactory system have been influenced by hidden changes in the environment over the duration from January to May for example due to seasonal clothing. We expect any hidden impact to be negligible compared to the effect caused by ablation.

3.7 Conclusions

This study demonstrates the usefulness of small animal PET with ^{18}F-FDG to image auditory system activations along nuclei of the central auditory pathway in normal hearing rats. For the strongest, non-adaptive stimulus (95dB, rippled noise) against background noise (55 dB) activations were consistently seen in NC, OC, MGB and IC with VOI and voxel-based analyses. A functional deactivation of the AC was measurable comparing a continuous white noise to both previous mentioned auditory conditions. Nevertheless, our data indicate, that sound deprivation to the greatest possible extent is necessary for the reference condition to allow for detection of increased activation in the AC even when a strong non-adaptive stimulus is used for stimulation. Furthermore, we found evidence for neuronal plasticity following continuous complete sound deprivation (cochlea ablation) in the form of increase (compensatory) activity in the olfactory system. The specificity of auditory and cross-modal compensatory activations is supported

by the fact that no activations were detected in any reference non-auditory region (SC, CB). In summary, small animal ^{18}F-FDG PET appears to be very promising to evaluate the pathophysiology of hearing loss in rats and the process of hearing restoration following auditory / cochlear implantation. Due to the minimal invasive procedures of PET imaging, the combinability of ^{18}F-FDG imaging with other additional PET tracers, e.g. for different neurotransmitters [Dedeurwaerdere2009], further enables a more-extensive observation and characterization of hearing, hearing disorders and corresponding healing processes. Moreover, the applicability of PET in medium size animals and humans makes it a valuable tool for translational hearing research.

3.8 Acknowledgment

We would like to thank Jean-Marc Edeline, Auditory Perception & Neural Code, Université Paris Sud, Orsay, France for providing us rippled noise stimuli and the staff of the preclinical molecular imaging in the Medical School, A. Kanwischer, P. Felsch and S. Eilert, for their support.

3.9 References

Abbott, S. D., Hughes, L. F., Bauer, C. A., Salvi, R., Caspary, D. M. (1999). "Detection of glutamate decarboxylase isoforms in rat inferior colliculus following acoustic exposure." Neuroscience 93(4): 1375-1381.

Ahn, S. H., Oh, S. H., Lee, J. S., Jeong, J. M., Lim, D., Lee, D. S., et al. (2004). "Changes of 2-deoxyglucose uptake in the rat auditory pathway after bilateral ablation of the cochlea." Hear Res 196: 33-38.

Arno, P., De Volder, A. G., Vanlierde, A., Wanet-Defalque, M. C., Streel, E., Robert, A., et al. (2001). "Occipital activation by pattern recognition in the early blind using auditory substitution for vision." Neuroimage 13(4): 632-645.

Berding, G., Wilke, F., Rode, T., Haense, C., Joseph, G., Meyer, G. J., et al. (2015). "Positron Emission Tomography Imaging Reveals Auditory and Frontal Cortical Regions Involved with Speech Perception and Loudness Adaptation." PLoS ONE 10(6): e0128743.

Blamey, P. J., Maat, B., Baskent, D., Mawman, D., Burke, E., Dillier, N., et al. (2015). "A Retrospective Multicenter Study Comparing Speech Perception Outcomes for Bilateral Implantation and Bimodal Rehabilitation." Ear Hear 36(4): 408-416.

Chonde, D. B., Abolmaali, N., Arabasz, G., Guimaraes, A. R., Catana, C. (2013). "Effect of MRI acoustic noise on cerebral fludeoxyglucose uptake in simultaneous MR-PET imaging." Invest Radiol 48(5): 302-312.

Clark, W. W. (1991). "Recent studies of temporary threshold shift (TTS) and permanent threshold shift (PTS) in animals." The Journal of the Acoustical Society of America 90(1): 155-163.

Constantinescu, C. C., Mukherjee, J. (2009). "Performance evaluation of an Inveon PET preclinical scanner." Phys Med Biol 54(9): 2885-2899.

Dedeurwaerdere, S., Gregoire, M. C., Vivash, L., Roselt, P., Binns, D., Fookes, C., et al. (2009). "In-vivo imaging characteristics of two fluorinated flumazenil radiotracers in the rat." Eur J Nucl Med Mol Imaging 36(6): 958-965.

Deutscher, A., Kurt, S., Scheich, H., Schulze, H. (2006). "Cortical and subcortical sides of auditory rhythms and pitches." Neuroreport 17: 4.

Giraud, A. L., Truy, E., Frackowiak, R. (2001). "Imaging plasticity in cochlear implant patients." Audiol Neurootol 6: 381-393.

Hsu, W. C., Tzen, K. Y., Huy, P. T., Duet, M., Yeh, T. H. (2009). "An animal model of central auditory pathway imaging in the rat brain by high resolution small animal positron emission tomography." Acta Otolaryngol 129(4): 423-428.

Jang, D. P., Lee, K. M., Lee, S. Y., Oh, J. H., Park, C. W., Kim, I. Y., et al. (2012). "Auditory adaptation to sound intensity in conscious rats: 2-[F-18]-fluoro-2-deoxy-D-glucose PET study." Neuroreport 23(4): 228-233.

Kilkenny, C., Browne, W. J., Cuthill, I. C., Emerson, M., Altman, D. G. (2010). "Improving bioscience research reporting: the ARRIVE guidelines for reporting animal research." PLoS Biol 8(6): e1000412.

Knoop, B. O., Geworski, L., Hofmann, M., Munz, D. L., Knapp, W. H. (2002). "Use of recovery coefficients as a test of system linearity of response in positron emission tomography (PET)." Phys Med Biol 47: 1237-1254.

Kujawa, S. G., Liberman, M. C. (2009). "Adding insult to injury: cochlear nerve degeneration after "temporary" noise-induced hearing loss." J Neurosci 29(45): 14077-14085.

Lancaster, J. L., Woldorff, M. G., Parsons, L. M., Liotti, M., Freitas, C. S., Rainey, L., et al. (2000). "Automated Talairach Atlas labels for functional brain mapping." Human Brain Mapping 10: 120-131.

Laudanski, J., Edeline, J. M., Huetz, C. (2012). "Differences between spectro-temporal receptive fields derived from artificial and natural stimuli in the auditory cortex." PLoS ONE 7(11): e50539.

Lazard, D. S., Vincent, C., Venail, F., Van de Heyning, P., Truy, E., Sterkers, O., et al. (2012). "Pre-, per- and postoperative factors affecting performance of postlinguistically deaf adults using cochlear implants: a new conceptual model over time." PLoS ONE 7(11): e48739.

Lu, W., Xu, J., Shepherd, R. K. (2005). "Cochlear implantation in rats: a new surgical approach." Hear Res 205(1-2): 115-122.

Mamach, M., Wilke, F., Durisin, M., Beger, F. A., Finke, M., Buchner, A., et al. (2018). "Feasibility of 15O-water PET studies of auditory system activation during general anesthesia in children." EJNMMI Res 8(1): 11.

Merabet, L. B., Pascual-Leone, A. (2010). "Neural reorganization following sensory loss: the opportunity of change." Nat Rev Neurosci 11(1): 44-52.

Niparko, J. K., Tobey, E. A., Thal, D. J., Eisenberg, L. S., Wang, N. Y., Quittner, A. L., et al. (2010). "Spoken language development in children following cochlear implantation." JAMA 303(15): 1498-1506.

Parellada, E., Lomena, F., Font, M., Pareto, D., Gutierrez, F., Simo, M., et al. (2008). "Fluordeoxyglucose-PET study in first-episode schizophrenic patients during the

hallucinatory state, after remission and during linguistic-auditory activation." Nucl Med Commun 29(10): 894-900.

Paul, A. K., Lobarinas, E., Simmons, R., Wack, D., Luisi, J. C., Spernyak, J., et al. (2009). "Metabolic imaging of rat brain during pharmacologically-induced tinnitus." Neuroimage 44(2): 312-318.

Paxinos, G., Watson, C. "The Rat Brain in Stereotaxic Coordinates." 3rd ed. New York: Academic Press; 1998.

Pietrini, P., Alexander, G. E., Furey, M. L., Dani, A., Mentis, M. J., Horwitz, B., et al. (2000). "Cerebral metabolic response to passive audiovisual stimulation in patients with Alzheimer's disease and healthy volunteers assessed by PET." J Nucl Med 41: 575-583.

Rao, D. B., Fechter, L. D. (2000). "Increased noise severity limits potentiation of noise induced hearing loss by carbon monoxide." Hear Res 150(1): 206-214.

Rausch, I., Cal-Gonzalez, J., Dapra, D., Gallowitsch, H. J., Lind, P., Beyer, T., et al. (2015). "Performance evaluation of the Biograph mCT Flow PET/CT system according to the NEMA NU2-2012 standard." EJNMMI Phys 2(1): 26.

Ruytjens, L., Willemsen, A. T., Van Dijk, P., Wit, H. P., Albers, F. W. (2006). "Functional imaging of the central auditory system using PET." Acta Otolaryngol 126(12): 1236-1244.

Schiffer, W. K., Mirrione, M. M., Biegon, A., Alexoff, D. L., Patel, V., Dewey, S. L. (2006). "Serial microPET measures of the metabolic reaction to a microdialysis probe implant." J Neurosci Methods 155: 272-284.

Schwarz, A. J., Danckaert, A., Reese, T., Gozzi, A., Paxinos, G., Watson, C., et al. (2006). "A stereotaxic MRI template set for the rat brain with tissue class distribution maps and co-registered anatomical atlas: application to pharmacological MRI." Neuroimage 32(2): 13.

Smith, J. J., Shionoya, K., Sullivan, R. M., Wilson, D. A. (2009). "Auditory stimulation dishabituates olfactory responses via noradrenergic cortical modulation." Neural Plast 2009: 754014.

Soto-Montenegro, M. L., Vaquero, J. J., Pascau, J., Gispert, J. D., Garcia-Barreno, P., Desco, M. (2009). "Detection of visual activation in the rat brain using 2-deoxy-2-[18F]fluoro-D: -glucose and statistical parametric mapping (SPM)." Mol Imaging Biol 11(2): 94-99.

Wehr, M., Zador, A. M. (2005). "Synaptic mechanisms of forward suppression in rat auditory cortex." Neuron 47(3): 437-445.

Willmore, B. D., King, A. J. (2009). "Auditory cortex: representation through sparsification?" Curr Biol 19(24): R1123-1125.

Wilson, B. S., Dorman, M. F. (2008). "Cochlear implants: a remarkable past and a brilliant future." Hear Res 242(1-2): 3-21.

Zhou, Y., Fang, F. H., Pan, P., Liu, Z. R., Ji, Y. H. (2017). "Visual deprivation induce cross-modal enhancement of olfactory perception." Biochem Biophys Res Commun 486(3): 833-838.

Zucker, R. S., Regehr, W. G. (2002). "Short-term synaptic plasticity." Annu Rev Physiol 64: 355-405.

3.10 Supporting information

Table 7: Supplement 7 - ANCOVA of study with FDG uptake as the dependent variable

Source	Degrees of Freedom	F Ratio	Prob. > F
Condition	2	15.8442	< 0.0001
Order of Condition	2	0.5685	0.5670
Animal position	2	0.5604	0.5716
Anatomical area	8	387.2309	< 0.0001

Results of ANCOVA with the condition, the order of condition and animals as well as anatomical area as fixed effects – uptake in the PET scan as dependent variable and animal as a random effect (performed using JMP10 software). ANCOVA was performed without the ablation data as stimulation conditions are only possible before ablation.

4 General discussion

4.1 Summary

Molecular imaging and particularly PET provide powerful tools for imaging central neuronal processing in adult humans. The applicability in subjects before and after auditory implantation opens up unique diagnostic perspectives. The ability to depict brain activity based on perfusion or metabolism using ^{15}O-water and ^{18}F-FDG respectively gives insides in the biological processes underlying auditory analysis with and without impairment. As the number of patients with hearing impairment and auditory implants increases, the understanding of underlying mechanisms along the auditory pathway will influence future concepts and performance of hearing aids and is, therefore, a major goal in hearing research.

In our first study in this context, we investigated the transferability of an established method for imaging activation of the auditory system in adult humans to small children. The most important difference is the necessity to perform imaging during general anesthesia since small children are not able to cooperate like adults during the study. According datasets from adults and children that had been collected on the basis of clinical indications were retrospectively analyzed. Different parameters like acquisition frame duration, smoothing of 3D datasets and criteria used for statistical inferences were compared in awake adults and children before or after CI implantation. Children were studied during EEG-controlled opioid-based general anesthesia. The following auditory conditions were applied during measurements of cerebral perfusion using ^{15}O-water PET: (i) direct stimulation of cochlea electrically via a needle electrode placed at the promontory, (ii) feeding of music directly into the CI processor and (iii) silence as a reference condition. Based on similar final hearing performances of all groups after auditory rehabilitation, we expected activations in all groups but slightly reduced in anesthesia. No significant difference was found between stimulation via promontory and CI in children. The preferred (strong) smoothing kernel in adults proved to be optimal. Moreover, no statistical difference in the frequency of detected activations could be observed between different acquisition times. However, one parameter, namely the level of significance used for statistical inference had to be adapted to achieve an appropriate sensitivity – in order to accommodate for the anesthesia effects.

The second study was designed to elaborate activation studies of the central auditory pathway and cortex in normal hearing rats. Structures in the brainstem and midbrain were included additionally to the cortex in contrast to activation studies in human, which are typically focused on the cortex. As an additional reference condition for the assessment of activity in auditory brain regions during stimulation, a model of profound

hearing loss as status of sensory deprivation was also included. ^{18}F-FDG was chosen as an indicator of neuronal activity based on metabolism. As expected, neuronal activations of all examined regions along the auditory pathway were observed in normal hearing rats. Interestingly, activity in the auditory cortex was not found by an increase with advanced stimulation but indirectly due to an inhibition during the compared reference condition broadband noise. These results show a good applicability of auditory activation studies using small animal PET in rats. The usefulness of the method is further substantiated by compensatory activations of brain regions related to the olfactory system we saw in the deaf animals – which are in line with experimental studies in animals after visual deprivation.

4.2 Translatability

Translational research on disorders of the auditory system is a powerful way to disentangle pathophysiology and in the development of new treatment strategies [Le Prell2016]. On the other hand, translational auditory research itself faces considerable difficulties regarding e.g. usefulness of auditory stimuli only for specific species [Gourevitch2015], the usefulness of animal models only for specific research questions [Reis2017] and differences in auditory functions between species [Baizer2018]. Nevertheless, functional and molecular imaging can support translational research as a tool applicable across species.

4.2.1 Characterization of the auditory cortex

PET enabled the demonstration of activated regions in the central auditory system in both humans and animals. While showing a general transferability, characteristic differences were observed in the extent and pattern of activations between awake adult humans, anesthetized children, and awake rats. Both studies presented in this thesis showed results corresponding to previous studies in humans, e.g. [Berding2015, Suh2015], and animals [Hsu2009, Jang2012]. Characteristic activation patterns using high-intensity stimulation vs. silence were seen in complementary areas: in humans in the auditory as well as auditory associated cortices and in animals in the auditory regions of the midbrain along with all major auditory areas in the brainstem. A study comparing in humans normal hearing subjects and rehabilitated CI users showed differences in extent and magnitude of cortical activations [Coez2008]. In comparison to this study, our results in CI users revealed smaller cortical activations, which could be explained by the heterogeneity of our patient groups and the inclusion of patients without cortical activation in the analyses. Concerning the animal model, our results are in accord with results obtained with another imaging modality – manganese-enhanced MRI – which showed after 24h stimulation only limited significant activations in unilateral substructures of the auditory cortex in rats [Kim2014] using intensity and frequency

modulated pulsed pure tone stimuli. Hence, it could be hypothesized that either processing in auditory cortex in rats is only sensitive to specific stimuli or that non-negligible activation occurs due to laboratory background noises. Our results in rats in agreement with [Ahn2004] and [Hsu2009] showed a high basal activity in the AC if silence is compared to the profound hearing loss. Our observation of reduced cortical activity with the white noise stimulus is consistent with [Jang2012] in animals but does not agree with increase activation in human cortices for similar conditions [Leaver2016]. It has to be noted that in humans different acoustic stimuli activate several brain areas to different extents as shown for white noise and speech by [Naito1995, Coez2008]. A similar effect could take place in rats with the applied stimuli and background conditions. Therefore, more specific meaningful stimuli for rats would be desirable. Such stimuli might push the extent of the activation in the auditory cortex in rats within the current limits of small animal PET or confirm the difference in activation on a cortical level between human and rats.

4.2.2 Studying sub-cortical activations

With respect to the central auditory pathway, we were able to measure increased neuronal activation in rats in all major sub-cortical auditory nuclei along the pathway. Electrophysiological studies revealed that auditory brainstem responses and auditory event-related potentials share some common characteristics in humans and rats [Shaw1988]. Nevertheless, profound differences are present as well [Sambeth2003].

In humans, activations in auditory regions such as IC [Riecke2018] and OC [Giraud2001] have been detected only in a few studies using 7 T fMRI and ^{15}O-water PET in conjunction with dedicated stimuli. One reason as laid out in the discussion of study II (chapter 3.6) might be partial volume effects with the sub-cortical nuclei being smaller in humans compared to rats [Kretschmann1992, Paxinos1998, Constantinescu2009, Rausch2015] in relation to the spatial resolution of corresponding PET systems. Particularly the IC is relatively small in this respect in humans (about 300 mm³ [Kretschmann1992, Riecke2018]) compared to rats ([Paxinos1998, Schwarz2006]). In contrast, imaging in rats following auditory stimulation provided activation of sub-cortical structures like the IC regularly [Jang2012] and similar to our results activation in the AC was scarce. There is evidence that specific auditory functions, like frequency specific attention, are represented at a sub-cortical level in rats but a cortical level in humans [Riecke2018]. This could explain the finding of more sub-cortical activation in rats compared to cortical activation in humans related to auditory stimuli with inherent complexity in terms of frequency.

Therefore, measurements of sub-cortical structures in animals are of particular interest and are included by multiple modalities of *in vivo* imaging such as fMRI [Kim2014,

Gao2015] and PET [Jang2012, Kang2013] as well as other modalities like *ex vivo* studies [Argence2008] and electrophysiology [Mokri2015]. In these measurements, PET is especially helpful in quantifying the effect size. Fast modalities of fMRI have a good temporospatial resolution but the absolute effect size in BOLD signal is with about 5% [Gao2015] smaller e.g. than our observation with >12.5%. Furthermore, PET enables detection of bilateral activation in normal hearing rats in all major sub-cortical structures NC, OC, IC and MGB. This could not be achieved in manganese-enhanced fMRI [Kim2014]. Although we were able to measure significant increases of activity due to auditory stimulation in small structures such as OC and MGB, it has to be kept in mind that we still underestimate the effect due to resolution limits respectively partial volume effects [Knoop2002]. In such small areas, measured effect size might be corrected using approaches for recovery correction [Knoop2002]. Such correction could possibly be implemented effectively in multimodal imaging e.g. using PET-MR [Chen2018].

4.2.3 Selection of analysis parameter

Our studies in humans showed that the selection of parameters during data analysis has a large impact on the results.

Similar to our study in patients, we analyzed our data in rats first without smoothing and then with a kernel of [2 mm]³, which was adapted to the smaller size of the structures we intended to measure [Mamach2015] and the resolution of the Inveon small animal PET system [Constantinescu2009] which we used. A too strong smoothing kernel includes the risk to mask activations in regions as AC or MGB due to differences in size [Blobel1998, Knoop2002]. Hence, the smoothing was omitted to enable imaging of partial activation as was seen for example by [Kim2014]. Small effects in human studies are typically related to statistical noise [Knoop2002] and correspondingly omitted. In preclinical PET studies of normal hearing rats, such noise is not yet a problem as activation in auditory regions typically is the predominant effect. More optimized smoothing might be necessary for the future to study models of gradual hearing loss with smaller differences between auditory conditions.

Similar to [Apostolova2012, Jang2012], we employed SPM to detect regional specific effects. For moderate effect sizes [Woo2014] recommended the use of an extend threshold for refinement which was applied e.g. by [Jang2012]. As no smoothing was applied, we accounted for statistical noise by applying an alternative ‘occupancy’ threshold. This threshold takes the size of the VOI into account. The concept of partial activation of the AC in [Kim2014] motivated this and a threshold of 1% was chosen. As our results agreed well with references [Ahn2004, Hsu2009, Jang2012], the selected value proved to be functional. In sum, we compensated for noise by adhering to a more

conservative significance threshold as recommended in [Woo2014] and the use of an alternative cluster-independent extend threshold.

4.3 Outlook and potentials

4.3.1 Radiopharmaceuticals for molecular imaging of the auditory system

Our results in rats showed particularly good applicability in the characterization of subcortical areas along the auditory pathway. Nevertheless, preclinical molecular imaging might also be used for further the characterization of the auditory cortex employing other stimuli and radiotracer with more adapted properties.

Especially the inhibitory GABAergic neurotransmitter system is of interest in this context as it is hypothesized to be a major pathophysiologic factor in age-related hearing loss [Caspary1999], in neuronal plasticity in the auditory system [Sanes2011] and in tinnitus [Eggermont2004]. The pharmaceutical Flumazenil (FMZ) labeled with the positron emitter ^{11}C or ^{18}F has been used preclinically [Mandema1991, Dedeurwaerdere2009] and in humans [Odano2009]. It is able to bind to the benzodiazepine recognition site of $GABA_A$-receptors [Mandema1991]. Both radiotracers enable absolute quantification of receptor density using complex methodology and procedures for data analysis [Dedeurwaerdere2009, Vivash2014]. In preliminary studies, we evaluated simplified bio-kinetic models for quantification of the relative non-displaceable binding potential BP_{ND} of ^{18}F-FMZ [Kessler2016, Mamach2017] using time activity curves from blood samples or the pons as a reference. The results were consistent across multiple models and showed good agreement. Hence, we used this quantitative approach for an exploratory longitudinal study of two animal models of profound hearing loss [Mamach2016]. We combined measurements of the GABAergic receptors with measurements of auditory system activation using ^{18}F-FDG in the same animals. We observed after acute acoustic trauma against a baseline with normal hearing animals as expected significant decreases of activity in AC and IC by 9% and 11%, persisting for at least 5 weeks. With respect to $GABA_A$-receptor PET, a significant decrease in binding potential in AC from 1.24 to 1.10 occurred after 5 weeks. This is consistent with the combined electrophysiological and pharmacological findings of [Salvi2016]. Nevertheless, we did not observe any significant short-term or long-term changes in binding potential in the IC. The reason might be that reduced activity of the GABAergic system occurs later in the IC as suggested by results of [Liao2000] after 7-8 weeks. This indicates that plasticity proceeds at different time scales in AC and IC. The use of multiple tracers in the same subjects enables more complex analyses of interaction and dependencies of auditory processing in animals and humans as the basis of age-related hearing loss.

Another approach worth to follow for hearing research would be a perfusion marker still allowing to study awake animals (as FDG) but with a faster tracer accumulation avoiding adaptation to auditory stimuli as seen e.g. in [Berding2015]. A tracer with such characteristics but for SPECT imaging is ^{99m}Tc-hexametylpropylenamineoxime (^{99m}Tc - HPMAO), which has already been used in auditory research [De Rossi1994, Goycoolea2011, Apostolova2012]. HMPAO is a chemical microsphere. After high first pass extraction via the blood-brain barrier, it is taken up into the cell and metabolized into a hydrophilic substance which is trapped in the cell [Leveille1992, van Dyck1996, Apostolova2012]. The fast fixation during less than 5 min in humans [van Dyck1996] reduces expected adaptation effects and the fixation in the cell enables longer scanning. An exploratory study of auditory activation in rats clearly indicated a lack in counting statistics related to the SPECT method [Mamach2014]. Therefore, we started to develop a procedure for labeling HMPAO with the positron emitter ^{68}Ga for imaging in PET with superior spatial resolution and sensitivity compared to SPECT.

All mentioned tracers can be established in animal models of auditory disorders and be translated to patients. As the pharmaceutical HMPAO labeled with ^{99m}Tc is already used in humans [Allen2004], translatability is very likely. Furthermore, ^{18}F-Flumazenil has also been already applied in humans [Duncan2013].

These two specific radiotracers were showcased as both of them resulted directly from our studies. Limitations such as adaptation and an interest for molecular characterization of auditory animal models motivated the implementation and start of development respectively. Both tracers give an indication in the possible impact of the development of new radiopharmaceuticals for auditory research.

4.3.2 Potentials in technological development

Beside tracer development, technological progress with respect to imaging equipment also broadens the significance of radiotracer diagnostics. Focusing on the PET devices, two defining properties, spatial resolution and sensitivity, have improved substantially over the last decades.

For example, the spatial resolution (i.e. the FWHM) of commercially available PET devices from one manufacturer improved from 9mm [Jin Su2004] to 4mm [Rausch2015]. Current experimental devices are able to scan images with a resolution of about 2 mm [Schmidt2018]. With respect to our study I (chapter 2), which employed a PET scanner with 7 mm spatial resolution, in the future 3-4 times smaller structures or substructures of the auditory system could be approached. This should enable PET to image the non-cortical structures in humans similar to rats and would lower the limit of detectable effect sizes. Similar to the proposal for animals, multimodal imaging could provide correction [Chen2018] for measured effect sizes with PET. Analogous devel-

opments are occurring in small animal PET imaging but are at last limited due to the physical resolution limits. They improved from 1.4 mm [Constantinescu2009] to 0.8 mm [Gaitanis2017].

Another important improvement is an increase in sensitivity. It has been enhanced from 0.7 kcps/MBq (BGO crystal based 2D PET) and 3.3 kcps/MBq (BGO crystal based 3D PET) – both in a scanner introduced in the late 1990s [Jin Su2004] to currently 9.6 kcps/MBq (LSO crystal based 3D PET) [Rausch2015]. The data is representatively given for commercially available products of one manufacturer. This improvement combined with additional software and reconstruction optimizations for scatter correction and contrast recovery [Rausch2015] created an overall more than 10 times better sensitivity in humans. This is particularly important for a diagnostic approach to be used in young patients with hearing disorders and in follow-up investigations during auditory rehabilitation. Even in oncology, which used to omit the radiation exposure by diagnostic procedures less rigidly due to the life-threatening character of the illness, processes are clearly optimized toward lower radiation doses [Colleran2017]. Children are in sensitive stages of their development and therefore by law specially protected also in the term of radiation safety [Vogt2011]. An increase in sensitivity as laid out above reduces the amount of radiotracer needed and hence the effective dose. This is desirable since radiation dose has accumulative effect according to current knowledge [Vogt2011]. The radiation dose induced by ^{15}O-water has been assessed by the ICRP [ICRP1988, 1998]. It is given as 0.00093 mSv/MBq in adults. A typical activity given for single injection in the frame of multiple injections for later statistical evaluation would be 370 MBq [Chmielowska1999]. A study with two conditions and 6 injections given for each condition would end up with a radiation exposure of 4.1 mSv. Reducing the injected activity by factor 10, based on the increased sensitivity as mentioned above, would bring the radiation exposure below 1 mSv even if 3 conditions are included. With respect to studies in children, the radiation exposure per MBq is relatively higher e.g. 0.0038 mSv/MBq for a 5-year-old child [ICRP1988, 1998]. Proceeding from a weight-adjusted activity of 125 MBq (factor 0.34 for 20 kg), this would result in a radiation exposure of 5.7 mSv for two conditions. Again a reduction of the injected activity by a factor of 10 would bring the radiation exposure below 1 mSv even if 3 conditions are included. This is a comparatively low value of radiation exposure for a diagnostic procedure utilizing ionizing radiation. It is even below the dose limit provided for the protection of the general population by the German radiation protection legislation (1 mSv) [Vogt2011, Veith2016, 2018]. Theoretically, such an advancement enables more than 20 follow-up investigations according to the dose limits for research studies according to the German radiation protection legislation. The aforementioned figures make it clear that based on the increased sensitivity of current state PET scanners, ^{15}O-water activation studies are possible with such a low amount of radioactivity that e.g. in hearing research follow-up

studies of rehabilitation after auditory implantation are possible with an acceptable radiation exposure. Moreover, radiation exposure would be small compared to the annual dose from natural sources with 2 mSv in Germany [Vogt2011]. Hence, such low dose PET would enable longitudinal observation with very limited risk.

5 Conclusions

In our first study, we illustrated that PET activation studies can show the functionality of the central auditory pathway by demonstrating cortical activation even in cochlear implanted small children during anesthesia. With respect to preclinical imaging, activity along the central auditory pathway could be shown in rats for all important auditory nuclei if suitable stimuli and reference conditions were applied. We demonstrated the relevance of adaptation to stimuli in both humans and rats. Considering the current difference of spatial resolution between small animal and human PET in proportion to the size of the imaged auditory brain regions, results cannot be directly comparable between species. Moreover, biological differences of processing in auditory nuclei and cortex might contribute to different activation patterns between rats (primarily sub-cortical) and humans (primarily cortical). The pathophysiology of hearing disorder and their treatment cannot solely be targeted using biomarkers of neuronal activity. This means molecular markers e.g. of neurotransmission are also of interest. In a preliminary study of the inhibitory GABAergic system, we found hints for reduced binding capacity in deafened rats, indicating compensatory and – according to experimental data – possibly neuronal plastic changes. Last but not least technical advances in emission tomographic scanning devices for humans (patients) offer novel options for auditory research: (i) improved spatial resolution allows to explore activations in nuclei of the central auditory pathway with a considerable improvement in signal recovery (ii) the gain in resolution will also give improved options to study animal model of medium size which are of particular interest in hearing research like born deaf white cats and finally (iii) profoundly improved sensitivity enables to reduce the applied amounts of radioactivity drastically. This will allow for the first time multiple follow-up investigations after auditory implantation helping to understand mechanisms underlying successful auditory rehabilitation. In addition, it will accommodate patient concerns with respect to radiation risks.

6 References

Abbott, S. D., Hughes, L. F., Bauer, C. A., Salvi, R., Caspary, D. M. (1999). "Detection of glutamate decarboxylase isoforms in rat inferior colliculus following acoustic exposure." Neuroscience **93**(4): 1375-1381.

Absalom, A., Adapa, R. "Anaesthesia and PET of the Brain." In: Dierckx, R. A., Otto, A., de Vries, E. F. J.,von Waarde, A., editors. PET and SPECT in Neurology. Heidelberg: Springer; 2014. p. 987-1009.

Ahn, S. H., Oh, S. H., Lee, J. S., Jeong, J. M., Lim, D., Lee, D. S., et al. (2004). "Changes of 2-deoxyglucose uptake in the rat auditory pathway after bilateral ablation of the cochlea." Hear Res **196**: 33-38.

Akeroyd, M. A. (2008). "Are individual differences in speech reception related to individual differences in cognitive ability? A survey of twenty experimental studies with normal and hearing-impaired adults." Int J Audiol **47 Suppl 2**: S53-71.

Alavi, A., Dann, R., Chawluk, J., Alavi, J., Kushner, M., Reivich, M. (1986). "Positron emission tomography imaging of regional cerebral glucose metabolism." Semin Nucl Med **16**(1): 2-34.

Allen, A., Barnes, A., Singh, R. S., Patterson, J., Hadley, D. M., Wyper, D. (2004). "Perfusion SPECT in cochlear implantation and promontory stimulation." Nucl Med Commun **25**: 521-525.

Angulo-Perkins, A., Concha, L. (2014). "Music perception: information flow within the human auditory cortices." Adv Exp Med Biol **829**: 293-303.

Antunes, F. M., Nelken, I., Covey, E., Malmierca, M. S. (2010). "Stimulus-specific adaptation in the auditory thalamus of the anesthetized rat." PLoS ONE **5**(11): e14071.

Apostolova, I., Wunder, A., Dirnagl, U., Michel, R., Stemmer, N., Lukas, M., et al. (2012). "Brain perfusion SPECT in the mouse: normal pattern according to gender and age." Neuroimage **63**(4): 1807-1817.

Argence, M., Vassias, I., Kerhuel, L., Vidal, P. P., de Waele, C. (2008). "Stimulation by cochlear implant in unilaterally deaf rats reverses the decrease of inhibitory transmission in the inferior colliculus." Eur J Neurosci **28**: 1589-1602.

Arno, P., De Volder, A. G., Vanlierde, A., Wanet-Defalque, M. C., Streel, E., Robert, A., et al. (2001). "Occipital activation by pattern recognition in the early blind using auditory substitution for vision." Neuroimage **13**(4): 632-645.

Baizer, J. S., Wong, K. M., Salvi, R. J., Manohar, S., Sherwood, C. C., Hof, P. R., et al. (2018). "Species Differences in the Organization of the Ventral Cochlear Nucleus." Anat Rec (Hoboken) **301**(5): 862-886.

Ballanger, B., Jahanshahi, M., Broussolle, E., Thobois, S. (2009). "PET functional imaging of deep brain stimulation in movement disorders and psychiatry." J Cereb Blood Flow Metab **29**(11): 1743-1754.

Bandettini, P. A. (2012). "Twenty years of functional MRI: the science and the stories." Neuroimage **62**(2): 575-588.

Berding, G., Lenarz, T. (2017). "Imaging in hearing using radiotracers." Current Directions in Biomedical Engineering **3**(2).

Berding, G., Wilke, F., Rode, T., Haense, C., Joseph, G., Meyer, G. J., et al. (2015). "Positron Emission Tomography Imaging Reveals Auditory and Frontal Cortical Regions Involved with Speech Perception and Loudness Adaptation." PLoS ONE **10**(6): e0128743.

Blamey, P. J., Maat, B., Baskent, D., Mawman, D., Burke, E., Dillier, N., et al. (2015). "A Retrospective Multicenter Study Comparing Speech Perception Outcomes for Bilateral Implantation and Bimodal Rehabilitation." Ear Hear **36**(4): 408-416.

Blobel, V., Lohrmann, E. "Statistische und numerische Methoden der Datenanalyse. Stuttgard: Teubner Studienbücher; 1998. 358 p.

Boellaard, R., Delgado-Bolton, R., Oyen, W. J., Giammarile, F., Tatsch, K., Eschner, W., et al. (2015). "FDG PET/CT: EANM procedure guidelines for tumour imaging: version 2.0." Eur J Nucl Med Mol Imaging **42**(2): 328-354.

Bol, A., Vanmelckenbeke, P., Michel, C., Cogneau, M., Goffinet, A. M. (1990). "Measurement of cerebral blood flow with a bolus of oxygen-15-labelled water: comparison of dynamic and integral methods." Eur J Nucl Med **17**(5): 234-241.

Campbell, M. C., Karimi, M., Weaver, P. M., Wu, J., Perantie, D. C., Golchin, N. A., et al. (2008). "Neural correlates of STN DBS-induced cognitive variability in Parkinson disease." Neuropsychologia **46**(13): 3162-3169.

Caobelli, F., Wollenweber, T., Bavendiek, U., Kuhn, C., Schutze, C., Geworski, L., et al. (2017). "Simultaneous dual-isotope solid-state detector SPECT for improved tracking of white blood cells in suspected endocarditis." Eur Heart J **38**(6): 436-443.

Carter, S. J., Martin, J. J., Middlemiss, J. H., Ross, F. G. M. (1963). "Polytome tomography." Clinical Radiology **14**(4): 405-413.

Caspary, D. M., Holder, T. M., Hughes, L. F., Milbrandt, J. C., McKernan, R. M., Naritoku, D. K. (1999). "Age-related changes in $GABA_A$ receptor subunit composition and function in rat auditory system." Neuroscience **93**: 307-312.

Celesia, G. G., Polcyn, R. D., Holden, J. E., Nickles, R. J., Gatley, J. S., Koeppe, R. A. (1982). "Visual evoked potentials and positron emission tomographic mapping of regional cerebral blood flow and cerebral metabolism: can the neuronal potential generators be visualized?" Electroencephalogr Clin Neurophysiol **54**(3): 243-256.

Cetas, J. S., Price, R. O., Velenovsky, D. S., Sinex, D. G., McMullen, N. T. (2001). "Frequency organization and cellular lamination in the medial geniculate body of the rabbit." Hear Res **155**(1): 113-123.

Chen, K. T., Salcedo, S., Gong, K., Chonde, D. B., Izquierdo-Garcia, D., Drzezga, A. E., et al. (2018) "An Efficient Approach to Perform MR-assisted PET Data

Optimization in Simultaneous PET/MR Neuroimaging Studies." J Nucl Med DOI: 10.2967/jnumed.117.207142

Cherry, S. R., Jones, T., Karp, J. S., Qi, J., Moses, W. W., Badawi, R. D. (2018). "Total-Body PET: Maximizing Sensitivity to Create New Opportunities for Clinical Research and Patient Care." J Nucl Med **59**(1): 3-12.

Chmielowska, J., Coghill, R. C., Carson, R. E., Ishii, K., Chen, R., Hallett, M., et al. (1999). "Comparison of PET [^{15}O]water studies with 6-minute and 10-minute interscan intervals: single-subject and group analyses." J Cereb Blood Flow Metab **19**: 570-582.

Chmielowska, J., Coghill, R. C., Maisog, J. M., Carson, R. E., Herscovitch, P., Honda, M., et al. (1998). "Positron emission tomography [^{15}O]water studies with short interscan interval for single-subject and group analysis: influence of background subtraction." J Cereb Blood Flow Metab **18**: 433-443.

Chonde, D. B., Abolmaali, N., Arabasz, G., Guimaraes, A. R., Catana, C. (2013). "Effect of MRI acoustic noise on cerebral fludeoxyglucose uptake in simultaneous MR-PET imaging." Invest Radiol **48**(5): 302-312.

Chu, R. C. (1980). "Positron Emission Tomography - An Emerging Technology." Proceedings of the Annual Symposium on Computer Application in Medical Care **1**: 469-475.

Church, M. W., Hotra, J. W., Holmes, P. A., Anumba, J. I., Jackson, D. A., Adams, B. R. (2012). "Auditory brainstem response (ABR) abnormalities across the life span of rats prenatally exposed to alcohol." Alcohol Clin Exp Res **36**(1): 83-96.

Clark, W. W. (1991). "Recent studies of temporary threshold shift (TTS) and permanent threshold shift (PTS) in animals." The Journal of the Acoustical Society of America **90**(1): 155-163.

Clarke, S., Morosan, P. "Architecture, Connectivity, and Transmitter Receptors of Human Auditory Cortex." In: Poeppel, D., Overath, T., Popper, A. N.,Fay, R. R., editors. The Human Auditory Cortex. New York: Springer; 2012. p. 11-38.

Coez, A., Zilbovicius, M., Ferrary, E., Bouccara, D., Mosnier, I., Ambert-Dahan, E., et al. (2008). "Cochlear implant benefits in deafness rehabilitation: PET study of temporal voice activations." J Nucl Med **49**(1): 60-67.

Coez, A., Zilbovicius, M., Ferrary, E., Bouccara, D., Mosnier, I., Ambert-Dahan, E., et al. (2009). "Processing of voices in deafness rehabilitation by auditory brainstem implant." Neuroimage **47**(4): 1792-1796.

Colleran, G. C., Kwatra, N., Oberg, L., Grant, F. D., Drubach, L., Callahan, M. J., et al. (2017). "How we read pediatric PET/CT: indications and strategies for image acquisition, interpretation and reporting." Cancer Imaging **17**(1): 28.

Constantinescu, C. C., Mukherjee, J. (2009). "Performance evaluation of an Inveon PET preclinical scanner." Phys Med Biol **54**(9): 2885-2899.

Dávila, H. O., Ovalle, S. A. M., Pérez, H., Castro, H. (2017). "Determination of Spatial Resolution of Positron Emission Tomograph of Clear PET-XPAD3/CT System." Universal Journal of Physics and Application **11**(4): 97-101.

Davis, M. H., Coleman, M. R., Absalom, A. R., Rodd, J. M., Johnsrude, I. S., Matta, B. F., et al. (2007). "Dissociating speech perception and comprehension at reduced levels of awareness." Proc Natl Acad Sci U S A **104**(41): 16032-16037.

Davison, C. M., O'Brien, J. T. (2014). "A comparison of FDG-PET and blood flow SPECT in the diagnosis of neurodegenerative dementias: a systematic review." Int J Geriatr Psychiatry **29**(6): 551-561.

De Rossi, G., Giordano, A., Calcagni, M. L., Di Nardo, W., Galli, J., Paludetti, G. (1994). "Brain SPET and auditory cortex perfusion. Technical notes and preliminary results." Nucl Med Commun **15**: 565-568.

Dedeurwaerdere, S., Gregoire, M. C., Vivash, L., Roselt, P., Binns, D., Fookes, C., et al. (2009). "In-vivo imaging characteristics of two fluorinated flumazenil radiotracers in the rat." Eur J Nucl Med Mol Imaging **36**(6): 958-965.

Demarquay, G., Royet, J. P., Mick, G., Ryvlin, P. (2008). "Olfactory hypersensitivity in migraineurs: a $H_2{}^{15}O$-PET study." Cephalalgia **28**(10): 1069-1080.

Deutscher, A., Kurt, S., Scheich, H., Schulze, H. (2006). "Cortical and subcortical sides of auditory rhythms and pitches." Neuroreport **17**: 4.

Di Nardo, W., Picciotti, P., Di Giuda, S., De Rossi, G., Paludetti, G. (2004). "SPET assessment of auditory cortex stimulation and tonotopic spatial distribution in auditory brainstem implant." Acta Otorhinolaryngol Ital **24**: 321-325.

DIN. "6855-4:2016-11, Constancy testing of nuclear medicine instruments - Part 4: Positron emission tomographs (PET)." Berlin: Beuth; 2016.

Duncan, N. W., Gravel, P., Wiebking, C., Reader, A. J., Northoff, G. (2013). "Grey matter density and $GABA_A$ binding potential show a positive linear relationship across cortical regions." Neuroscience **235**: 226-231.

Eggermont, J. J., Roberts, L. E. (2004). "The neuroscience of tinnitus." Trends Neurosci **27**(11): 676-682.

Ell, P. J., Jarritt, P. H., Costa, D. C., Cullum, I. D., Lui, D. (1987). "Functional imaging of the brain." Semin Nucl Med **17**(3): 214-229.

Elsinga, P. H. "Nuclear Medicine Imaging Tracers for Neurology " In: Dierckx, R. A., Otto, A., de Vries, E. F. J.,von Waarde, A., editors. PET and SPECT in Neurology. Heidelberg: Springer; 2014.

Fox, P. T., Raichle, M. E. (1984). "Stimulus rate dependence of regional cerebral blood flow in human striate cortex, demonstrated by positron emission tomography." J Neurophysiol **51**(5): 1109-1120.

Frackowiak, R. S., Friston, K. J. (1994). "Functional neuroanatomy of the human brain: positron emission tomography - a new neuroanatomical technique." J Anat **184**(Pt2): 211-225.

Frackowiak, R. S., Lenzi, G. L., Jones, T., Heather, J. D. (1980). "Quantitative measurement of regional cerebral blood flow and oxygen metabolism in man using ^{15}O and positron emission tomography: theory, procedure, and normal values." J Comput Assist Tomogr **4**(6): 727-736.

Fragoso Costa, P., Santos, A., Vidovič, B., editors. "Brain Imaging - A Technologist's Guide. Vienna: European Association of Nuclear Medicine; 2016.

Friederici, A. D. (2012). "The cortical language circuit: from auditory perception to sentence comprehension." Trends Cogn Sci **16**(5): 262-268.

Froklage, F. E., Syvänen, S., Hendrikse, N. H., Huisman, M. C., Molthoff, C. F., Tagawa, Y., et al. (2012). "[^{11}C]Flumazenil brain uptake is influenced by the blood-brain barrier efflux transporter P-glycoprotein." EJNMMI research **2**: 12.

Fujiki, N., Naito, Y., Hirano, S., Kojima, H., Shiomi, Y., Nishizawa, S., et al. (2000). "Brain activities of prelingually and postlingually deafened children using cochlear implants." Ann Otol Rhinol Laryngol Suppl **185**: 12-14.

Fukuda, M., Barnes, A., Simon, E. S., Holmes, A., Dhawan, V., Giladi, N., et al. (2004). "Thalamic stimulation for parkinsonian tremor: correlation between regional cerebral blood flow and physiological tremor characteristics." Neuroimage **21**(2): 608-615.

Gaitanis, A., Kastis, G. A., Vlastou, E., Bouziotis, P., Verginis, P., Anagnostopoulos, C. D. (2017). "Investigation of Image Reconstruction Parameters of the Mediso nanoScan PC Small-Animal PET/CT Scanner for Two Different Positron Emitters Under NEMA NU 4-2008 Standards." Mol Imaging Biol **19**(4): 550-559.

Gao, P. P., Zhang, J. W., Fan, S. J., Sanes, D. H., Wu, E. X. (2015). "Auditory midbrain processing is differentially modulated by auditory and visual cortices: An auditory fMRI study." Neuroimage **123**: 22-32.

Giraud, A. L., Truy, E., Frackowiak, R. (2001). "Imaging plasticity in cochlear implant patients." Audiol Neurootol **6**: 381-393.

Gourevitch, B., Occelli, F., Gaucher, Q., Aushana, Y., Edeline, J. M. (2015). "A new and fast characterization of multiple encoding properties of auditory neurons." Brain Topogr **28**(3): 379-400.

Goycoolea, M., Mena, I., Neubauer, S. (2011). "Functional studies (NeuroSPECT) of the human auditory pathway after stimulating binaurally with pure tones." Acta Otolaryngol **131**(4): 371-376.

Gunther, W. (1992). "MRI-SPECT and PET-EEG findings on brain dysfunction in schizophrenia." Prog Neuropsychopharmacol Biol Psychiatry **16**: 445-462.

Hariz, M., Blomstedt, P., Zrinzo, L. (2013). "Future of brain stimulation: new targets, new indications, new technology." Mov Disord **28**(13): 1784-1792.

Heinke, W., Schwarzbauer, C. (2002). "In vivo imaging of anaesthetic action in humans: approaches with positron emission tomography (PET) and functional magnetic resonance imaging (fMRI)." Br J Anaesth **89**(1): 112-122.

Herzog, H., Lamprecht, A., Kuhn, A., Roden, W., Vosteen, K. H., Feinendegen, L. E. (1991). "Cortical activation in profoundly deaf patients during cochlear implant stimulation demonstrated by $H_2{}^{15}O$ PET." J Comput Assist Tomogr **15**(3): 369-375.

Hevesy, G. (1923). "The Absorption and Translocation of Lead by Plants: A Contribution to the Application of the Method of Radioactive Indicators in the Investigation of the Change of Substance in Plants." Biochemical Journal **17**(4-5): 439-445.

Hirano, S., Naito, Y., Kojima, H., Honjo, I., Inoue, M., Shoji, K., et al. (2000). "Functional differentiation of the auditory association area in prelingually deaf subjects." Auris Nasus Larynx **27**: 303-310.

Hochmair-Desoyer, I., Schulz, E., Moser, L., Schmidt, M. (1997). "The HSM sentence test as a tool for evaluating the speech understanding in noise of cochlear implant users." The American journal of otology **18**: S83.

Horga, G., Fernandez-Egea, E., Mane, A., Font, M., Schatz, K. C., Falcon, C., et al. (2014). "Brain metabolism during hallucination-like auditory stimulation in schizophrenia." PLoS ONE **9**(1): e84987.

Hsu, W. C., Tzen, K. Y., Huy, P. T., Duet, M., Yeh, T. H. (2009). "An animal model of central auditory pathway imaging in the rat brain by high resolution small animal positron emission tomography." Acta Otolaryngol **129**(4): 423-428.

ICRP (1988). "ICRP Publication 53 - Radiation Dose to Patients from Radiopharmaceuticals." Annals of the ICRP **18**(1-4).

ICRP (1991). "ICRP Publication 60 - 1990 Recommendations of the International Commission on Radiological Protection." Annals of the ICRP **21**(1-3).

ICRP (1998). "ICRP Publication 80 - Radiation Dose to Patients from Radiopharmaceuticals (Addendum to ICRP Publication 53)." Annals of the ICRP **28**(3).

Jakoby, B. W., Bercier, Y., Conti, M., Casey, M. E., Bendriem, B., Townsend, D. W. (2011). "Physical and clinical performance of the mCT time-of-flight PET/CT scanner." Phys Med Biol **56**(8): 2375-2389.

Jana, J. J., Vaid, N., Shanbhag, J. (2013). "Effect of total intravenous anaesthesia on intraoperative monitoring of cochlear implant function in paediatric patients." Cochlear Implants Int **14**(3): 169-173.

Jang, D. P., Lee, K. M., Lee, S. Y., Oh, J. H., Park, C. W., Kim, I. Y., et al. (2012). "Auditory adaptation to sound intensity in conscious rats: 2-[F-18]-fluoro-2-deoxy-D-glucose PET study." Neuroreport **23**(4): 228-233.

Jeffries, K. J., Fritz, J. B., Braun, A. R. (2003). "Words in melody: an H(2)15O PET study of brain activation during singing and speaking." Neuroreport **14**(5): 749-754.

Jin Su, K., Jae Sung, L., Dong Soo, L., June-Key, J., Myung Chul, L. "Performance evaluation of SIEMENS CTI ECAT EXACT 47 PET scanner USING NEMA NU2-2001." IEEE Symposium Conference Record Nuclear Science 2004; 2004 16-22 Oct. 2004; Rome, Italy: IEEE. p. 3118-3120. DOI: 10.1109/NSSMIC.2004.1466341

Johnsrude, I. S., Giraud, A. L., Frackowiak, R. S. (2002). "Functional imaging of the auditory system: the use of positron emission tomography." Audiol Neurootol **7**: 251-276.

Jonckers, E., Shah, D., Hamaide, J., Verhoye, M., Van der Linden, A. (2015). "The power of using functional fMRI on small rodents to study brain pharmacology and disease." Front Pharmacol **6**: 231.

Kang, H. H., Wang, C. H., Chen, H. C., Li, I. H., Cheng, C. Y., Liu, R. S., et al. (2013). "Investigating the effects of noise-induced hearing loss on serotonin transporters in rat brain using 4-[^{18}F]-ADAM/small animal PET." Neuroimage **75**: 262-269.

Kanno, I., Iida, H., Miura, S., Murakami, M. (1991). "Optimal scan time of oxygen-15-labeled water injection method for measurement of cerebral blood flow." J Nucl Med **32**: 1931-1934.

Kanno, I., Iida, H., Miura, S., Murakami, M., Takahashi, K., Sasaki, H., et al. (1987). "A System for Cerebral Blood Flow Measurement Using an $H_2{}^{15}O$ Autoradiographic Method and Positron Emission Tomography." J Cereb Blood Flow Metab **7**: 143-153.

Kerssens, C., Hamann, S., Peltier, S., Hu, X. P., Byas-Smith, M. G., Sebel, P. S. (2005). "Attenuated brain response to auditory word stimulation with sevoflurane: a functional magnetic resonance imaging study in humans." Anesthesiology **103**(1): 11-19.

Kessler, M., Mamach, M., Bankstahl, J. P., Ross, T. L., Wilke, F., Geworski, L., et al. (2016). "Evaluation of Logan's graphical method with reference tissue input as a simplified approach for quantification of $GABA_A$ receptor binding in rats." Eur J Nucl Med Mol Imaging **43**(Supplement 1): S100-S101.

Kilkenny, C., Browne, W. J., Cuthill, I. C., Emerson, M., Altman, D. G. (2010). "Improving bioscience research reporting: the ARRIVE guidelines for reporting animal research." PLoS Biol **8**(6): e1000412.

Kim, H., Cho, J., Kim, Y. R., Song, Y., Chun, S. I., Suh, J. Y., et al. (2014). "Response of the primary auditory and non-auditory cortices to acoustic stimulation: a manganese-enhanced MRI study." PLoS ONE **9**(3): e90427.

Klinge, P. A., Brooks, D. J., Samii, A., Weckesser, E., van den Hoff, J., Fricke, H., et al. (2008). "Correlates of local cerebral blood flow (CBF) in normal pressure

hydrocephalus patients before and after shunting - A retrospective analysis of O-15 H_2O PET-CBF studies in 65 patients." Clinical Neurology and Neurosurgery **110**(4): 369-375.

Knoop, B. O., Geworski, L., Hofmann, M., Munz, D. L., Knapp, W. H. (2002). "Use of recovery coefficients as a test of system linearity of response in positron emission tomography (PET)." Phys Med Biol **47**: 1237-1254.

Kral, A., O'Donoghue, G. M. (2010). "Profound Deafness in Childhood." New England Journal of Medicine **363**(15): 1438-1450.

Krause, B. J., Müller-Gärtner, H.-W., editors. "Bildgebung des Gehirns und Kognition. Landsberg: ecomed; 2003.

Kretschmann, H.-J., Weinrich, W. "Cranial Neuroimaging and Clinical Neuroanatomy." 2nd ed. New York: Thieme Medical Publisher; 1992.

Kreuer, S., Biedler, A., Larsen, R., Altmann, S., Wilhelm, W. (2003). "Narcotrend monitoring allows faster emergence and a reduction of drug consumption in propofol-remifentanil anesthesia." Anesthesiology **99**(1): 34-41.

Kujawa, S. G., Liberman, M. C. (2009). "Adding insult to injury: cochlear nerve degeneration after "temporary" noise-induced hearing loss." J Neurosci **29**(45): 14077-14085.

Lammertsma, A. A., Wise, R. J., Jones, T. (1983). "In vivo measurements of regional cerebral blood flow and blood volume in patients with brain tumours using positron emission tomography." Acta Neurochir (Wien) **69**(1-2): 5-13.

Lancaster, J. L., Woldorff, M. G., Parsons, L. M., Liotti, M., Freitas, C. S., Rainey, L., et al. (2000). "Automated Talairach Atlas labels for functional brain mapping." Human Brain Mapping **10**: 120-131.

Lange, C., Suppa, P., Frings, L., Brenner, W., Spies, L., Buchert, R. (2015). "Optimization of Statistical Single Subject Analysis of Brain FDG PET for the Prognosis of Mild Cognitive Impairment-to-Alzheimer's Disease Conversion." J Alzheimers Dis **49**(4): 945-959.

Lange, D. "Physikalisch-technische Grundlagen der Nuklearmedizin." In: Schlegel, W.,Bille, J., editors. Medizinische Physik. 2 Medizinische Strahlenphysik. Berlin: Springer; 2002. p. 171-210.

Laudanski, J., Edeline, J. M., Huetz, C. (2012). "Differences between spectro-temporal receptive fields derived from artificial and natural stimuli in the auditory cortex." PLoS ONE **7**(11): e50539.

Lazard, D. S., Vincent, C., Venail, F., Van de Heyning, P., Truy, E., Sterkers, O., et al. (2012). "Pre-, per- and postoperative factors affecting performance of postlinguistically deaf adults using cochlear implants: a new conceptual model over time." PLoS ONE **7**(11): e48739.

Le Prell, C. G., Lobarinas, E. "Perspectives on Auditory Translational Research." In: Le Prell, C. G., Lobarinas, E., Fay, R. R.,Popper, A. N., editors. Translational

Research in Audiology, Neurology and the Hearing Sciences. 1st ed. New York: Springer; 2016. p. 265.

Leaver, A. M., Rauschecker, J. P. (2016). "Functional Topography of Human Auditory Cortex." J Neurosci **36**(4): 1416-1428.

Lee, C. C. (2013). "Thalamic and cortical pathways supporting auditory processing." Brain Lang **126**(1): 22-28.

Lee, D. S., Lee, J. S., Oh, S. H., Kim, S. K., Kim, J. W., Chung, J. K., et al. (2001). "Cross-modal plasticity and cochlear implants." Nature **409**(6817): 149-150.

Lee, Y. S., Kim, J. S., Kim, K. M., Kang, J. H., Lim, S. M., Kim, H. J. (2014). "Performance measurement of PSF modeling reconstruction (True X) on Siemens Biograph TruePoint TrueV PET/CT." Ann Nucl Med **28**(4): 340-348.

Lenarz, M., Matthies, C., Lesinski-Schiedat, A., Frohne, C., Rost, U., Illg, A., et al. (2002). "Auditory brainstem implant part II: subjective assessment of functional outcome." Otol Neurotol **23**(5): 694-697.

Lenarz, T., Lim, H. H., Reuter, G., Patrick, J. F., Lenarz, M. (2006). "The auditory midbrain implant: a new auditory prosthesis for neural deafness-concept and device description." Otol Neurotol **27**: 838-843.

Leveille, J., Demonceau, G., Walovitch, R. C. (1992). "Intrasubject comparison between technetium-99m-ECD and technetium-99m-HMPAO in healthy human subjects." J Nucl Med **33**(4): 480-484.

Liao, W. H., Van Den Abbeele, T., Herman, P., Frachet, B., Huy, P. T., Lecain, E., et al. (2000). "Expression of NMDA, AMPA and $GABA_A$ receptor subunit mRNAs in the rat auditory brainstem. II. Influence of intracochlear electrical stimulation." Hear Res **150**: 12-26.

Lin, V. Y. W., Black, S. E. (2017). "Linking Deafness and Dementia: Challenges and Opportunities." Otol Neurotol **38**(8): e237-e239.

Ljunggren, K. (1968). "Review of the use of radioactive tracers for evaluating parameters pertaining to the flow of material in plant and natural systems." Science **162**(3849): 303-349.

Logan, J., Fowler, J. S., Volkow, N. D., Ding, Y. S., Wang, G.-J., Alexoff, D. L. (2001). "A Strategy for Removing the Bias in the Graphical Analysis Method." J Cereb Blood Flow Metab **21**: 307-320.

Logan, J., Fowler, J. S., Volkow, N. D., Wang, G.-J., Ding, Y.-S., Alexoff, D. L. (1996). "Distribution Volume Ratios Without Blood Sampling from Graphical Analysis of PET Data." J Cereb Blood Flow Metab **16**: 834-840.

Lu, W., Xu, J., Shepherd, R. K. (2005). "Cochlear implantation in rats: a new surgical approach." Hear Res **205**(1-2): 115-122.

Mamach, M., Berding, G., Bankstahl, J. P., Bengel, F. M., Kurt, S. (2015). "Revealing asymmetric activations in the auditory cortex in rats with FDG PET." Eur J Nucl Med Mol Imaging **42**(Supplement 1): S544.

Mamach, M., Berding, G., Bankstahl, J. P., Wilke, F., Geworski, L., Bengel, F. M., et al. (2014). "Feasibility of imaging auditory activation in the rat brain using emission tomography " Eur J Nucl Med Mol Imaging **41**(Supplement 2): S634.

Mamach, M., Kessler, M., Bankstahl, J. P., Ross, T. L., Bengel, F. M., Geworski, L., et al. (2017). "Quantitative PET of GABA-A receptor binding in gerbils after intra-peritoneal F-18-Flumazenil injection does not resemble accurate results obtain in rats after intravenous administration." Eur J Nucl Med Mol Imaging **44**(Supplement 2): S365-S366.

Mamach, M., Kessler, M., Bankstahl, J. P., Ross, T. L., Geworski, L., Bengel, F. M., et al. (2016). "Complete hearing loss changes activity pattern and inhibitory neurotransmission in the auditory system of rodents detected with PET." Eur J Nucl Med Mol Imaging **43**(Supplement 1): S98-S99.

Mamach, M., Wilke, F., Durisin, M., Beger, F. A., Finke, M., Buchner, A., et al. (2018). "Feasibility of ^{15}O-water PET studies of auditory system activation during general anesthesia in children." EJNMMI Res **8**(1): 11.

Mandema, J. W., Gubbens-Stibbe, J. M., Danhof, M. (1991). "Stability and pharmacokinetics of flumazenil in the rat." Psychopharmacology **103**: 384-387.

Mason, A., Mason, M. (2007). "Psychologic Impact of Deafness on the Child and Adolescent." Primary Care: Clinics in Office Practice **34**(2): 407-426.

Matzke, K. H., Meyer, G. J., Hundeshagen, H. (1993). "An advanced system for the administration of ^{15}O-water." J Labelled Comp Radiopharm **32**: 459-460.

Mazziotta, J. C., Phelps, M. E. (1984). "Human sensory stimulation and deprivation: positron emission tomographic results and strategies." Ann Neurol **15 Suppl**: S50-60.

McIntosh, A. R., Gonzalez-Lima, F. (1993). "Network analysis of functional auditory pathways mapped with fluorodeoxyglucose: associative effects of a tone conditioned as a Pavlovian excitor or inhibitor." Brain Res **627**: 129-140.

Merabet, L. B., Pascual-Leone, A. (2010). "Neural reorganization following sensory loss: the opportunity of change." Nat Rev Neurosci **11**(1): 44-52.

Meyer, J. P., Adumeau, P., Lewis, J. S., Zeglis, B. M. (2016). "Click Chemistry and Radiochemistry: The First 10 Years." Bioconjug Chem **27**(12): 2791-2807.

Miyamoto, R. T., Wong, D. (2001). "Positron emission tomography in cochlear implant and auditory brainstem implant recipients." J Commun Disord **34**: 473-478.

Miyamoto, R. T., Wong, D., Pisoni, D. B., Hutchins, G., Sehgal, M., Fain, R. (1999). "Positron emission tomography in cochlear implant and auditory brain stem implant recipients." The American journal of otology **20**: 596-601.

Mokri, Y., Worland, K., Ford, M., Rajan, R. (2015). "Effect of background noise on neuronal coding of interaural level difference cues in rat inferior colliculus." Eur J Neurosci **42**(1): 1685-1704.

Møller, A. R. "Hearing : anatomy, physiology, and disorders of the auditory system." 2nd ed. Oxford: Academic Press 2006. 328 p.

Moreno-Cantu, J. J., Thompson, C. J., Meyer, E., Fiset, P., Zatorre, R. J., Klein, D., et al. (2000). "Enhancement of the signal-to-noise ratio in $H_2{}^{15}O$ bolus PET activation images: a combined cold-bolus, switched protocol." J Nucl Med **41**: 926-933.

Morosan, P., Rademacher, J., Schleicher, A., Amunts, K., Schormann, T., Zilles, K. (2001). "Human primary auditory cortex: cytoarchitectonic subdivisions and mapping into a spatial reference system." Neuroimage **13**(4): 684-701.

Morris, J. S., Friston, K. J., Dolan, R. J. (1998). "Experience-dependent modulation of tonotopic neural responses in human auditory cortex." Proc Biol Sci **265**: 649-657.

Mortensen, M. V., Madsen, S., Gjedde, A. (2005). "Cortical responses to promontorial stimulation in postlingual deafness." Hear Res **209**(1-2): 32-41.

Mueller, T. (2012). "What is the Thalamus in Zebrafish?" Frontiers in Neuroscience **6**(64).

Mullani, N. A., Herbst, R. S., O'Neil, R. G., Gould, K. L., Barron, B. J., Abbruzzese, J. L. (2008). "Tumor blood flow measured by PET dynamic imaging of first-pass ^{18}F-FDG uptake: a comparison with ^{15}O-labeled water-measured blood flow." J Nucl Med **49**(4): 517-523.

Muzik, O., Chugani, D. C., Juhasz, C., Shen, C., Chugani, H. T. (2000). "Statistical parametric mapping: assessment of application in children." Neuroimage **12**(5): 538-549.

Nadol, J. B., Jr. (1988). "Comparative anatomy of the cochlea and auditory nerve in mammals." Hear Res **34**(3): 253-266.

Naito, Y., Okazawa, H., Honjo, I., Hirano, S., Takahashi, H., Shiomi, Y., et al. (1995). "Cortical activation with sound stimulation in cochlear implant users demonstrated by positron emission tomography." Brain Res Cogn Brain Res **2**: 207-214.

Nenov, V. I., Halgren, E., Smith, M. E., Badier, J. M., Ropchan, J., Blahd, W. H., et al. (1991). "Localized brain metabolic response correlated with potentials evoked by words." Behav Brain Res **44**: 101-104.

Nikolopoulos, T. P., Mason, S. M., O'Donoghue, G. M., Gibbin, K. P. (1999). "Integrity of the auditory pathway in young children with congenital and postmeningitic deafness." Ann Otol Rhinol Laryngol **108**(4): 327-330.

Niparko, J. K., Tobey, E. A., Thal, D. J., Eisenberg, L. S., Wang, N. Y., Quittner, A. L., et al. (2010). "Spoken language development in children following cochlear implantation." JAMA **303**(15): 1498-1506.

Nishimura, H., Doi, K., Iwaki, T., Hashikawa, K., Oku, N., Teratani, T., et al. (2000). "Neural plasticity detected in short- and long-term cochlear implant users using PET." Neuroreport **11**: 811-815.

NRC, National Research Council. "Brain and Cognition: Some New Technologies. Washington, DC: The National Academies Press; 1989. 90 p.

Odano, I., Halldin, C., Karlsson, P., Varrone, A., Airaksinen, A. J., Krasikova, R. N., et al. (2009). "[^{18}F]flumazenil binding to central benzodiazepine receptor studies by PET--quantitative analysis and comparisons with [^{11}C]flumazenil." Neuroimage **45**(3): 891-902.

Okazawa, H., Naito, Y., Yonekura, Y., Sadato, N., Hirano, S., Nishizawa, S., et al. (1996). "Cochlear implant efficiency in pre- and postlingually deaf subjects. A study with $H_2{}^{15}O$ and PET." Brain **119 (Pt 4**: 1297-1306.

Okuda, T., Nagamachi, S., Ushisako, Y., Tono, T. (2013). "Glucose metabolism in the primary auditory cortex of postlingually deaf patients: an FDG-PET study." ORL J Otorhinolaryngol Relat Spec **75**(6): 342-349.

OpenStax-College (2016a). "Cross Section of the Cochlea " 1406_Cochlea.jpg (https://cnx.org/contents/FPtK1zmh@8.25:s3XqfSLV@7/Sensory-Perception, 18.06.2016)

OpenStax-College (2016b). "Structures of the Ear." 1404_The_Structures_of_the_Ear.jpg (https://cnx.org/contents/FPtK1zmh@8.25:s3XqfSLV@7/Sensory-Perception, 18.05.2016)

Orr, J. S., Gillespie, F. C. (1968). "Occupancy principle for radioactive tracers in steady-state biological systems." Science **162**(3849): 138-139.

Parellada, E., Lomena, F., Font, M., Pareto, D., Gutierrez, F., Simo, M., et al. (2008). "Fluordeoxyglucose-PET study in first-episode schizophrenic patients during the hallucinatory state, after remission and during linguistic-auditory activation." Nucl Med Commun **29**(10): 894-900.

Paul, A. K., Lobarinas, E., Simmons, R., Wack, D., Luisi, J. C., Spernyak, J., et al. (2009). "Metabolic imaging of rat brain during pharmacologically-induced tinnitus." Neuroimage **44**(2): 312-318.

Paxinos, G., Watson, C. "The Rat Brain in Stereotaxic Coordinates." 3rd ed. New York: Academic Press,; 1998.

Petersen, S. E., Fox, P. T., Posner, M. I., Mintun, M., Raichle, M. E. (1988). "Positron emission tomographic studies of the cortical anatomy of single-word processing." Nature **331**(6157): 585-589.

Pickles, J. O. "An Introduction to the Physiology of Hearing." 4th ed. Leiden: Brill; 2013.

Pietrini, P., Alexander, G. E., Furey, M. L., Dani, A., Mentis, M. J., Horwitz, B., et al. (2000). "Cerebral metabolic response to passive audiovisual stimulation in patients with Alzheimer's disease and healthy volunteers assessed by PET." J Nucl Med **41**: 575-583.

Plourde, G., Belin, P., Chartrand, D., Fiset, P., Backman, S. B., Xie, G., et al. (2006). "Cortical processing of complex auditory stimuli during alterations of consciousness with the general anesthetic propofol." Anesthesiology **104**(3): 448-457.

PubMed. PubMed: National Center for Biotechnilogy Information, US National Library of Medicine; [09.07.2018]. Search: ((auditory OR hearing[Title] OR ear[Title]) AND (animal)) Available from: https://www.ncbi.nlm.nih.gov/pubmed/.

Qin, P., Duncan, N. W., Wiebking, C., Gravel, P., Lyttelton, O., Hayes, D. J., et al. (2012). "$GABA_A$ receptors in visual and auditory cortex and neural activity changes during basic visual stimulation." Front Hum Neurosci **6**: 337.

Raichle, M. E. (1981). "Measurement of local cerebral blood flow and metabolism in man with positron emission tomography." Fed Proc **40**(8): 2331-2334.

Rajan, R., Dubaj, V., Reser, D. H., Rosa, M. G. (2013). "Auditory cortex of the marmoset monkey - complex responses to tones and vocalizations under opiate anaesthesia in core and belt areas." Eur J Neurosci **37**(6): 924-941.

Rao, D. B., Fechter, L. D. (2000). "Increased noise severity limits potentiation of noise induced hearing loss by carbon monoxide." Hear Res **150**(1): 206-214.

Rausch, I., Cal-Gonzalez, J., Dapra, D., Gallowitsch, H. J., Lind, P., Beyer, T., et al. (2015). "Performance evaluation of the Biograph mCT Flow PET/CT system according to the NEMA NU2-2012 standard." EJNMMI Phys **2**(1): 26.

Reimold, M., Slifstein, M., Heinz, A., Mueller-Schauenburg, W., Bares, R. (2006). "Effect of spatial smoothing on t-maps: arguments for going back from t-maps to masked contrast images." J Cereb Blood Flow Metab **26**(6): 751-759.

Reis, A. d., Dalmolin, S. P., Dallegrave, E. (2017). "Animal models for hearing evaluations: a literature review." Revista CEFAC **19**(3): 417-428.

Reivich, M., Kuhl, D., Wolf, A., Greenberg, J., Phelps, M., Ido, T., et al. (1979). "The [^{18}F]fluorodeoxyglucose method for the measurement of local cerebral glucose utilization in man." Circ Res **44**(1): 127-137.

Riecke, L., Peters, J. C., Valente, G., Poser, B. A., Kemper, V. G., Formisano, E., et al. (2018). "Frequency-specific attentional modulation in human primary auditory cortex and midbrain." Neuroimage **174**: 274-287.

Roy, C. S., Sherrington, C. S. (1890). "On the Regulation of the Blood-supply of the Brain." The Journal of Physiology **11**(1-2): 85-158.117.

Ruytjens, L., Willemsen, A. T., Van Dijk, P., Wit, H. P., Albers, F. W. (2006). "Functional imaging of the central auditory system using PET." Acta Otolaryngol **126**(12): 1236-1244.

Salvi, R., Sun, W., Ding, D., Chen, G. D., Lobarinas, E., Wang, J., et al. (2016). "Inner Hair Cell Loss Disrupts Hearing and Cochlear Function Leading to Sensory Deprivation and Enhanced Central Auditory Gain." Front Neurosci **10**: 621.

Sambeth, A., Maes, J. H., Van Luijtelaar, G., Molenkamp, I. B., Jongsma, M. L., Van Rijn, C. M. (2003). "Auditory event-related potentials in humans and rats: effects of task manipulation." Psychophysiology **40**(1): 60-68.

Sanes, D. H., Kotak, V. C. (2011). "Developmental plasticity of auditory cortical inhibitory synapses." Hear Res **279**(1-2): 140-148.

Schiffer, W. K., Mirrione, M. M., Biegon, A., Alexoff, D. L., Patel, V., Dewey, S. L. (2006). "Serial microPET measures of the metabolic reaction to a microdialysis probe implant." J Neurosci Methods **155**: 272-284.

Schmidt, F. P., Kolb, A., Pichler, B. J. (2018). "Optimization, evaluation and calibration of a cross-strip DOI detector." Phys Med Biol **63**(4): 045022.

Schmidt, K., Mies, G., Sokoloff, L. (1991). "Model of kinetic behavior of deoxyglucose in heterogeneous tissues in brain: a reinterpretation of the significance of parameters fitted to homogeneous tissue models." J Cereb Blood Flow Metab **11**(1): 10-24.

Schmuck, S., Mamach, M., Wilke, F., von Klot, C. A., Henkenberens, C., Thackeray, J. T., et al. (2017). "Multiple Time-Point ^{68}Ga-PSMA I&T PET/CT for Characterization of Primary Prostate Cancer: Value of Early Dynamic and Delayed Imaging." Clin Nucl Med **42**(6): e286-e293.

Schulz, G. M., Varga, M., Jeffires, K., Ludlow, C. L., Braun, A. R. (2005). "Functional neuroanatomy of human vocalization: an $H_2{}^{15}O$ PET study." Cereb Cortex **15**(12): 1835-1847.

Schwartz, M. S., Otto, S. R., Shannon, R. V., Hitselberger, W. E., Brackmann, D. E. (2008). "Auditory brainstem implants." Neurotherapeutics **5**(1): 128-136.

Schwarz, A. J., Danckaert, A., Reese, T., Gozzi, A., Paxinos, G., Watson, C., et al. (2006). "A stereotaxic MRI template set for the rat brain with tissue class distribution maps and co-registered anatomical atlas: application to pharmacological MRI." Neuroimage **32**(2): 13.

Schwender, D., Kaiser, A., Klasing, S., Peter, K., Poppel, E. (1994). "Midlatency auditory evoked potentials and explicit and implicit memory in patients undergoing cardiac surgery." Anesthesiology **80**(3): 493-501.

Selimoglu, E. (2007). "Aminoglycoside-induced ototoxicity." Curr Pharm Des **13**(1): 119-126.

Sharma, A., Tobey, E., Dorman, M., Bharadwaj, S., Martin, K., Gilley, P., et al. (2004). "Central auditory maturation and babbling development in infants with cochlear implants." Arch Otolaryngol Head Neck Surg **130**(5): 511-516.

Shaw, N. A. (1988). "The auditory evoked potential in the rat-a review." Progress in Neurobiology **31**: 19-45.

Signorini, M., Paulesu, E., Friston, K., Perani, D., Colleluori, a., Lucignani, G., et al. (1999). "Rapid assessment of regional cerebral metabolic abnormalities in single subjects with quantitative and nonquantitative [18F]FDG PET: A clinical validation of statistical parametric mapping." Neuroimage **9**: 63-80.

Silbersweig, D. A., Stern, E., Frith, C. D., Cahill, C., Schnorr, L., Grootoonk, S., et al. (1993). "Detection of thirty-second cognitive activations in single subjects with positron emission tomography: a new low-dose $H_2{}^{15}O$ regional cerebral blood flow three-dimensional imaging technique." J Cereb Blood Flow Metab **13**(4): 617-629.

Singer, W., Zuccotti, A., Jaumann, M., Lee, S. C., Panford-Walsh, R., Xiong, H., et al. (2013). "Noise-induced inner hair cell ribbon loss disturbs central arc mobilization: a novel molecular paradigm for understanding tinnitus." Mol Neurobiol **47**(1): 261-279.

Smith, J. J., Shionoya, K., Sullivan, R. M., Wilson, D. A. (2009). "Auditory stimulation dishabituates olfactory responses via noradrenergic cortical modulation." Neural Plast **2009**: 754014.

Soto-Montenegro, M. L., Vaquero, J. J., Pascau, J., Gispert, J. D., Garcia-Barreno, P., Desco, M. (2009). "Detection of visual activation in the rat brain using 2-deoxy-2-[^{18}F]fluoro-D: -glucose and statistical parametric mapping (SPM)." Mol Imaging Biol **11**(2): 94-99.

Suh, M. W., Park, K. T., Lee, H. J., Lee, J. H., Chang, S. O., Oh, S. H. (2015). "Factors Contributing to Speech Performance in Elderly Cochlear Implanted Patients: An FDG-PET Study: A Preliminary Study." J Int Adv Otol **11**(2): 98-103.

Talairach, J., Tournoux, P. "Co-Planar Stereotaxic Atlas of the Human Brain. Stuttgart: Thieme; 1988.

Ter-Pogossian, M. M. (1992). "The origins of positron emission tomography." Semin Nucl Med **22**(3): 140-149.

Theobald, T. "Sampson's Textbook of Radiopharmacy." 4th edition ed. London: Pharmaceutical Press; 2010.

Tzourio-Mazoyer, N., Landeau, B., Papathanassiou, D., Crivello, F., Etard, O., Delcroix, N., et al. (2002). "Automated anatomical labeling of activations in SPM using a macroscopic anatomical parcellation of the MNI MRI single-subject brain." Neuroimage **15**(1): 273-289.

Vallez Garcia, D., Casteels, C., Schwarz, A. J., Dierckx, R. A., Koole, M., Doorduin, J. (2015). "A standardized method for the construction of tracer specific PET and

SPECT rat brain templates: validation and implementation of a toolbox." PLoS ONE **10**(3): e0122363.

van Dyck, C. H., Lin, C. H., Smith, E. O., Wisniewski, G., Cellar, J., Robinson, R., et al. (1996). "Comparison of technetium-99m-HMPAO and technetium-99m-ECD cerebral SPECT images in Alzheimer's disease." J Nucl Med **37**(11): 1749-1755.

van Horik, J., Emery, N. J. (2011). "Evolution of cognition." Wiley Interdiscip Rev Cogn Sci **2**(6): 621-633.

Vaska, P., Woody, C. L., Schlyer, D. J., Shokouhi, S., Stoll, S. P., Pratte, J. F., et al. (2004). "RatCAP: miniaturized head-mounted PET for conscious rodent brain imaging." IEEE Transactions on Nuclear Science **51**(5): 2718-2722.

Veith, H.-M. "Strahlenschutzverordnung / Textausgabe mit einer erläuternden Einführung." (2016). Köln: Bundesanzeiger Verlag GmbH;

Veith, H.-M. "Strahlenschutzgesetz mit Strahlenschutzverordnung : Textausgabe mit einer erläuternden Einführung." (2018). Köln: Bundesanzeiger Verlag GmbH;

Vincenti, V., Bacciu, A., Guida, M., Marra, F., Bertoldi, B., Bacciu, S., et al. (2014). "Pediatric cochlear implantation: an update." Ital J Pediatr **40**: 72.

Vivash, L., Gregoire, M. C., Bouilleret, V., Berard, A., Wimberley, C., Binns, D., et al. (2014). "In vivo measurement of hippocampal $GABA_A$/cBZR density with [^{18}F]-flumazenil PET for the study of disease progression in an animal model of temporal lobe epilepsy." PLoS ONE **9**(1): e86722.

Vogt, H.-G., Schultz, H. "Grundzüge des praktischen Strahlenschutz." 6th revised ed. Wien: Hanser; 2011. 603 p.

Volkow, N. D., Mullani, N., Gould, L. K., Adler, S. S., Gatley, S. J. (1991). "Sensitivity of Measurements of Regional Brain Activation with Oxygen-15-Water and PET to Time of Stimulation and Period of Image Reconstruction." J Nucl Med **32**(1): 58-61.

von Gablenz, P., Hoffmann, E., Holube, I. (2017). "Prevalence of hearing loss in Northern and Southern Germany." Hno **65**(8): 663-670.

Warburton, E., Price, C. J., Swinburn, K., Wise, R. J. (1999). "Mechanisms of recovery from aphasia: evidence from positron emission tomography studies." J Neurol Neurosurg Psychiatry **66**: 155-161.

Wehr, M., Zador, A. M. (2005). "Synaptic mechanisms of forward suppression in rat auditory cortex." Neuron **47**(3): 437-445.

WHO. "Addressing the rising prevalence of hearing loss. Geneva: World Health Organization; 2018. Available at http://www.who.int/iris/handle/10665/260336 p.

Willis, M. W., Benson, B. E., Ketter, T. A., Kimbrell, T. A., George, M. S., Speer, A. M., et al. (2008). "Interregional cerebral metabolic associativity during a continuous performance task (Part I): healthy adults." Psychiatry Res **164**(1): 16-29.

Willmore, B. D., King, A. J. (2009). "Auditory cortex: representation through sparsification?" Curr Biol **19**(24): R1123-1125.

Wilson, B. S., Dorman, M. F. (2008). "Cochlear implants: a remarkable past and a brilliant future." Hear Res **242**(1-2): 3-21.

Woo, C. W., Krishnan, A., Wager, T. D. (2014). "Cluster-extent based thresholding in fMRI analyses: pitfalls and recommendations." Neuroimage **91**: 412-419.

Woods, R. P., Grafton, S. T., Holmes, C. J., Cherry, S. R., Mazziotta, J. C. (1998). "Automated image registration: I. General methods and intrasubject, intramodality validation." J Comput Assist Tomogr **22**: 139-152.

Wu, H. M., Huang, S. C., Choi, Y., Hoh, C. K., Hawkins, R. A. (1995). "A modeling method to improve quantitation of fluorodeoxyglucose uptake in heterogeneous tumor tissue." J Nucl Med **36**(2): 297-306.

Xu, J., Yu, L., Cai, R., Zhang, J., Sun, X. (2010). "Early continuous white noise exposure alters auditory spatial sensitivity and expression of GAD65 and GABAA receptor subunits in rat auditory cortex." Cereb Cortex **20**(4): 804-812.

Yao, R., Lecomte, R., Crawford, E. S. (2012). "Small-animal PET: what is it, and why do we need it?" J Nucl Med Technol **40**(3): 157-165.

Zhou, Y., Fang, F. H., Pan, P., Liu, Z. R., Ji, Y. H. (2017). "Visual deprivation induce cross-modal enhancement of olfactory perception." Biochem Biophys Res Commun **486**(3): 833-838.

Zucker, R. S., Regehr, W. G. (2002). "Short-term synaptic plasticity." Annu Rev Physiol **64**: 355-405.

List of Figures

Figure 1 Anatomy of a) the human ear [OpenStax-College2016b] and the cochlea [OpenStax-College2016a] 2
Figure 2 Schematic simplified view of the afferent auditory pathway 4
Figure 3 Schematic locations of auditory relevant Brodmann areas in humans 5
Figure 4 Schematic view of the structure of the auditory pathway in rats [Mueller2012]....8
Figure 5 Structure of the radiopharmaceutical ^{18}F-FDG and imaging principle of PET. 12
Figure 6 Comparison of spatial resolution of a dedicated small animal PET with an animal anatomical atlas 16
Figure 7 Impact of resolution on contrast. 17
Figure 8 Exemplary interindividual differences shown on similar transaxial planes of patients on both sides in comparison to a brain template (middle) and between each other. 18
Figure 9 Examples of activations in auditory and extra-auditory regions (AR and eAR separated by blue line), during general anesthesia in a child and awake state in an adult patient detected with different cut-off levels used for statistical inferences (all smoothed with a filter kernel of [20mm]³) 34
Figure 10 Examples of activations in auditory and extra-auditory regions (AR and eAR separated by blue line) detected with different smoothing filter kernels (always using a cut-off for statistical inferences of $p < 0.01$) 36
Figure 11 Timelines for a) general experimental setup and b) a single scan procedure 49
Figure 12 Schematic view of the custom made sound attenuating box 50
Figure 13 Mean normalized images for all conditions and in different coronal levels....55
Figure 14 Results of voxel-wise pairwise comparison in SPM 58

List of Tables

Table 1 Comparison of speech intelligibility 6 years after PET, between patients studied with and without anesthesia.....27

Table 2 Comparison of peak height (t_{max} values) of auditory activations obtained with different scan durations (60 vs. 90s) and depending on anesthesia (no vs. yes). 31

Table 3 Mean relative sizes of activations in AR and eAR – both given as percent of the overall size of the auditory region. 32

Table 4 Frequency of activations in AR and eAR – dependency on selected threshold for statistical inferences and applied smoothing filter-kernel. 35

Table 5 Mean and standard deviation (SD) of pairwise differences of average normalized VOI values shown for all comparisons of conditions.....56

Table 6 T-values and coverage of VOIs for each condition comparison with SPM 57

Table 7: Supplement 1 - ANCOVA of study with FDG uptake as the dependent variable...66

List of Abbreviations

ABI	Auditory brainstem implant
ABL	Bilateral cochlea ablation
ABR	Auditory brainstem response
AC	Auditory cortex
AMI	Auditory midbrain implant
AR	Auditory brain region
BA	Brodmann area
BG	Background noise
BGO	Bismuth germanate (scintillator material)
Bq	Becquerel
BOLD	Blood-oxygen-level dependent contrast
BPND	Non-displaceable binding potential
CB	Cerebellum
CBF	Cerebral blood flow
CI	Cochlear implant
cps	Counts per second
CT	Computer tomography
dB SPL	Decibel sound pressure level
eAR	Extra-auditory brain region
EEG	Electroencephalography
e.g.	For example
FDG	2-fluoro-2-deoxyglucose
FMZ	Flumazenil
FWHM	Full width at half maximum

GABA	Gamma-amino-butyric acid
HMPAO	Hexametylpropylenamineoxime
HSM	Hochmair-Schulz-Moser sentence test
IC	Inferior colliculus
ICRP	International Commission on Radiological Protection
i.e.	That is
LL	Lateral lemniscus
LSO	Lutetium oxyorthosilicate (scintillator material)
MGB	Medial geniculate body
MRI	Magnetic resonance imaging
NC	Nucleus cochlearis
ng	Nanogram (weight)
p	Probability
OC	Superior olivary complex
ON	Olfactory nucleus
OSEM	Ordered subset expectation maximization
PET	Positron emission tomography
pmol	Picomol (amount of substance)
PN	Promontory needle electrode stimulation
RN	Pulsed rippled noise
S	Second(s)
S/N	Signal to noise ratio
SC	Somatosensory cortex
SPECT	Single photon emission computed tomography
SPM	Statistical parametric mapping
SUV	Standard uptake value

T	Tesla (SI unit of magnetic flux density)
T-value	Experimental design dependent indicator for statistical significance
VOI	Volume of interest
WN	White noise

Contribution

My responsibilities in all studies were the analysis and additionally for animal experiments contribution to the design, execution of scan procedures and care of the animals. Detailed contributions in both published study are specified in the following paragraphs.

Study I

The first study was a retrospective analysis of data. The clinical setting was designed by Georg Berding and Anke Lesinski-Schiedat. Imaging time and parameters for the default analysis were set by Georg Berding and Florian Wilke. The patients were selected by Anke Lesinski-Schiedat based on clinical indications. Speech performance was retrospectively retrieved from the patient files by Martin Durisin, Mareike Finke, and Andreas Büchner. The concept of anesthesia was designed by Frank Beger, Barbara Schultz, and Arthur Schultz. All anesthesia were carried out by Frank Beger.

Brain region to be evaluated were selected by Georg Berding and Martin Mamach. Parameters for the systematic variation in smoothing were chosen by Martin Mamach. The evaluated levels of significance for statistical inferences were selected by Georg Berding and Martin Mamach. Analyses were performed by Martin Mamach. Scripts from Florian Wilke were adapted by Martin Mamach for implementation of automated analysis on multiple patients in SPM. The first draft of the manuscript was written by Martin Mamach with the support of Georg Berding. The final manuscript was additionally revised by Anke Lesinski-Schiedat, Martin Durisin, and Mareike Finke. All authors approved before submission and after editorial revision. The retrospective analysis was supported by the DFG Cluster of Excellence EXC 1077 “Hearing4all”.

Study II

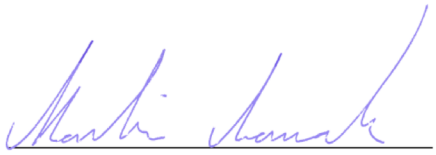
The study was developed and designed by Martin Mamach, Simone Kurt, and Georg Berding. Experiments were carried out by Martin Mamach. Cochlea ablation was operated by Simone Kurt with help of Martin Mamach. Post-operative animal care was realized by Martin Mamach under the supervision of Simone Kurt and Jens Bankstahl. Imaging was performed by Martin Mamach in cooperation with the technical staff of the preclinical imaging facility Silvia Eilert, Petra Felsch and Alexander Kanwischer. The Schwarz-atlas was adapted by Martin Mamach. The analyses were designed by Martin Mamach with the support of Simone Kurt and Georg Berding. Data were analyzed by Martin Mamach and in later animal groups in cooperation with Mariella Kessler. The manuscript was written by Martin Mamach with the support of Georg Berding and Simone Kurt. Additionally, Jens Bankstahl and Marielle Kessler revised the manuscript. All authors approved before submission. The study was supported by the DFG Cluster of Excellence EXC 1077 “Hearing4all”.

Declaration

Herewith, I confirm that I have written the present PhD thesis myself and independently, and that I have not submitted it at any other university worldwide.

Herewith, I agree that MHH can check my thesis using plagiarism detection software as well as randomly check the primary data. I am aware that in case of suspicion, ombudsman review procedure according to §9 of MHH 'Guidelines of Hannover Medical School to guarantee good scientific practice and dealing with scientific fraud' will be initiated. During that procedure, the thesis evaluation procedure is halted.

Hannover, (August 15th 2018)



Acknowledgments

I would like to thank here all the wonderful people without whom this thesis would not have been possible.

First and foremost, I thank my supervisor **Prof. Dr. Georg Berding**. He has taken the chance and has welcomed me as a newcomer to this field. Time and time again, he showed the perfect balance between patience and pressure to push for posters, talks, papers and this work. He restricted my sometimes naive approaches but gave a lot of freedom to pursue our studies in my own way.

I also would like to thank **Prof. Dr. Simone Kurt** who was another strong influence on the animal studies and my supervisor in animal studies. Her expert knowledge and contacts helped e.g. to create arrays of conditions and the stimulation box. She was crucial in the models of profound hearing loss as an operator, providing resources and with her knowledge about animals.

I would like to further express my deep gratitude to both of my co-supervisors **Prof. Dr. Peter Behrens** and **Prof. Dr. Karin Weißenborn**. They accompanied my academic way over the years and made sure realistic goals were set. Both took the time to evaluate the progress not with a focus on the interest of the cluster or the university but for my own sake.

I would like to especially thank **Florian Wilke** who helped me as a mentor to get started at the MHH and taught me all basics of analyses and corresponding programs I used. He provided me with an excellent professional framework I could build on.

In addition, I am much obliged to **Prof. Dr. Lilli Geworski** and my colleagues of the Department of Medical Physics and Radiation Protection, who adopted me in the middle of my thesis into their department and provided the ability to finish this research.

Very special thanks go to my fellow PhD-student **Mariella Kessler** with whom I had the pleasure of working together. Not only was she an eager student who let me at times feel like a supervisor but a good teacher, a marvelous colleague and best friend as well. The constructive discussions and exchanges substantially enhanced the working environment and the quality of research.

Relating to this, I also like to thank the other **PhD-students**, **postdocs, the clinical** and **the preclinical staff** of the department of nuclear medicine, in particular, **Silvia Eilert**, **Petra Felsch**, **Alexander Kanwischer**, **Elke Krischke** and **Maria Nierada**, for the stimulating and friendly environment they provided.

Also, my **fellow PhD-students** and other **members of the cluster of Excellency Hearing4All** deserve credit for providing an excellent structure for research and education. In particular, the former PhD-coordinator in Hannover **Dr. Odett Kaiser** and the cur-

rent PhD-coordinator **Dr. Christine Baumhoff** deserve thanks for their organization and support and answering all the important and unimportant questions I had over the years.

Thank goes to all **human participants** for their data. Even if we never met, I am grateful for their trust and commitment to research. Additionally, very special thanks go to all my **laboratory animals** with which I was able to work. For the limited time we had, I felt a bond and ongoing deep gratitude for the sacrifices they made. In particular, I would like to thank **Jane the rat** as an outstanding friendly and cooperative animal which will forever have a place in my heart.

Finally, I would like to thank my family and in particular my mother **Gabriele Mamach** and my father **Wolfgang Mamach**. This work is a big milestone of a road they started and helped me to pave, fix and rebuild no matter in which direction I chose to steer or across which terrain. The importance of their undying support and love is beyond my capabilities to explain. I thank you from the bottom of my heart.

Curriculum Vitae

Contact Information Martin Mamach mamach.martin@mh-hannover.de

General Born on the 15th of February 1985 in Berlin, Germany

Citizenship German

Graduate School

Medical School Hannover, Hanover, Germany
PhD Program "Auditory Sciences"

- November 15th 2013 to November 15th 2015, PhD Student, Department of Nuclear Medicine
- Since November 15th 2015, Employee, Department of Medical Physics and Radiation Protection
- Student representative to the board of the cluster of excellency Hearing4All (January 2014 to August 2016)

Degrees

Humboldt University of Berlin, Berlin, Germany

M.S., Department of Physics, February 15th 2013

- Thesis topic: *Quantification of Monte-Carlo event generator scale uncertainties of Sherpa with an example ATLAS analysis studying Underlying Event properties*

B.S., Department of Physics, July 20th 2008

- Thesis topic: *Study of the production and decay processes of a heavy b quark of a serial fourth fermion family*

Academic experiences

- *Radiation Safety Expert* S2.3, S4.2, S5, S6.4 (March 2018, Hanover, Germany)
- *Basics in Laboratory Animal Science* (March 2015, Hanover, Germany)
- *PMOD Software Course* (September 29th to October 2nd 2014, Zurich, Switzerland)
- *Monte-Carlo School 2011* (March 2011, Hamburg, Germany)
- *CERN Summer Student Program 2010* (July 6th 2010 to September 17th 2010, Geneva, Switzerland)
- *Year-in-Japan-Program* (September 2008 to May 2009, Kobe, Japan)

Professional experience

- *Student assistant*, **Humboldt University of Berlin**, Berlin, Germany, April 2010 to May 2012, Supervision of solid-state-detector experiment
- *Student assistant*, **Kobe University**, Japan, October 2008 to May 2009, Teacher in German and intercultural competences
- *Intern*, **Helmholtz Center for Materials and Energy**, Berlin, Germany, Design of a database for storage ring components

Publications

Articles

Berding, G., Wilke, F., Rode, T., Haense, C., Joseph, G., Meyer, G. J., **Mamach, M.**, et al. (2015). "Positron Emission Tomography Imaging Reveals Auditory and Frontal Cortical Regions Involved with Speech Perception and Loudness Adaptation." PLoS ONE 10(6): e0128743.

Schmuck, S., **Mamach, M.**, Wilke, F., von Klot, C. A., Henkenberens, C., Thackeray, J. T., Sohns, J. M., et al. (2017). "Multiple Time-Point ^{68}Ga-PSMA I&T PET/CT for Characterization of Primary Prostate Cancer: Value of Early Dynamic and Delayed Imaging." Clin Nucl Med **42**(6): e286-e293.

Mamach, M., Wilke, F., Durisin, M., Beger, F. A., Finke, M., Buchner, A., Schultz, B., et al. (2018). "Feasibility of ^{15}O-water PET studies of auditory system activation during general anesthesia in children." EJNMMI Res **8**(1): 11.

Mamach, M., Kessler, M., Bankstahl, J. P., Wilke, F., Geworski, L., Bengel, F. M., et al. (2018). "Visualization of the auditory pathway in rats with ^{18}F-FDG PET activation studies based on different auditory stimuli and reference conditions including cochlea ablation" PLoS One **13**(10):e0205044.

Conference contributions (first author)

Mamach, M., Berding, G., Bankstahl, J. P., Wilke, F., Geworski, L., Bengel, F. M., et al. (2014a). "Feasibility of imaging auditory activation in the rat brain using emission tomography " Eur J Nucl Med Mol Imaging 41(Supplement 2): S634.

Mamach, M., Berding, G., Wilke, F., Durisin, M., Finke, M., Büchner, A., et al. (2014b). "Impact of narcosis on results in PET activation studies of the auditory system." Eur J Nucl Med Mol Imaging 41(Supplement 2): S325.

Mamach, M., Berding, G., Bankstahl, J. P., Bengel, F. M., Kurt, S. (2015a). "Revealing asymmetric activations in the auditory cortex in rats with FDG PET." Eur J Nucl Med Mol Imaging 42(Supplement 1): S544.

Mamach, M., Berding, G., Bankstahl, J. P., Ross, T. L., Bengel, F. M., Kurt, S. (2015b). "Quantification of GABA-A receptor binding in the auditory system of rats using F-18-Flumazenil PET." Eur J Nucl Med Mol Imaging 42(Supplement 1): S545.

Mamach, M., Berding, G., Bankstahl, J. P., Wilke, F., Geworski, L., Bengel, F. M., et al. "Feasibility of statistical parametric mapping for analysis of auditory activation studies with PET in rats." 53. Jahrestagung der Deutschen Gesellschaft für Nukelarmedizin; 2015c; Hannover.

Mamach, M., Berding, G., Bankstahl, J. P., Wilke, F., Geworski, L., Kurt, S. (2015d). "Inverse translation of PET auditory system activation studies to rats using F-18-FDG PET." Eur J Nucl Med Mol Imaging 42(Supplement 1): S23.

Mamach, M., Berding, G., Wilke, F., Durisin, M., Finke, M., Büchner, A., et al. "Implementation of O-15-water PET for the assessment of auditory implants – methodological issues " 53. Jahrestagung der Deutschen Gesellschaft für Nukelarmedizin; 2015e; Hannover.

Mamach, M., Kessler, M., Bankstahl, J. P., Ross, T. L., Geworski, L., Bengel, F. M., et al. (2016). "Complete hearing loss changes activity pattern and inhibitory neurotransmission in the auditory system of rodents detected with PET." Eur J Nucl Med Mol Imaging 43(Supplement 1): S98-S99.

Mamach, M., Kessler, M., Bankstahl, J. P., Ross, T. L., Bengel, F. M., Geworski, L., et al. (2017). "Quantitative PET of GABA-A receptor binding in gerbils after intra-peritoneal F-18-Flumazenil injection does not resemble accurate results obtain in rats after intravenous administration." Eur J Nucl Med Mol Imaging 44(Supplement 2): S365-S366.